



저작자표시-비영리-변경금지 2.0 대한민국

이용자는 아래의 조건을 따르는 경우에 한하여 자유롭게

- 이 저작물을 복제, 배포, 전송, 전시, 공연 및 방송할 수 있습니다.

다음과 같은 조건을 따라야 합니다:



저작자표시. 귀하는 원저작자를 표시하여야 합니다.



비영리. 귀하는 이 저작물을 영리 목적으로 이용할 수 없습니다.



변경금지. 귀하는 이 저작물을 개작, 변형 또는 가공할 수 없습니다.

- 귀하는, 이 저작물의 재이용이나 배포의 경우, 이 저작물에 적용된 이용허락조건을 명확하게 나타내어야 합니다.
- 저작권자로부터 별도의 허가를 받으면 이러한 조건들은 적용되지 않습니다.

저작권법에 따른 이용자의 권리는 위의 내용에 의하여 영향을 받지 않습니다.

이것은 [이용허락규약\(Legal Code\)](#)을 이해하기 쉽게 요약한 것입니다.

[Disclaimer](#)

보건학 박사 학위논문

**The effects of fecal elements on  
metabolic disease and gut microbiome**

장내 원소가 대사성 질환과  
장내 마이크로비옴에 미치는 영향

2019년 2월

서울대학교 대학원  
보건학과 환경보건학 전공  
차 광 현

# **ABSTRACT**

## **The effects of fecal elements on metabolic disease and gut microbiome**

**Kwang Hyun Cha**

**Department of Environmental Health Sciences**

**Graduate School of Public Health**

**Seoul National University**

Metabolic syndrome (MetS) including obesity and diabetes is one of the major global public health concerns. Recent studies suggest a possible role of gut microbiota in MetS, demonstrating that microbial alteration could affect energy intake by changing the digestive capacity as well as induce low-grade inflammation by metabolic endotoxemia. Meanwhile, with the importance of gut microbiota on MetS being emphasized, there has also been considerable evidence that exposure to environmental chemicals could be associated with MetS. In particular, the elements including essential minerals and metals play an important part in host metabolic homeostasis. Most elements studies on MetS were conducted on the host side without considering the role of gut microbiota, and have only been done with a few elements such as As and Cd. Thus, in this thesis, we studied the relationships of fecal elements with gut microbiota and MetS.

First, we elucidated the association of various fecal elements with human gut microbiome and MetS status. We analyzed 29 elements from

human feces samples and performed the correlation study between fecal elements, MetS, and gut microbiota. Beryllium (Be), calcium (Ca), and thallium (Tl) had the significant odds ratios for MetS, and MetS-related biomarkers had a significant positive correlation with Be and Tl, whereas Ca showed a significant negative correlation with those. Be and Tl also had the high relationships with the reduction of microbial diversity. Besides, Be and Ca showed conflicting associations with the MetS-related gut microbiota, *Akkermansia* and *Bifidobacterium*. We additionally confirmed that the abundance of two elements had a link with gut microbial functions using metagenomics-based or metabolomics-based function predictions.

Second, we evaluated whether a low dose of Be exposure could affect gut microbial changes and promote MetS. In mice fed a high fat diet (HFD), 30 ppb of Be exposure resulted in significant body weight gain as well as adiposity increase, whereas normal diet groups did not show obvious changes. The shifts in the gut microbial community were caused by the exposure to both 3 ppb and 30 ppb of Be in HFD groups, with the microbial diversity reduction and the significant decrease of *Akkermansia*. *In vitro* human feces culture experiments also showed the reduction of species evenness and MetS-related *Bifidobacterium* due to a low dose of Be. The changes in cecal short chain fatty acids (SCFAs) profiles (increase in acetate, but decrease in propionate and butyrate) in HFD groups were related to appetite increase with a significant decrease in the anorexigenic hormone. Furthermore, the expression of inflammation-related genes and plasma LPS levels significantly increased in HFD groups, showing the evidence of metabolic endotoxemia and low-grade inflammation.

Third, we assessed and compared the effects of two different Ca

supplements, Ca-carbonate and Ca-citrate, on the improvement of host metabolic homeostasis in HFD mice. High concentration of Ca-citrate supplementation showed significant decreases in body weight and MetS-related plasma biomarkers compared to Ca-carbonate groups. Although both Ca-carbonate and Ca-citrate supplementations led to similar changes in gut microbial composition, Ca-citrate groups showed more noticeable differences in the metabolic production of SCFAs, especially propionate, with the increase in anorexigenic GLP-1 gene expression. Also, Ca-citrate groups significantly reduced the expression of inflammatory cytokines, with the increases in the expression of the mucosal barrier function-related genes.

In conclusion, this study indicated that fecal elements were highly associated with MetS, and some elements had strong relationships with gut microbiota. Exposure to Be could affect the changes in gut microbial composition and worsen MetS in HFD mice even at very low concentrations. Ca supplementations effectively helped attenuate MetS with the increase in MetS-suppressing microbiota, and Ca-citrate showed greater improvement in MetS compared to Ca-carbonate. These data suggest that fecal elements analysis will provide important information to understand the relationship between gut microbiota and diseases and further research will be required in the future.

**Keyword:** Metabolic syndrome, gut microbiota, fecal elements, beryllium, calcium

**Student Number:** 2014-30750

# CONTENTS

<b>ABSTRACT</b> .....	<b>i</b>
<b>CONTENTS</b> .....	<b>iv</b>
<b>LIST OF TABLES</b> .....	<b>vi</b>
<b>LIST OF FIGURES</b> .....	<b>vii</b>
<b>LIST OF ABBREVIATIONS</b> .....	<b>xi</b>
<b>CHAPTER I.</b> .....	<b>1</b>
<b>BACKGROUNDS</b>	
Gut Microbiome Research .....	2
Metabolic Syndrome and Gut Microbiome .....	3
Elements and Metabolic Syndrome .....	5
Objectives and Hypotheses .....	8
<b>CHAPTER II.</b> .....	<b>9</b>
<b>ASSOCIATIONS OF FECAL ELEMENTS WITH METABOLIC SYNDROME, HUMAN GUT MICROBIOME, AND THEIR FUNCTION</b>	
Introduction .....	10
Materials and Methods .....	12
Results .....	20
Discussion.....	41

<b>CHAPTER III.</b> .....	<b>46</b>
<b>LOW DOSE OF BERYLLIUM INFLUENCES GUT MICROBIOTA PROMOTING METABOLIC SYNDROME</b>	
Introduction .....	47
Materials and Methods .....	49
Results .....	55
Discussion .....	82
 <b>CHAPTER IV.</b> .....	 <b>89</b>
<b>CALCIUM SUPPLEMENTS IMPROVE HOST METABOLIC HOMEOSTASIS IN HIGH FAT DIET MICE WITH CHANGES IN GUT MICROBIOTA</b>	
Introduction .....	90
Materials and Methods .....	92
Results .....	96
Discussion .....	112
 <b>CHAPTER V.</b> .....	 <b>118</b>
<b>CONCLUSIONS</b>	
 <b>REFERENCES</b> .....	 <b>122</b>
<b>APPENDICES</b> .....	<b>142</b>
<b>국문초록</b> .....	<b>152</b>

# LIST OF TABLES

Table 2.1 Characteristics of the study population. ....	22
Table 2.2 Major fecal element levels of healthy and MetS groups. ....	23
Table 2.3 Fecal trace element levels of healthy and MetS groups. ....	24
Table 2.4 Odds ratios for the association between tertiles of fecal elements and risk of MetS. ....	25

# LIST OF FIGURES

## CHAPTER II

Figure 2.1 Schematic diagram of this study. ....	19
Figure 2.2 Spearman's rank correlation between fecal elements and MetS-related clinical biomarkers. ....	26
Figure 2.3 Differences in the gut microbiota composition between the healthy and MetS groups. ....	30
Figure 2.4 $\alpha$ -diversity indexes according to fecal element status. ....	31
Figure 2.5 Spearman's rank correlation between fecal elements and gut microbiota (genus level). ....	32
Figure 2.6 Multivariate correlation analysis between fecal elements and microbial taxa using MaAsLin. ....	33
Figure 2.7 Correlation network between two fecal elements (Ca and Be) and major microbiota (genus level). ....	34
Figure 2.8 Histograms of the linear discriminant analysis (LDA) scores for differentially abundant gut microbial functions according to fecal (A) Be and (B) Ca status. ....	38
Figure 2.9 Partial least squares discriminant analysis (PLS-DA) of fecal metabolites based on the fecal Be and Ca status. ....	39
Figure 2.10 Overview of metabolite pathway analysis from Be and Ca clustering. ....	40

## CHAPTER III

Figure 3.1 Body weight gain (%) and feed intake over time in the control and Be-exposed mice. ....	57
--	----

Figure 3.2 Weekly water intake and Be exposure from drinking water in ND and HFD mice. ....	58
Figure 3.3 Effect of Be exposure on host metabolism in ND mice. ....	59
Figure 3.4 Effect of Be exposure on host metabolism in HFD mice. ....	60
Figure 3.5 The cecal microbiome composition profiles at the family level in the control and Be-exposed mice fed (A) ND or (B) HFD. ....	64
Figure 3.6 Diversity analysis of the cecal microbial community based on Be exposure in (A) ND and (B) HFD. ....	65
Figure 3.7 Non-metric multidimensional scaling plots of cecal microbiota based on Be exposure in (A) ND and (B) HFD. ....	66
Figure 3.8 Non-metric multidimensional scaling plot of fecal microbiota based on Be exposure over time in HFD mice. ....	67
Figure 3.9 Cecal microbiota perturbation and composition based on Be exposure. ....	69
Figure 3.10 The cultured human fecal microbiome composition profiles at the genus level based on Be concentration. ....	71
Figure 3.11 Diversity analysis of the cultured human fecal microbial community based on Be concentration. ....	73
Figure 3.12 Cultured human fecal microbiota perturbation and composition based on different Be concentration. ....	75
Figure 3.13 Cecal SCFAs profiles based on Be exposure in ND and HFD mice. ....	78
Figure 3.14 mRNA levels of the indicated genes in proximal colons based on Be exposure in HFD mice. ....	79
Figure 3.15 The ratios of Gram-positive / Gram-negative bacteria in (A) <i>in</i>	

<i>in vivo</i> mice experiments and (B) <i>in vitro</i> anaerobic cultivation, and the plasma LPS level based on Be exposure. ....	80
Figure 3.16 Effect of Be and colonic culture with Be on nitrite level. ....	81
Figure 3.17 Possible mechanisms explaining the effects of Be on gut microbiota and MetS. ....	88

## CHAPTER IV

Figure 4.1 Body weight gain (%) and feed intake over time in the control (0.4% Ca) groups and Ca supplementation groups (1.2% Ca) under a high fat diet. ....	97
Figure 4.2 Effect of Ca-carbonate and Ca-citrate supplementation on host metabolism under a high fat diet. ....	98
Figure 4.3 The cecal microbiome composition profiles at the family level with Ca supplementations under a high fat diet. ....	100
Figure 4.4 $\alpha$ -Diversity analysis of the cecal microbial community based on Ca supplementations. ....	101
Figure 4.5 $\beta$ -Diversity analysis of the cecal microbial community based on Ca supplementations. ....	102
Figure 4.6 Cecal microbiota changes and composition based on Ca supplementations. ....	104
Figure 4.7 The ratios of Gram-positive/Gram-negative bacteria based on Ca supplementations. ....	105
Figure 4.8 Cecal SCFAs profiles based on Ca supplementations. ....	108
Figure 4.9 Gene expression for (A) appetite suppression, (B) inflammation, and (C) mucosal barrier function in proximal colons based on Ca	

supplementations. ....	109
Figure 4.10 Plasma LPS level based on Ca supplementation. ....	110
Figure 4.11 Comparison of cecal Ca content between Ca-carbonate and Ca-citrate based on Ca supplementations. ....	111
Figure 4.12 Possible mechanisms explaining the effects of two different Ca supplements on gut microbiota and MetS. ....	117

# LIST OF ABBREVIATIONS

As: arsenic

ALT: alanine transaminase

ANOVA: analysis of variance

AST: aspartate transaminase

BATMAN: Bayesian automated metabolite analyzer for NMR

Be: beryllium

BMI: body mass index

Ca: calcium

CCV: continuous calibration verification

Cd: cadmium

CI: confidence intervals

DBP: diastolic blood pressure

DZ: dizygotic

EDTA: ethylenediaminetetraacetic acid

ELISA: enzyme-linked immunosorbent assay

eWAT: epididymal white adipose tissue

FBInsulin: fasting blood insulin

FBS: fasting blood sugar

FDR: false discovery rate

GC-FID: gas chromatography with flame ionization detector

GLP-1: glucagon-like peptide-1

HDL: high-density lipoprotein cholesterol

HFD: high fat diet

hsCRP: high sensitivity C-reactive protein

IARC: International Agency for Research on Cancer

ICP-MS: inductively coupled plasma mass spectrometry

IQR: interquartile range

IRB: Institutional Review Board

LDA: linear discriminant analysis

LDL: low-density lipoprotein cholesterol

LEfSe: linear discriminant analysis effect size

LPS: lipopolysaccharide

MaAsLin: multivariate association with linear models

MetS: metabolic syndrome

MZ: monozygotic

Na: sodium

ND: normal diet

NMDS: non-metric multidimensional scaling

NMR: nuclear magnetic resonance

NOAEL: no observed adverse effect level

ORs: odds ratios

OSHA: Occupational Safety and Health Administration

OTU: operational taxonomic unit

Pb: lead

PBS: phosphate-buffered saline

PCoA: principal coordinate analysis

PEL: permissible exposure limit

PERMANOVA: permutational multivariate analysis of variance

PICRUST: phylogenetic investigation of communities by reconstruction of unobserved states

PLS-DA: partial least squares discriminant analysis

ppb: parts per billion

ppm: parts per million

PYY: peptide YY

QIIME: quantitative insights into microbial ecology

qPCR: quantitative polymerase chain reaction

RDP: ribosomal database project

SBP: systolic blood pressure

SCFAs: short chain fatty acids

SD: standard deviation

SEM: standard error of the mean

tCholesterol: total cholesterol

TDI: tolerable daily intake

TG: triglyceride

Tl: thallium

TWA: time-weighted average

VIP: variable importance of projection

WHO: World Health Organization

Zn: zinc

**CHAPTER I.**

**BACKGROUNDS**

## Gut Microbiome Research

Humans are associated in a symbiotic relationship with up to  $10^{14}$  microorganisms. The majority of these host-associated microbes reside within the gastrointestinal tract and have extraordinary metabolic potential, playing a pivotal role in human health<sup>(1)</sup>. The gut microbiota enhances the host's response to pathogen invasion, modulates host gene expression and immune response, and ultimately influences overall health<sup>(2)</sup>. Normal inhabitants of the gastrointestinal tract facilitate the metabolism of polysaccharides consumed by the host<sup>(3)</sup>, and interactions between microbes within the microbiota enhance this metabolic potential, further improving polysaccharide utilization<sup>(4)</sup>. Other health-supporting functions of gut microorganisms include disease protection through immunomodulation as has been shown for *Bifidobacterium longum*, which strongly stimulates the production of interleukin-10 and proinflammatory cytokines, including TNF- $\alpha$  that protects the host against tumor proliferation<sup>(5)</sup>. Furthermore, *Bifidobacterium* and other lactic acid bacteria often produce exopolysaccharides, complex polymers that can be used as fermentable substrates by other gut microbes aiding in microbial community structure and stability<sup>(6)</sup>.

Compositional perturbations of the microbiota (dysbiosis) have been associated with diseases, including obesity, diabetes, colorectal cancer, and allergies<sup>(7,8)</sup>. Hence, maintaining compositional and functional stability within the gut microbiome is essential to host health, as demonstrated by dysbiosis detected at the onset of nonpathogenic chronic diseases such as Crohn's disease, where the gut microbiome had a significant decrease in

beneficial *Bifidobacteriaceae* populations while exhibiting an increase in groups containing potential pathogens, including *Enterobacteriaceae*, *Pasteurellaceae*, *Fusobacteriaceae*, and *Neisseriaceae*<sup>(9)</sup>.

Current high-throughput sequencing technologies provide important information about the composition and functionality of the gut microbiome. However, to better understand mechanistic interactions between the gut microbiota and its host and the importance of the gut microbiome in maintaining health, it is critical to explore new research approaches and integrate several emerging omics technologies such as metabolomics, meta-transcriptomics, meta-proteomics, and culturomics<sup>(10)</sup>.

## **Metabolic Syndrome and Gut Microbiome**

Metabolic syndrome, which consists of the obesity-related metabolic abnormalities that lead to high risk of developing type 2 diabetes and cardiovascular disease, has been increasingly prevalent globally, indicating that approximately 20-30% of adults are suffering from MetS all over the world<sup>(11-13)</sup>. Although the high incidence of MetS is generally thought to result from the excessive nutrient intake and reduced physical activity<sup>(14,15)</sup>, lots of studies suggest a possible role of gut microbiota in MetS<sup>(16-21)</sup>.

Comparisons between obese and lean individuals have demonstrated that obese individuals have increased levels of Firmicutes and reduced levels of Bacteroidetes<sup>(22)</sup>. Similar alterations were observed in obese versus lean mice<sup>(16)</sup>, suggesting that the microbiota may contribute to the pathogenesis of obesity. The consensus is that obesity is associated with

reduced microbial diversity<sup>(23)</sup>. Metagenomic analysis has revealed increased harvest of energy from indigestible carbohydrates in the microbiome of obese mice, clarifying the role of an altered microbiota in obesity<sup>(17)</sup>. Similar findings were observed upon transfer of fecal samples from twins discordant for obesity, and cohousing of lean and obese recipient mice resulted in the invasion of *Bacteroides sp.* from the lean to the obese animals, which prevented the development of obesity in a diet-dependent fashion<sup>(19)</sup>. The use of germ-free mice allows the interactions between diet and the microbiota, and the underlying mechanisms of the development of obesity, to be investigated in detail. Germ-free mice are resistant to diet-induced obesity when fed a western diet, which is rich in saturated fat and sucrose, despite a similar level of food intake compared to conventionally raised animals<sup>(24,25)</sup>.

Type 2 diabetes in humans was also associated with a reduced abundance of butyrate-producing bacteria and an increased abundance of *Lactobacillus sp.*<sup>(26-28)</sup>. Computational models based on the gut metagenome were able to predict type 2 diabetes-associated phenotype in patients with impaired glucose tolerance, suggesting that the gut microbiome may constitute a novel biomarker for prediction of type 2 diabetes. Vancomycin treatment in patients with metabolic syndrome reduced the abundance of Gram-positive bacteria, such as butyrate-producing bacteria; this was associated with reduced insulin sensitivity, suggesting that the decreased levels of butyrate-producing bacteria observed in patients with type 2 diabetes may contribute to disease<sup>(29)</sup>. In a landmark study, Vrieze et al. used fecal microbiota transplantation from lean donors to insulin-resistant patients with metabolic syndrome and demonstrated that feces from lean

subjects, but not autologous transplantation, improved insulin sensitivity and was associated with enhanced numbers of butyrate-producing bacteria<sup>(30)</sup>. Thus, there are accumulating evidence to suggest that the microbiome may directly modulate insulin sensitivity in humans. However, how the microbiota modulates host glucose metabolism remains unclear. Therefore, more mechanistic studies are warranted.

*Akkermansia muciniphila*, which exhibits mucin-degrading properties and has attracted considerable attention, was found to be enriched in a Chinese cohort of patients with type 2 diabetes<sup>(27)</sup>. However, this finding was not corroborated in a European cohort<sup>(28)</sup>. Instead, in a European population, it was demonstrated that obese individuals with less severe metabolic syndrome had increased levels of *A. muciniphila* and this was associated with increased microbial diversity compared with subjects with more impaired metabolic status<sup>(31)</sup>. Thus, there may be population-specific associations between *A. muciniphila* and type 2 diabetes. Supplementation with *A. muciniphila* in diet-induced obese mice reduced circulating lipopolysaccharide (LPS) levels and enhanced lipid oxidation<sup>(32)</sup>, and was related to improved glucose tolerance and reduced inflammation<sup>(33)</sup>.

## Elements and Metabolic Syndrome

Elements including essential minerals and metals play an important part in biological functions in human<sup>(34)</sup>. An excess of toxic trace elements or a deficiency of essential minerals has been linked with chronic MetS. Globally, high levels of arsenic in water supplies have been associated with

increased incidence of type 2 diabetes<sup>(35-37)</sup>. Mechanistic studies suggest arsenic may impair insulin secretion from pancreatic beta cells and induce changes in gene expression affecting pancreatic insulin secretion and insulin resistance in peripheral tissues<sup>(38)</sup>. While a diabetogenic effect of another metal, cadmium, was noted in rats exposed neonatally<sup>(39)</sup>, and suggestive evidence on fasting glucose levels in humans was reported<sup>(40)</sup>, no mechanism of action has been identified. Also, the increased plasma lead levels are related to hypertension and peripheral vascular disease. On the other hand, calcium or zinc supplementation can reduce body weight and improve host adiposity<sup>(41-44)</sup>.

The composition, diversity and enzymatic capacities of the gut microbiota are readily affected by various environmental factors, and several metals have also been shown to inhibit gut bacterial growth or to induce dysbiosis *in vitro* and *in vivo*. In mice supplied with cadmium-containing drinking water, a sharp decrease in the populations of all microbial species was observed<sup>(45)</sup>. Breton et al. also reported minor but specific changes in the composition of the colonic microbiota at the family and genus levels, following chronic treatment with cadmium and lead in mice. Heavy metal-consuming animals had smaller numbers of Lachnospiraceae and larger numbers of Lactobacillaceae and Erysipelotrichaceae than control animals<sup>(46)</sup>. Exposures to these heavy metals were subtoxic and not associated with hepatotoxicity, changes in behavior, organ and body weights, food intake, stool consistency or gut motility. However, a low number of Lachnospiraceae has been previously linked to intestinal inflammation and suggested as a predisposition to colitis<sup>(47)</sup>. Similarly, 4-week arsenic treatment induced a significant decrease

in mouse fecal populations of Firmicutes, but not in Bacteroidetes. These taxonomic changes were associated with an alteration of the metabolic activity of the gut microbiome as demonstrated by the variation of some microbial co-metabolites, such as indole derivatives, observed in urine or feces of exposed animals<sup>(48)</sup>.

## **Objectives and Hypotheses**

### **Objectives:**

The objectives of this study were 1) to assess the associations of fecal elements with metabolic syndrome, human gut microbiome and their function, 2) to determine whether low dose of beryllium could impact gut microbiota promoting metabolic syndrome, and 3) to evaluate and compare the effects of two different calcium supplements on the improvement of host metabolic homeostasis with changes in gut microbiota.

### **Hypothesis 1**

Fecal elements analysis from human feces will reflect individual exposure to each element.

### **Hypothesis 2**

Some fecal elements will affect the gut microbial composition and their metabolic function.

### **Hypothesis 3**

Metabolic syndrome will be influenced by gut microbiota or their metabolites.

**CHAPTER II.**

**ASSOCIATIONS OF FECAL ELEMENTS  
WITH METABOLIC SYNDROME, HUMAN  
GUT MICROBIOME, AND THEIR  
FUNCTION**

### **Introduction**

Metabolic syndrome (MetS), which consists of the obesity-related metabolic abnormalities that lead to high risk of developing type 2 diabetes and cardiovascular disease, has been increasingly prevalent globally, indicating that approximately 20-30% of adults are suffering from MetS all over the world<sup>(11-13)</sup>. Although the high incidence of MetS is generally thought to result from the excessive nutrient intake and reduced physical activity<sup>(14,15)</sup>, lots of studies suggest a possible role of gut microbiota in MetS<sup>(16-21)</sup>. Especially, the results from recent works indicate that the effects of dietary intake on the gut microbiome can surpass the genetic factors and immune response of individuals, emphasizing the crucial role of external factors such as diet, antibiotics, drugs, and environmental chemicals<sup>(20,21,49,50)</sup>.

Elements including essential minerals and metals play an important part in biological functions in human<sup>(34)</sup>. An excess of toxic trace elements or a deficiency of essential minerals has been linked with chronic MetS. Arsenic (As) exposure has been associated with diabetes or cardiovascular disease, and the increased plasma lead (Pb) levels are related to hypertension and peripheral vascular disease<sup>(36,51,52)</sup>. On the other hand, calcium (Ca) or zinc (Zn) supplementations can reduce body weight and improve host adiposity<sup>(41-44)</sup>.

Some studies suggest that the exposure to certain elements such as As, Cd, and Na can disturb intestinal microbiota and result in metabolic disorders<sup>(48,53-55)</sup>. Given that much of the elements are excreted in feces rather than absorbed into the host via the digestive tract<sup>(56)</sup>, and the close links between MetS and gut microbiota have recently been highlighted, we

hypothesized that the effects of elements on the MetS might be caused by the changes in gut microbiota. However, most elements studies have been conducted on the host side, and some approaches that consider the link between elements and gut microbiome were performed on animals, not on humans.

Thus, to elucidate the association of various elements with human gut microbiome and MetS status, we analyzed 29 fecal elements from Korean twins cohort that we had already used for the microbiome analysis in our previous study<sup>(57)</sup>. We then performed the correlation study between fecal elements, MetS, and gut microbiota. In addition, we evaluated the relationship of MetS-related fecal elements with the microbial functions based on both 16S rRNA gene sequences and fecal metabolites profiles obtained from NMR spectroscopy.

### **Materials and Methods**

**Subjects.** This study was approved by the Institutional Review Board of the Seoul National University (IRB No. 144-2011-07-11) and was performed by the principle of the Helsinki Declaration. Written informed consent was obtained from each participant. A total of 304 individuals from participants enrolled in the Healthy Twin Study in Korea<sup>(58)</sup> were selected for this study. The fecal samples from the participants were collected at home and immediately frozen in a home freezer, followed by transfer to clinics and stored at -80 °C until analysis. All participants were questionnaires covering lifestyle, medication, disease history, biochemical tests, and anthropometrical measurements. Demographic characteristics of the study subjects are shown in Table 2.1.

### **Measurements of MetS components and definition of MetS.**

Measurements of waist circumference, blood pressure, triglyceride, HDL cholesterol, and fasting blood sugar (FBS) have been previously published<sup>(57)</sup>. MetS was defined following the revised National Cholesterol Education Program Adult Treatment Panel III criteria<sup>(59)</sup> with the Korean-specific waist circumference cut-off values for abdominal obesity<sup>(60)</sup>. The subjects were considered to have MetS if they had three or more of the following five criteria: (1) waist circumference  $\geq 90$  cm in men or  $\geq 85$  cm in women, (2) blood pressure  $\geq 130/85$  mm Hg, (3) triglycerides  $\geq 150$  mg/dL (1.7 mmol/L), (4) HDL cholesterol  $<40$  mg/dL (1.03 mmol/L) in men or  $<50$  mg/dL (1.3 mmol/L) in women, and (5) FBS  $\geq 100$  mg/dL (5.6 mmol/L).

**16S rDNA amplicon sequence analysis.** DNA was extracted using a QIAamp DNA Stool Mini Kit (Qiagen, USA) with the additional bead-beating procedure to improve the DNA recovery for Gram-positive bacteria. The 16S rRNA genes were amplified using the Illumina-adapted universal primers 515F/806R for the V4 region. PCR products were purified using a MO BIO UltraClean PCR Clean-Up Kit (MO BIO Laboratories, Carlsbad, CA, USA) and quantified using a KAPA Library Quantification kit (KAPA Biosystems, Woburn, MA, USA). Sequencing was conducted on the MiSeq platform using a paired-end 2 × 300-bp reagent kit (Illumina, San Diego, CA, USA). Sequences generated from the MiSeq run were analyzed using QIIME software (V1.8.0) and were clustered into 97% identity using an open-reference operational taxonomic unit (OTU) picking protocol against the 13\_5 revision of the Greengenes database<sup>(61)</sup>. The taxonomy assignments for OTUs were based on the Greengenes reference sequence using the RDP classifier. Unclassified taxa at each taxonomic level were excluded from the analysis. The R package “vegan” was used to calculate Chao1 measure, Simpson and Shannon index for  $\alpha$ -diversity (diversity within populations) analysis from the resulting tables of OTU counts. The OTU tables were subsequently converted to relative abundance table.

**Pretreatment for fecal elements determination.** The inductively coupled plasma mass spectrometry (ICP-MS) calibration standard solutions were prepared from 10 mg/L multi-element standard solution (PerkinElmer, Waltham, MA, USA). The standard calibration solutions were prepared by dilution of the standard solutions with a suitable percentage of analytical grade concentrated HNO<sub>3</sub> (Dongwoo Fine Chem.Co., Ltd., Korea). De-

ionized water (18.2 M $\Omega$ -cm) was prepared by a Milli-Q water purification system (Millipore, Bedford, MA, USA). All chemicals and reagents used in this study were obtained from Sigma (St. Louis, MO, USA) and of analytical reagent grade unless otherwise stated. Before use, all plastic and glassware were soaked in 10% nitric acid for at least 24 h and then rinsed with deionized water several times. To measure the total metal concentration in the samples, microwave-assisted acid digestion was performed. Fecal samples (~0.5 g) were weighed directly into quartz microwave digestion tubes, and 4.0 mL concentrated HNO<sub>3</sub> was added. The 1.5 kW microwave was applied to reach 230°C for 20 min and the temperature was maintained during 15 min with a microwave digestion system (Ultrawave, Milestone srl, Italia), followed by allowing cooling without a microwave. The contents of the tubes were then transferred to polypropylene tubes and diluted to 50.0 g with deionized water. Sample blanks were prepared by following the above procedure.

**Fecal elements analysis with ICP-MS.** ICP-MS measurements were performed using a quadrupole ELAN DRC-e spectrometer (Perkin-Elmer SCIEX, Norwalk, CT, USA), equipped with a concentric nebulizer (Meinhard Associates, Golden, CO, USA), a cyclonic spray chamber (Glass Expansion, Inc., West Melbourne, Australia), a quartz torch with a quartz injector tube (2 mm i.d.), and an autosampler (AS-93 Plus, Perkin-Elmer) for the simultaneous determination of metals. The following operational conditions were used: radiofrequency power of 1.4 kW and plasma, auxiliary, and nebulizer gas flow rate of 16, 1.2, and 0.9 L/min, respectively. Quality control was conducted throughout the sample analysis. Quantitative

analysis of the sample was performed by external calibration. To monitor the consistency of the instruments, the calibration standards were analyzed as samples regularly. Continuous calibration verification (CCV) standard solutions were measured after every ten samples. Data were accepted only when CCV samples were 90–110% of the expected value. Deionized water blanks were also analyzed at regular intervals to check for cross-contamination or losses.

**NMR-based metabolomic analysis.** For NMR-based metabolomic analysis, samples were prepared according to Lamichhane's method with a slight modification<sup>(62)</sup>. Briefly, human fecal samples (~200 mg) were mixed with 1000  $\mu\text{L}$  DDW, vortexed for 30 s and homogenized by tissue homogenizer for 5 min. After centrifugation (14,000 g, 4°C) for 10 min, 300  $\mu\text{L}$  of supernatant was mixed with 60  $\mu\text{L}$  of deuterium oxide ( $\text{D}_2\text{O}$ ) containing 0.025 mg/mL 3-(trimethylsilyl) propionic acid-d<sub>4</sub> sodium salt, 60  $\mu\text{L}$  of 1 mM imidazole, 60  $\mu\text{L}$  of 2 mM  $\text{NaN}_3$ , and 120  $\mu\text{L}$  of 0.5 M  $\text{KH}_2\text{PO}_4$ . The mixtures were vortexed for 1 min and centrifuged at 14,000 g for 10 min. The clear supernatant was then transferred to a 5 mm NMR tube (Wilmad-Lab glass, UK) for NMR analysis. All  $^1\text{H}$ -NMR spectra were acquired using a Varian 500 MHz NMR system (Varian, Palo Alto, CA, USA) spectrometer equipped with a cold flow-probe.  $^1\text{H}$ -NMR spectra were collected at 25°C using the water presaturation pulse sequence. Spectra were collected with 64 transients using a 4 s acquisition time and a 2 s recycle delay. Tentative assignments of  $^1\text{H}$  NMR signals were carried out using the Bayesian automated metabolite analyzer for NMR (BATMAN) and confirmed by Chenomx NMR Suite 8.3 (Chenomx, Canada) according to

the Human Metabolome Database and the previous literature<sup>(63,64)</sup>. A total of 67 metabolites (acetate, acetoin, alanine, arginine, aspartate, betaine, butyrate, cadaverine, carnitine, carnosine, cholate, choline, creatine, cysteine, folate, formate, fructose, fucose, fumarate, galactose, glucose, glutarate, glyceraldehyde, glycerol, glycine, heptanoate, histamine, histidine, hypoxanthine, indole, indoxyl sulfate, isobutyrate, isoleucine, isovalerate, lactate, leucine, lysine, malate, malonate, mannose, methionine, methyl succinate, N-acetylglutamate, N-acetylneuraminate, proline, propionate, purine, putrescine, pyrimidine, pyruvate, ribose, sarcosine, succinate, threonine, thymine, trimethylamine, trimethylamine oxide, tryptophan, tyrosine, uracil, urocanate, valerate, valine, xanthine, xylose,  $\gamma$ -aminobutyrate,  $p$ -cresol) were assigned for analysis. The metabolomic data were imported into MetaboAnalyst 4.0 and normalized for multivariate pattern recognition analysis<sup>(65,66)</sup>. Partial least squares discriminant analysis (PLS-DA) was performed to obtain an overview of the complete metabolomic data set after mean centering scaling. Variable importance of projection (VIP) scores were assessed to rank the differential metabolites among each element status.

**Functional analysis.** Phylogenetic investigation of communities by reconstruction of unobserved states (PICRUSt) was used to infer putative functional metagenomes from 16S rDNA sequence profiles<sup>(67)</sup>. As the tool adapts OTUs with Greengene IDs, OTUs were picked with closed reference against May 2013 Greengenes database. The relative abundance of each functional pathway was obtained for each sample, and non-microbial functional pathways belonging to the ‘Organismal Systems’ and ‘Human

Diseases' categories were excluded from downstream analysis. To determine metabolic features that were differentially abundant between each element status (low and high level), linear discriminant analysis effect size (LEfSe) was applied under the condition  $\alpha = 0.05$ , with the linear discriminant analysis (LDA) score of at least two<sup>(68)</sup>. The data for metabolites concentrations from low and high level group of each element status were integrated to a MetaboAnalyst module for the analysis of the relevant pathways. Pathway enrichment analysis and pathway topology analysis are used to identify and visualize the matched metabolites from the datasets. The pathway impact represented the deviation of metabolic pathways between the two groups based on the position of metabolites. Log P reflected the deviation of metabolic pathways between the two batches based on the concentration of metabolites. The overall flow of the analyses is shown in Figure 2.1.

**Statistical analysis.** Each fecal element concentration was classified into tertiles for the analysis of odds ratios (ORs), microbial  $\alpha$ -diversity, and metabolic function. ORs and their 95% confidence intervals (CI) were computed for the second (middle level) and third tertile (high level) of each element with the first tertile (low level) as the reference. Logistic regression models were used in the calculation of multivariate-adjusted ORs, adjusted for age, sex, and smoking. The association between food intake data of four major dietary elements (Ca, P, K, and Na) and their fecal measurement data was analyzed by Spearman rank correlation analysis. The average daily intake of Ca, P, K, and Na was estimated from nutrition survey data (N=275). Association of fecal elements with MetS-related clinical

biomarkers and gut microbiota was assessed by Spearman's rank correlation analysis. A correlation heatmap was generated using the R package "Pheatmap". *P*-values were adjusted for multiple testing with the Benjamini-Hochberg method. Multivariate analysis using a multivariate association with linear models (MaAsLin) was performed to identify significant associations of microbial abundances with metabolic status or fecal elements status<sup>(69)</sup>. In the analysis, age, sex, and smoke were treated as fixed effects, and MZ, DZ twin, and family relationships were treated as random variables. Low abundance taxa (the average relative abundance across all the samples < 0.1%) were excluded from MaAsLin analysis. Co-occurrence network was visualized with Cytoscape 3.6.1 software if the  $|\text{Spearman's rank correlation coefficient}| > 0.15$ . Mediation analysis was performed to assess both the direct effects of specific fecal elements and their indirect effects through gut microbiota on MetS using the R package "mediation".

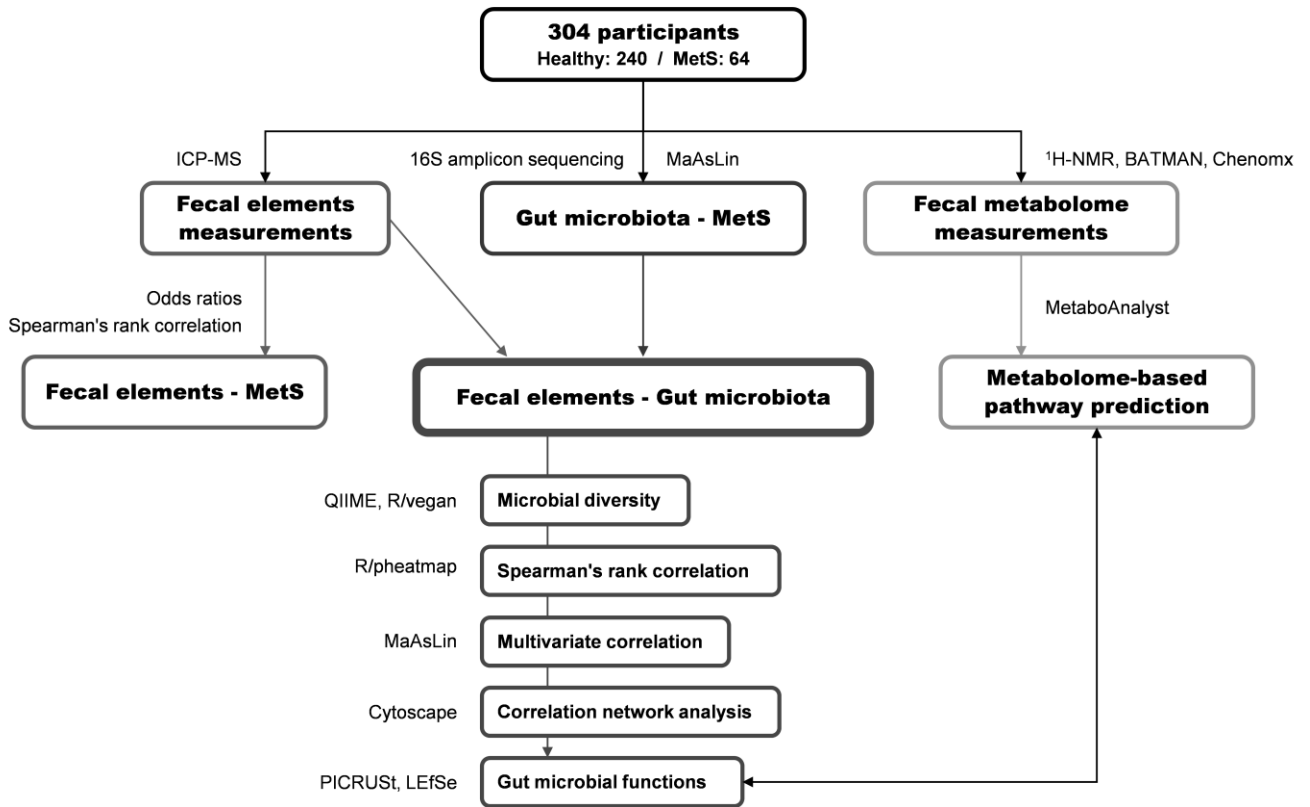


**Figure 2.1 Schematic diagram of this study.**

### **Results**

#### **Associations of fecal elements with clinical MetS indices**

We obtained human fecal samples and clinical metadata from 304 participants who were included in our previous study<sup>(57)</sup>. The subjects that conform to the MetS criteria were 21.1% of the total, 14.5% of MZ twins, 19.1% of DZ twins, and 29.4% of family members (Table 2.1). To assess the relationships between fecal elements and Met status, we measured the content of 29 elements from human feces. The elements were divided into two groups, major fecal elements group (Ca, P, K, Mg, S, and Na) and trace elements group (Fe, Zn, Al, Mn, Sr, Cu, Ti, Ba, Rb, Cr, Ga, As, Se, Cd, Co, V, Pb, U, Li, Cs, Bi, Tl, and Be) according to the relative abundance (1%) for the entire 29 elements (Table 2.2 and Table 2.3). Ca was the most abundant fecal element in the healthy group, whereas K was the highest in the MetS group. Total elements concentration was higher in the healthy group (~13,938 µg/g) compared to the MetS group (~11,381 µg/g). The average relative abundance values of K, Mg, S, Na, Al, Ti, Rb, Cr, As, Se, Cd, Co, Pb, Tl, and Be were higher in the MetS group than the healthy group.

We then stratified the healthy and MetS groups into tertiles of elements and calculated the ORs of MetS for each element using the low tertile of each element as a reference. The ORs of all elements were shown in Appendix A. Among 29 elements, Be, Ca, and Tl had the significant ORs, and the ORs were adjusted for age, sex, and smoking. Because Ca was already known to be associated with MetS, Be and Tl were additionally adjusted for MetS-related Ca (Table 2.4). The similar tendency was observed even after the adjustment. Be and Tl showed a significant increase

in ORs of MetS in the high tertile, whereas Ca had a noticeable decrease in ORs of MetS in the high tertile, indicating the possible link between the three elements and MetS.

To further investigate the fecal elements associated with MetS status, we analyzed the correlations between 29 fecal elements and each MetS-related indices, including HDL cholesterol (HDL), total cholesterol (tCholesterol), LDL cholesterol (LDL), BMI, triglyceride, uric acid, aspartate transaminase (AST), alanine transaminase (ALT), waist circumference (Waist), FBS, systolic and diastolic blood pressure (SBP and DBP), high sensitivity C-reactive protein (hsCRP), and fasting blood insulin (FBInsulin), using Spearman's rank correlation test (Figure 2.2). When the fecal elements were arranged in order of correlation with MetS, the three elements (Be, Tl, and Ca) also showed the strong correlation with MetS compared to other elements. Some single MetS-related biomarkers such as BMI, AST, ALT, Waist, hsCRP, and FBInsulin still had a significant positive correlation with Be or Tl. On the contrary, Ca showed a significant negative correlation with BMI, Waist, FBS, and SBP biomarkers. Thus, we concluded that some fecal elements could be associated with MetS status.

**Table 2.1 Characteristics of the study population.**

Characteristics	All participants	Family relationships		
		MZ twins	DZ twins	Non-twin
N	304	138	47	119
Age (years)	45.6 ± 13.6	41.9 ± 7.6	42.5 ± 8.0	52.0 ± 12.5
Sex:				
Males	166 (54.6)	70 (50.7)	29 (61.7)	67 (56.3)
Females	138 (45.4)	68 (49.3)	18 (38.3)	52 (43.7)
Smoking:				
Never	174 (57.2)	79 (57.2)	25 (53.2)	70 (58.8)
Ever	130 (42.8)	59 (42.8)	22 (46.8)	49 (41.2)
Waist ≥ 90 (M) or 85 (F) cm	80 (26.3)	33 (23.9)	7 (14.89)	40 (33.6)
BP ≥ 130/85 mm Hg	51 (16.8)	20 (14.5)	11 (23.4)	20 (16.8)
Triglyceride ≥ 150 mg/dL	95 (31.3)	39 (28.3)	13 (27.7)	43 (36.1)
HDL < 40 (M) or 50 (F) mg/dL	126 (41.4)	56 (40.6)	14 (29.8)	56 (47.1)
FBS ≥ 100 mg/dL	83 (27.3)	33 (23.9)	10 (21.3)	40 (33.6)
MetS <sup>a</sup>	64 (21.1)	20 (14.5)	9 (19.1)	35 (29.4)

Abbreviations: BP, blood pressure; DZ, dizygotic; F, female; FBS, fasting blood sugar; HDL, high-density lipoprotein cholesterol; M, male; MetS, metabolic syndrome; MZ, monozygotic; Non-twin, parents or siblings of twin pairs; waist, waist circumference. Values are mean ± SD or *n* (%)

<sup>a</sup>Abnormal values for at least three of the following: waist, BP, triglyceride, HDL, and FBS.

**Table 2.2 Major fecal element levels of healthy and MetS groups.**

	Concentration in feces <sup>a</sup>		Relative abundance	
	(µg/g fresh weight)		(%)	
	Healthy (N=240)	MetS (N=60)	Healthy	MetS
Ca	3,544.50±319.90	2,524.78±471.85	23.81±0.98	20.95±1.83
P	3,313.14±274.19	2,564.05±433.49	22.22±0.60	21.18±1.22
K	2,830.60±145.30	2,665.27±281.34	22.18±1.11	24.51±2.38
Mg	1,874.98±143.13	1,554.02±192.66	13.31±0.51	14.07±1.08
S	1,643.87±99.38	1,389.50±181.83	12.01±0.38	12.43±0.76
Na	415.72±46.55	433.83±124.63	4.25±0.66	4.71±1.38

Values are mean ± 95% confidence interval.

<sup>a</sup>Major and trace elements groups were separated on the basis of the relative abundance (1%) for the entire 29 elements.

**Table 2.3 Fecal trace element levels of healthy and MetS groups.**

	Concentration in feces (µg/g fresh weight)		Relative abundance (%)	
	Healthy (N=240)	MetS (N=60)	Healthy	MetS
Fe	88.8065±9.8438	61.7571±10.0764	0.6006±0.0449	0.5329±0.0493
Zn	88.6187±9.0036	63.1448±12.3407	0.5909±0.0371	0.5226±0.0529
Al	49.2368±9.1496	48.8734±18.4176	0.3466±0.0619	0.4351±0.1430
Mn	41.8780±3.4949	30.6845±4.6193	0.2893±0.0153	0.2669±0.0216
Sr	23.0480±2.7183	17.2947±3.1959	0.1536±0.0105	0.1531±0.0210
Cu	12.1870±1.0478	9.5266±1.6482	0.0843±0.0045	0.0840±0.0085
Ti	7.8892±1.4896	6.9829±2.7542	0.0536±0.0095	0.0579±0.0199
Ba	6.1758±0.6408	4.8304±1.0635	0.0427±0.0037	0.0399±0.0052
Rb	5.4851±0.3358	4.8045±0.5533	0.0414±0.0020	0.0437±0.0039
Cr	0.3499±0.0331	0.3030±0.0647	0.0025±0.0002	0.0028±0.0005
Ga	0.2737±0.0328	0.2006±0.0436	0.0019±0.0002	0.0017±0.0002
As	0.2608±0.0344	0.3096±0.1117	0.0020±0.0003	0.0031±0.0012
Se	0.2508±0.0246	0.2259±0.0485	0.0017±0.0001	0.0020±0.0003
Cd	0.1678±0.0192	0.1720±0.0502	0.0012±0.0001	0.0015±0.0004
Co	0.1415±0.0116	0.1507±0.0412	0.0010±0.0001	0.0013±0.0004
V	0.1311±0.0152	0.1066±0.0322	0.0009±0.0001	0.0009±0.0002
Pb	0.1233±0.0139	0.1299±0.0379	0.0009±0.0001	0.0013±0.0004
U	0.0485±0.0097	0.0362±0.0125	0.0003±0.0001	0.0003±0.0001
Li	0.0273±0.0047	0.0202±0.0048	0.0002±0.0000	0.0002±0.0000
Cs	0.0159±0.0015	0.0154±0.0034	0.0001±0.0000	0.0001±0.0000
Bi	0.0130±0.0065	0.0041±0.0023	0.0001±0.0000	0.0001±0.0000
Tl	0.0075±0.0008	0.0079±0.0017	0.0001±0.0000	0.0001±0.0000
Be	0.0040±0.0005	0.0047±0.0010	< 0.0001	< 0.001

Values are mean ± 95% confidence interval.

**Table 2.4 Odds ratios for the association between tertiles of fecal elements and risk of MetS.**

<b>Fecal elements<sup>a</sup> (tertile status)</b>	<b>Healthy (N=240)</b>	<b>MetS (N=64)</b>	<b>ORs<sup>b</sup> (95% CI)</b>	<b>Adjusted ORs<sup>c</sup> (95% CI)</b>	<b>p value<sup>d</sup></b>
Be:					
Low	87 (36.2%)	14 (21.9%)	reference	reference	reference
Middle	81 (33.8%)	20 (31.2%)	1.53 (0.72, 3.30)	2.09 (0.96, 4.71)	0.069
High	72 (30.0%)	30 (46.9%)	2.56 (1.28, 5.36)	2.53 (1.17, 5.90)	*0.022
Ca:					
Low	74 (30.8%)	27 (42.2%)	reference	reference	reference
Middle	79 (32.9%)	22 (34.4%)	0.77 (0.40, 1.46)	0.76 (0.39, 1.48)	0.424
High	87 (36.2%)	15 (23.4%)	0.48 (0.23, 0.95)	0.45 (0.21, 0.94)	*0.037
Tl:					
Low	84 (35.0%)	17 (26.6%)	reference	reference	reference
Middle	86 (35.8%)	15 (23.4%)	0.86 (0.40, 1.85)	1.59 (0.72, 3.53)	0.250
High	70 (29.2%)	32 (50.0%)	2.24 (1.16, 4.47)	2.59 (1.16, 6.01)	*0.023

<sup>a</sup>The fecal elements that indicated a significant odds ratios (ORs) were selected and represented. Appendix A shows the crude ORs of all elements. <sup>b</sup>The low, middle, and high level groups of each element were determined using the tertile values. The low tertile of each element was utilized as a reference. <sup>c</sup>Adjusted for age, sex, and smoking. Be and Tl were additionally adjusted for Ca, already known to be associated with MetS. <sup>d</sup>The significant values ( $P < 0.05$ ) were marked with an asterisk (\*).

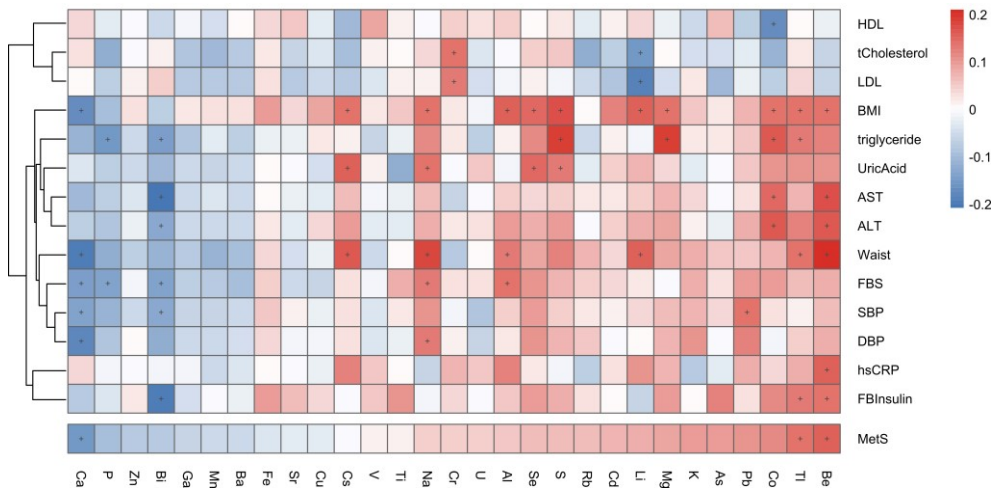


**Figure 2.2 Spearman’s rank correlation between fecal elements and MetS-related clinical biomarkers.**

Fecal elements were arranged in order of correlation with MetS. Asterisks represent significant associations at FDR adjusted *P* values of < 0.2 (N=304).

### **Associations of fecal elements with human gut microbial populations**

Before the correlation analysis between fecal elements and gut microbiota, we evaluate the MetS-related gut microbial taxa from 304 individuals in our study using MaAsLin analysis with adjustments for age, sex, smoke, identical twin, and family relationships (Figure 2.3). In genus taxa level, *Sutterella* and *Dorea* were increased in MetS group, while *Faecalibacterium*, *Bifidobacterium*, *Subdoligranulum*, *Eubacterium*, *Akkermansia*, *Odoribacter*, and *Rothia* were overrepresented in the healthy group. The positive correlation of *Sutterella* and the negative correlation of *Bifidobacterium*, *Akkermansia*, and *Odoribacter* with MetS were the same results with our previous study<sup>(57)</sup>, indicating that the decrease in the total number of samples (from 655 to 304) might not affect the microbial properties within the groups.

We next examined whether certain elements could affect the  $\alpha$ -diversity in the microbial community such as Chao1 richness, Simpson and Shannon indexes (Figure 2.4). When the diversity analysis was carried out based on the tertile levels of each element, some elements have shown a significant reduction in microbial diversity. Simpson and Shannon diversity indexes, which indicates species evenness, were significantly decreased in the high tertile of Be and Tl elements. K also showed a similar decreasing pattern in the Simpson diversity index.

To assess the overall correlation between fecal elements and gut microbiota, we filtered microbial taxa by excluding low-abundance taxa (< 0.1% of mean relative abundance) and calculated Spearman's rank correlation coefficient between 29 fecal elements and 29 gut microbiota genera (Figure 2.5). Some elements were clearly grouped in a separate

cluster, indicating that there might be a robust link between certain fecal elements and the shaping of the gut microbiota community. For example, K and Na had a negative correlation with *Bacteroides*, known as one of the representative three enterotypes<sup>(70)</sup>, and a positive correlation with *Prevotella*, one of another enterotype. On the other hand, Ca and P showed the strong positive correlation with *Bacteroides* along with negative correlation with *Prevotella*. Especially, the four genera (*Akkermansia*, *Bifidobacterium*, *Odoribacter*, and *Parabacteroides*) which showed a significant abundance in the healthy group in our previous study<sup>(57)</sup> were positively associated with Ca. Moreover, Be element had a strong positive correlation with *Sutterella*, the most significantly increased genera from MetS group in our study, and a robust negative correlation with both *Akkermansia* and *Bifidobacterium*, which were reported to attenuate MetS, respectively<sup>(6,31,32)</sup>.

To confirm the association by multivariate analysis, MaAsLin analysis was performed for fecal Be, Ca, and Tl with the adjustments for age, sex, smoke, MZ and DZ twin, and family relationship. Appendix B shows all significant associations of microbial genera with Be, Ca, and Tl. The results from Appendix B and Figure 2.6 indicated that MetS-related gut microbial genera such as *Akkermansia*, *Bifidobacterium* were still significantly associated with Be and Ca after the adjustment. However, Tl showed no significant association with those genera after the multivariate analysis. To visualize the microbial interaction by Be and Ca, we performed network analysis (Figure 2.7) using Cytoscape. *Akkermansia* and *Bifidobacterium* worked as one of the hubs having linkers for both Be and Ca. Two elements showed the opposite correlation with *Akkermansia* and *Bifidobacterium*.

We performed a mediation analysis to evaluate both the direct effects of specific fecal elements and their indirect effects through gut microbiota on MetS (Figure 2.8). The effects of Be on MetS was highly affected by the *Akkermansia* (10.22%) and *Bifidobacterium* mediator (33.08%), while the mediation effect of the two microbiota in Ca analysis indicated 9.99% and 5.42%, respectively. These results showed that Ca has a more direct effect on metabolic syndrome, apart from gut microbiota, compared to Be. The effects of Be on MetS was nearly affected by the *Sutterella* mediator (1.11%).

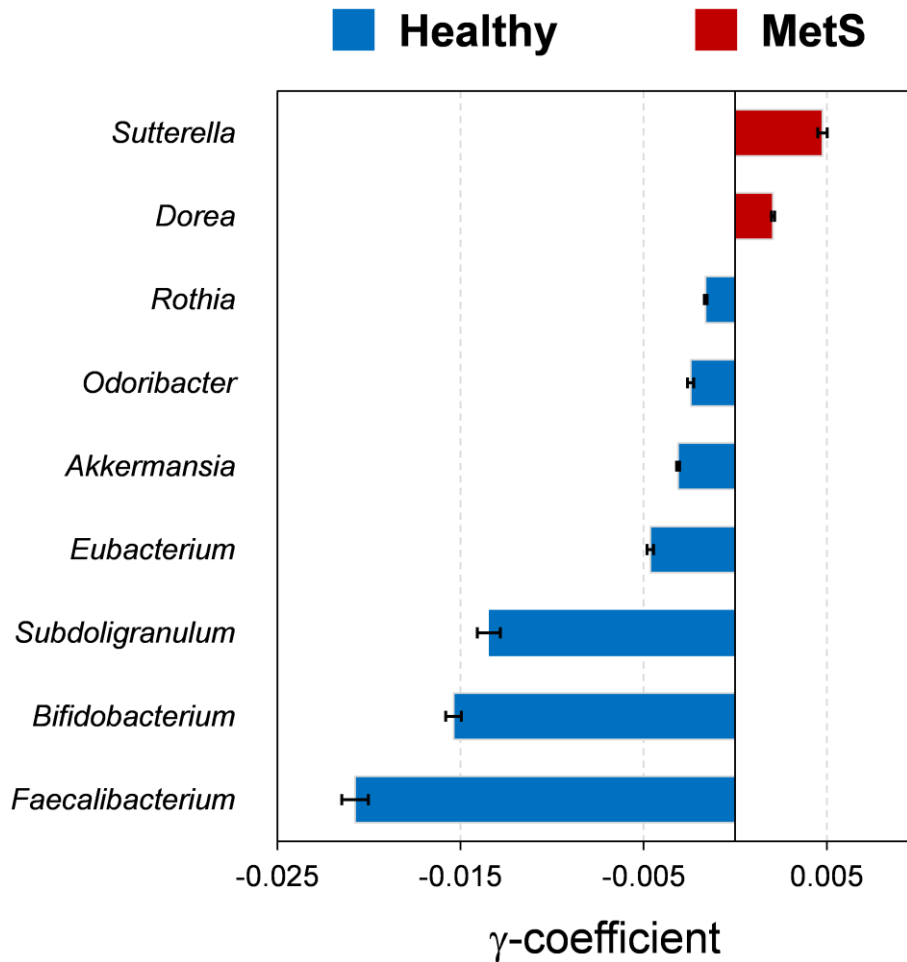


**Figure 2.3 Differences in the gut microbiota composition between the healthy and MetS groups.**

The  $\gamma$ -coefficients were calculated from MaAsLin analysis assessing associations between MetS status and microbial taxa (genus level) with adjustments for age, sex, and family structures (N=304). Red and blue bars represent taxa enriched in the MetS and healthy group, respectively. Error bars represent SEM.

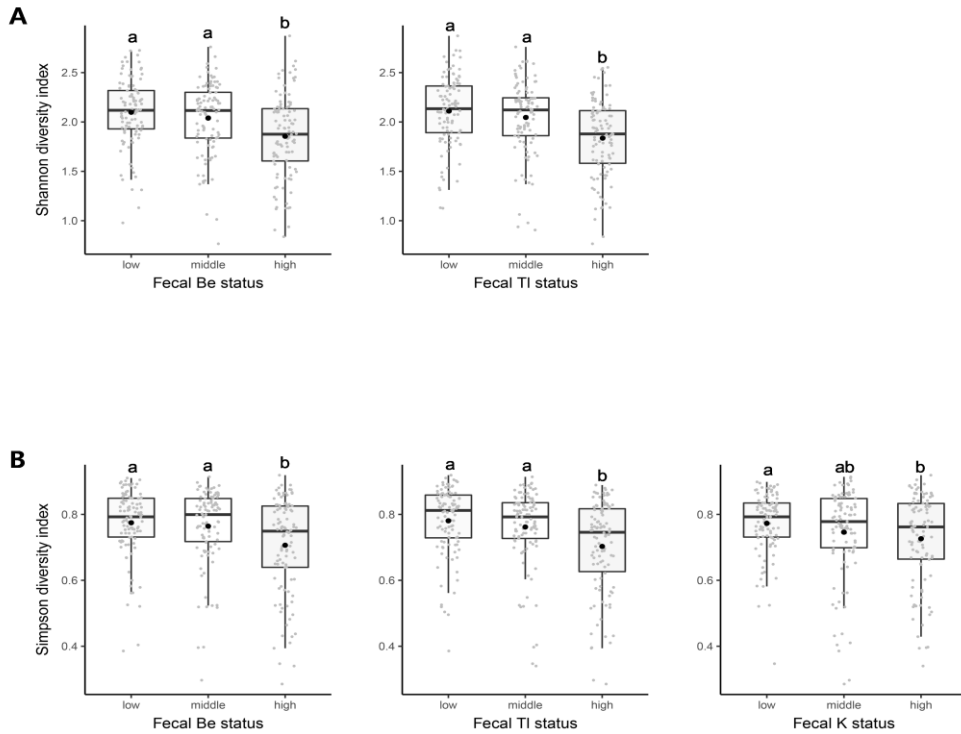


**Figure 2.4  $\alpha$ -diversity indexes according to fecal element status.**

(A) Shannon and (B) Simpson diversity index were calculated to investigate  $\alpha$ -diversity of the microbial community. The low, middle, and high level groups of each element were determined using the tertile values from the relative abundance of elements. The fecal elements that indicated a significant difference were represented. Different letters indicate significant differences (One-way ANOVA and Duncan's tests;  $P < 0.05$ ) (N=304).

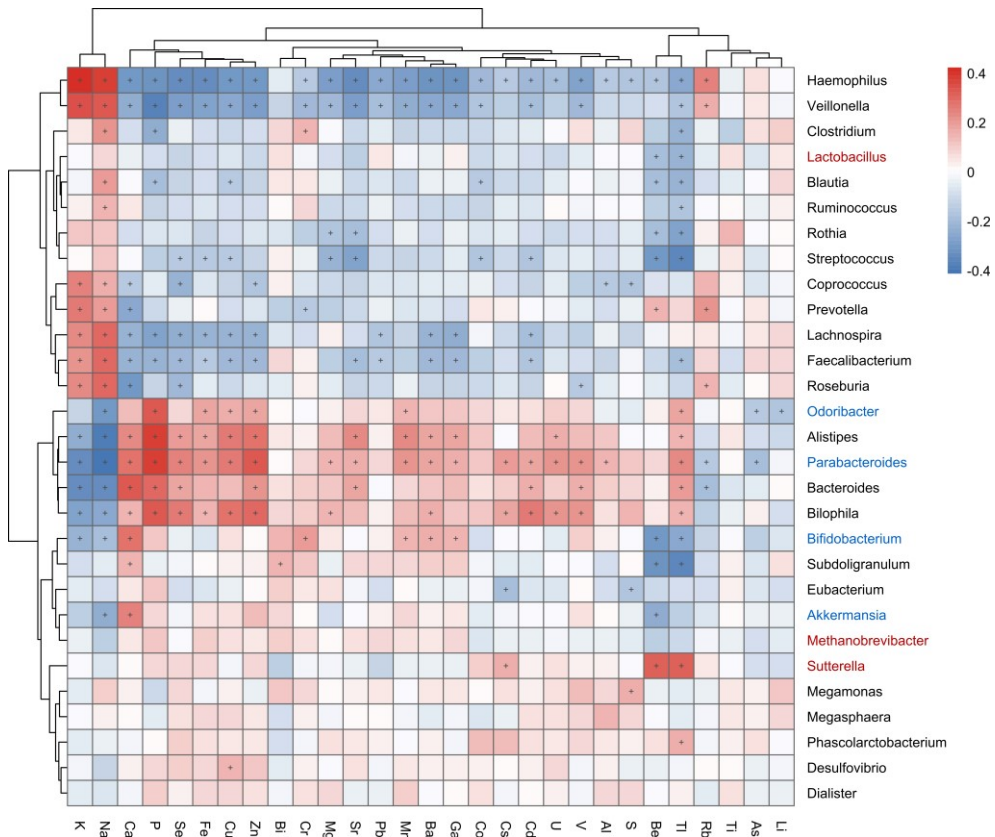


**Figure 2.5 Spearman's rank correlation between fecal elements and gut microbiota (genus level).**

The filtered set of taxa excluding low-abundance taxa ( $< 0.1\%$  of mean relative abundance) was used for correlation analysis. Asterisks represent significant associations at FDR adjusted  $P$  values of  $< 0.01$  (N=304). Blue and red microbiota respectively denote taxa significantly enriched in the healthy group and MetS group in the previous study<sup>(57)</sup>.

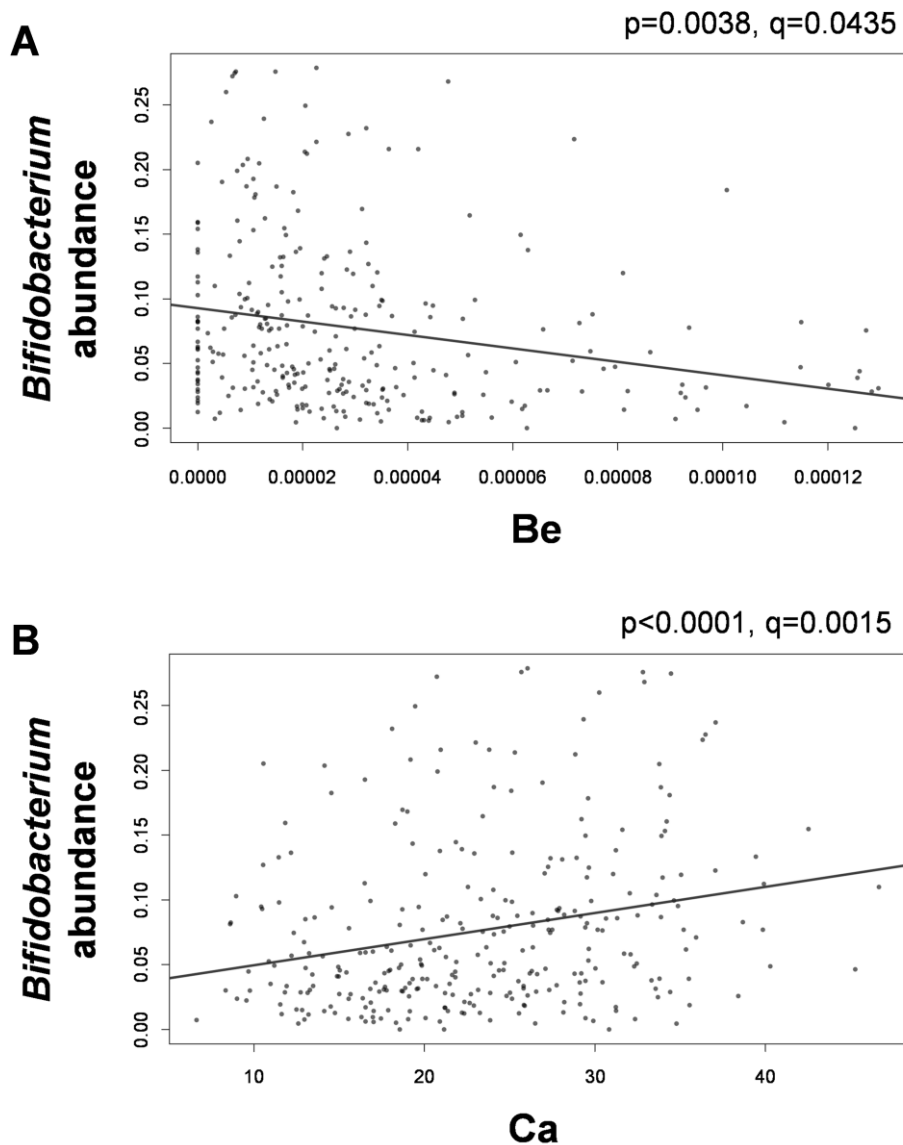


**Figure 2.6 Multivariate correlation analysis between fecal elements and microbial taxa using MaAsLin.**

The associations of *Bifidobacterium* enriched in a healthy group with fecal (A) Be and (B) Ca content were represented. Appendix B shows all significant associations of microbial taxa with fecal Be, Ca, and Tl. The *P* value and *q*-value indicated in each plot were determined by MaAsLin analysis (N=304).

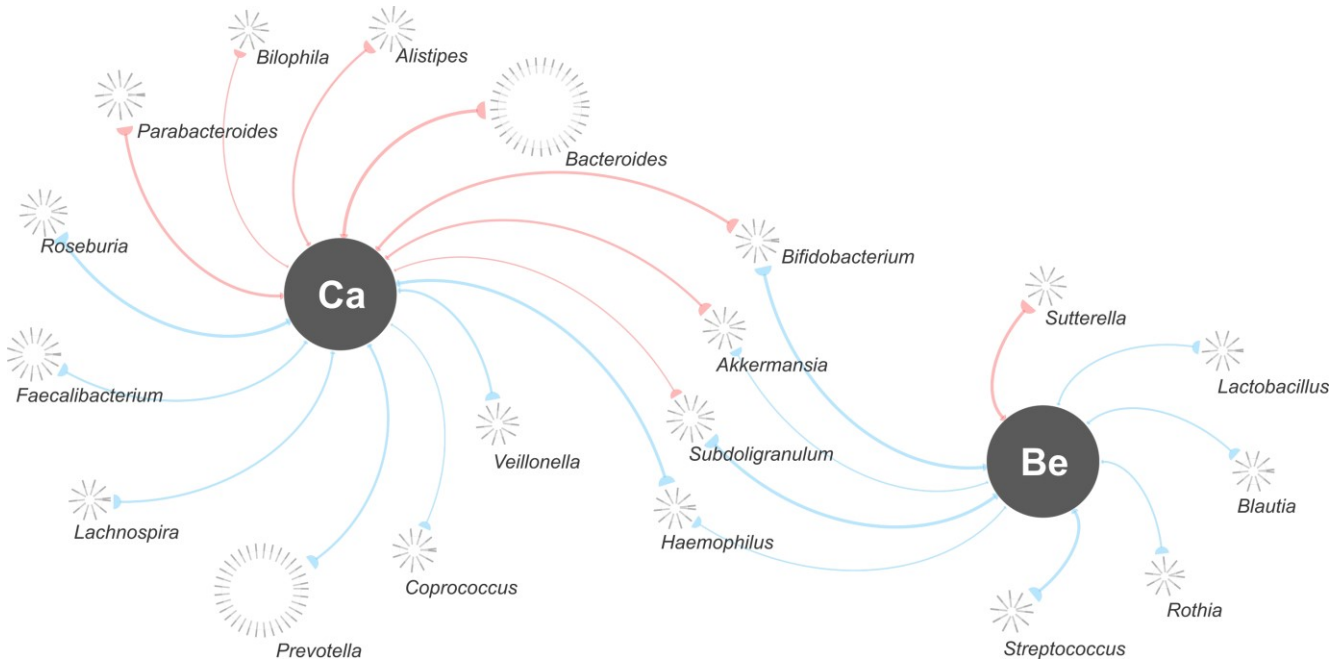


**Figure 2.7 Correlation network between two fecal elements (Ca and Be) and major microbiota (genus level).**

Red and blue edges denote positive and negative Spearman's rank correlation coefficient  $>0.15$  and  $<-0.15$ , respectively. The edge width represents the correlation between two nodes. The circle size of each taxon indicates the mean relative abundance from the 304-study population.

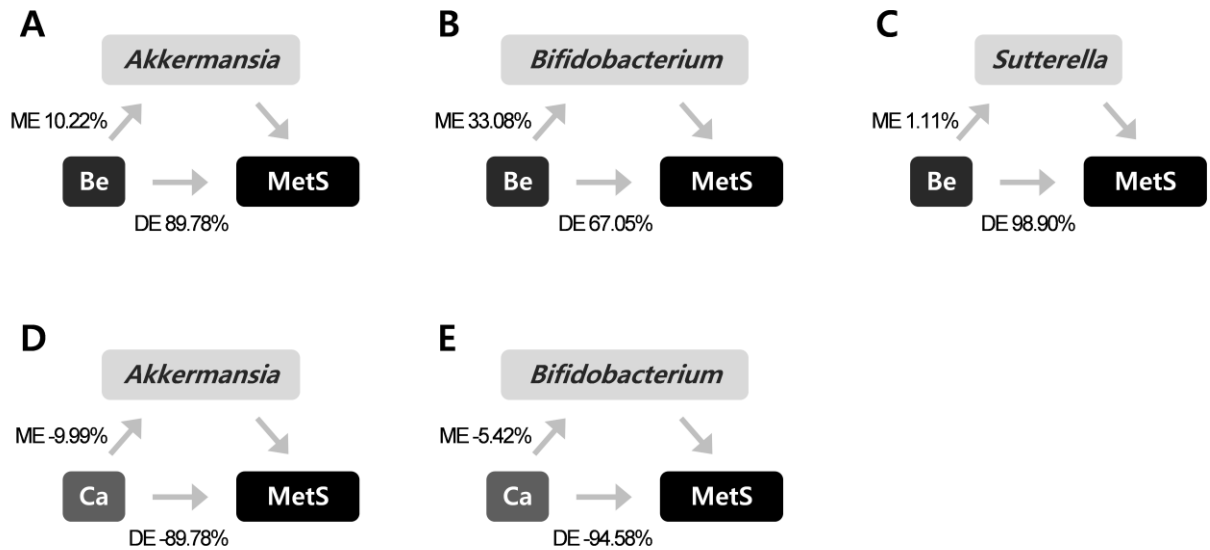


**Figure 2.8** Causal mediation analysis for the effects of Be and Ca with the gut microbiota mediator on MetS. The average causal mediation effects (ME) and the average direct effects (DE) were indicated. (A) direct factor: Be, mediator: *Akkermansia*; (B) direct factor: Be, mediator: *Bifidobacterium*; (C) direct factor: Be, mediator: *Sutterella*; (D) direct factor: Ca, mediator: *Akkermansia*; (E) direct factor: Ca, mediator: *Bifidobacterium*. The average mediated proportion from A, B, C, D and E were 10.22%, 33.08%, 1.11%, 9.99% and 5.42%, respectively.

### **Microbial functional analysis based on fecal Be and Ca status**

To evaluate the gut microbial functions according to MetS-related Be and Ca, we used PICRUST to infer functional metagenomes from 16S rRNA gene sequences and their reference genomes. Functional pathways that were differentially abundant between the low and high tertile of each element were identified and represented as histograms of the LDA scores (Figure 2.9). The oxidative phosphorylation pathway was overrepresented in Be high group, suggesting that Be was likely to be associated with the oxidative chemical reaction in the gut environment. We also observed that energy metabolism such as methane, pyruvate, arginine and proline metabolism was enriched in Be low group compared to Be high group. On the contrary, the energy metabolism was significantly increased in Ca high group, indicating Be low and Ca high group were a little closer to the healthy condition.

Next, we acquired high-resolution <sup>1</sup>H-NMR spectra, and 67 metabolites were assigned and quantified for the metabolomic analysis. These metabolites were analyzed using supervised multivariate analysis (PLS-DA). Although there were no clear clustering among each element tertile, we observed differences in the score plots between the low and high group for each element (Figure 2.10). According to the corresponding loading plot, 15 metabolites were identified as discriminating metabolites (VIP > 1). Fumaric acid, putrescine, glyceraldehyde, and cadaverine decreased proportionally to Be levels, whereas tryptophan increased in reverse. In the Ca groups, all 13 metabolites (lysine, isobutyric acid, isovaleric acid, pyruvate, alanine, methionine, cadaverine, malic acid, valine, methyl succinic acid, fumaric acid, tyrosine, and aspartate) were increased with a

dose-dependent manner. Especially, the acetate, one of the major microbial products was enriched in Be high group and decreased in Ca high group.

Finally, we performed the metabolome-based pathway prediction using MetaboAnalyst (Figure 2.11). For each element, the top 10 metabolic pathways with high pathway impact value were selected and compared with the results from PICRUSt analysis. Four (pyruvate, methane, arginine and proline metabolism, and glycolysis or gluconeogenesis) and five (pyruvate, methane, alanine, aspartate and glutamate, tryptophan metabolism, and citrate cycle) pathways matched the PICRUSt results from Be and Ca, respectively. The top two pathways (pyruvate and methane metabolism) were differentially important in both Be and Ca groups. Thus, we found that the Be and Ca status in the gut could influence not only the microbial composition but also their metabolic function.

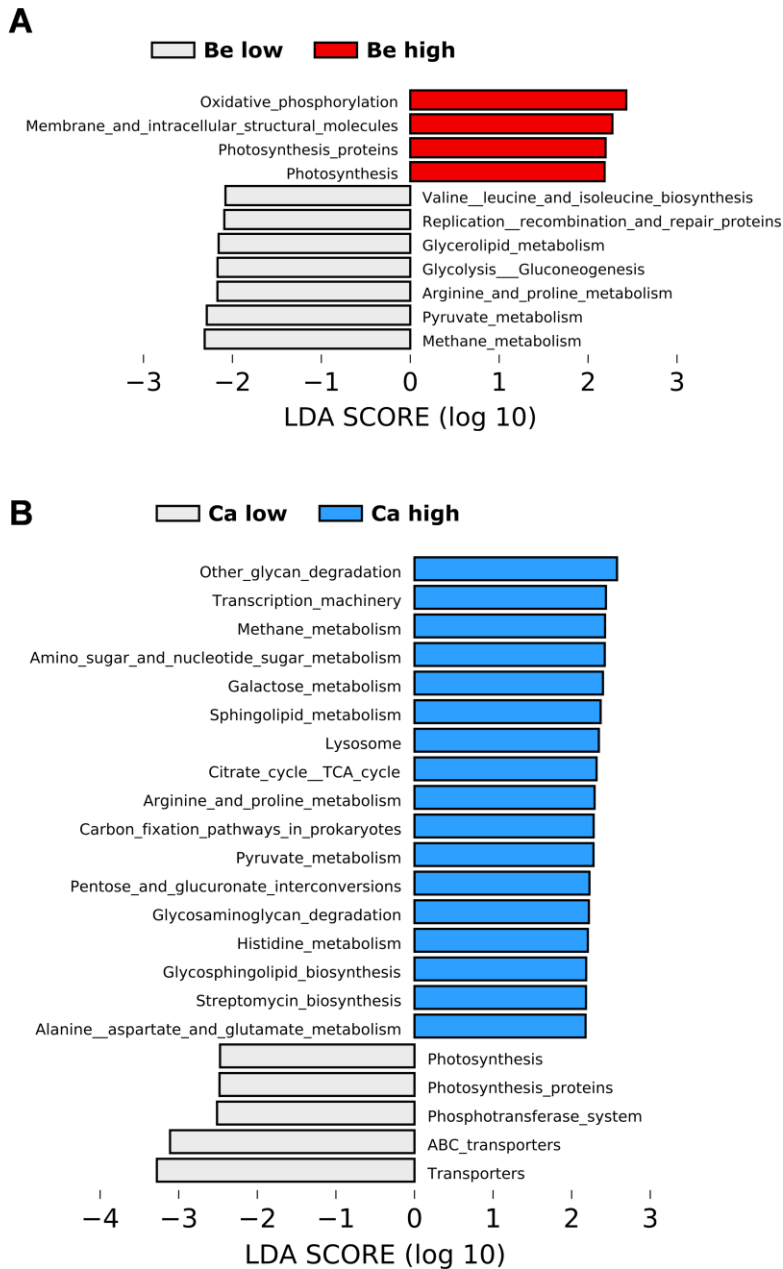


**Figure 2.9 Histograms of the linear discriminant analysis (LDA) scores for differentially abundant gut microbial functions according to fecal (A) Be and (B) Ca status.**

Microbial functional profiling was performed using PICRUSt. Features with LDA scores > 2 were presented (N=304).

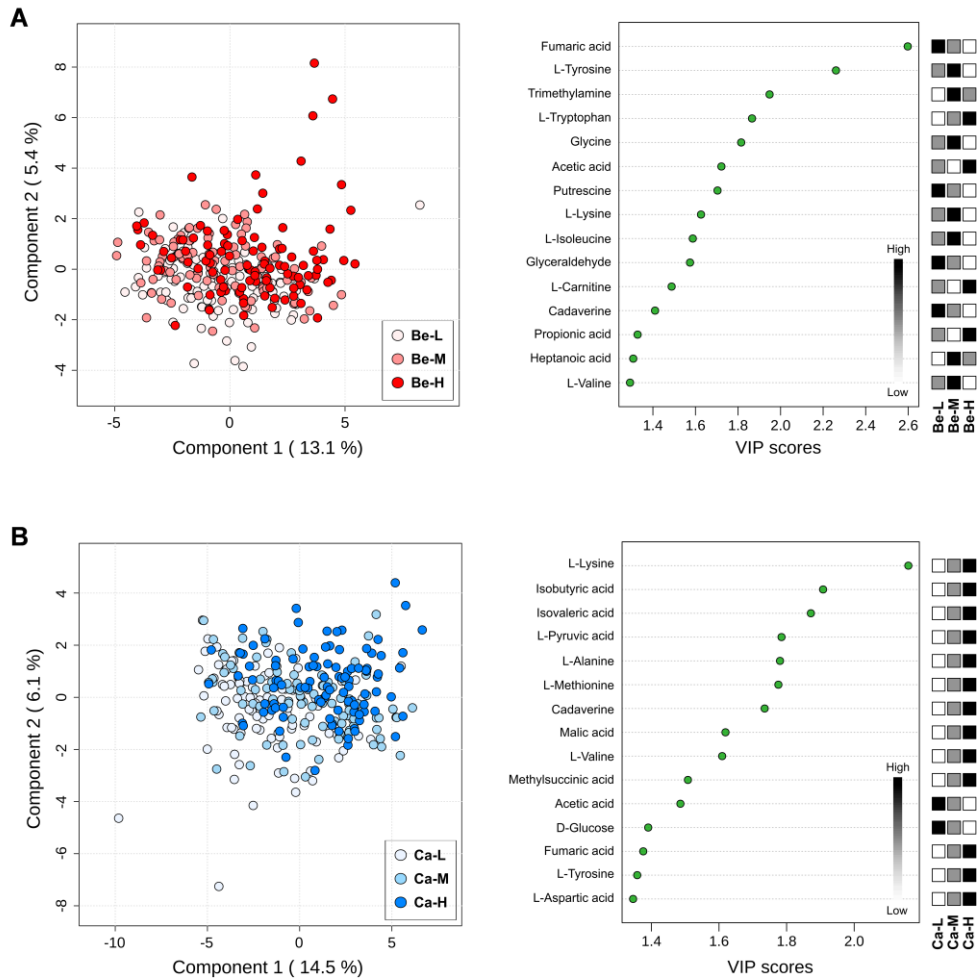


**Figure 2.10 Partial least squares discriminant analysis (PLS-DA) of fecal metabolites based on the fecal Be and Ca status.**

The PLS-DA score plot and loading plot of NMR-based fecal metabolomic datasets (N=300) for fecal (A) Be and (B) Ca status are presented. VIP plots indicate the most discriminating metabolites in descending order of importance. PLS-DA and VIP scores were assessed using MetaboAnalyst 4.0.

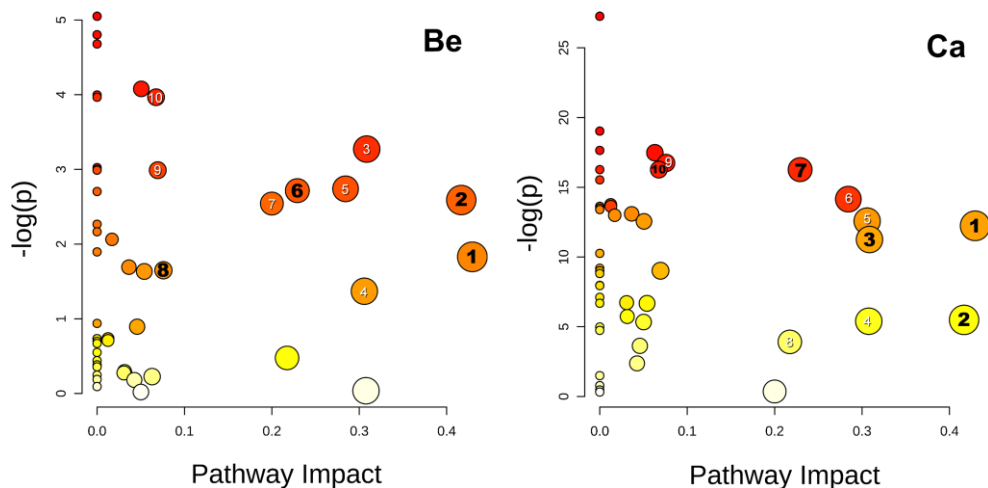


**Figure 2.11 Overview of metabolite pathway analysis from Be and Ca clustering.**

All the matched pathways are displayed as circles. The color and size of each circle were based on  $p$ -value and pathway impact value, respectively. The top 10 metabolic pathways with high impact value were denoted, and the black font color indicates the pathways differentially clustered in PICRUST analysis (Figure 2.8). Be group, 1: pyruvate metabolism; 2: methane metabolism; 3: alanine, aspartate and glutamate metabolism; 4: glycine, serine and threonine metabolism; 5: butanoate metabolism; 6: arginine and proline metabolism; 7: tryptophan metabolism; 8: glycolysis or gluconeogenesis; 9: sulfur metabolism; 10: citrate (TCA cycle). Ca group, 1: pyruvate metabolism; 2: methane metabolism; 3: alanine, aspartate and glutamate metabolism; 4: beta-alanine metabolism; 5: glycine, serine and threonine metabolism; 6: butanoate metabolism; 7: arginine and proline metabolism; 8: glycerolipid metabolism; 9: glycolysis or gluconeogenesis; 10: citrate cycle (TCA cycle).

### **Discussion**

In this study, we analyzed 29 human fecal elements. According to Table 2.2, the major elements of the human feces except for C, H, O, and N were Ca, P, K, Mg, S, and Na, which were the same as the main elements of a person's body composition<sup>(71)</sup>. Ca was the most detected mineral in both the human body and feces. When we compared the food intake data of four major elements (Ca, P, K, and Na) with their fecal measurement data, Ca and P indicated a significant association (Appendix C). Considering absorption efficiency of Ca (20%), P (55%), K (90%), and Na (90%), in the case of elements with low bioavailability, the results of measuring the element content through feces samples seemed to reflect the information of exposure through oral intake<sup>(72-75)</sup>.

The elements that were highly associated with MetS were Ca, Be, and Tl. In the case of Be, there were few reported studies related to MetS, but the association of Ca and metabolic disorders has already been reported in many other kinds of literature<sup>(42,43,76-79)</sup>. Meanwhile, because the diagnostic test using thallium-201 isotopes is conducted to check the blood circulation in the heart muscle from heart disease patients, the high correlation between MetS and Tl is likely to be attributed to the test<sup>(80)</sup>. When we performed the Spearman's rank correlation analysis among elements to check for the interaction between each element, Be was highly associated with Tl, and Ca indicated significant negative correlations with Na, K, and Rb (Appendix D). The high correlation between Be and Tl might be another reason for the Tl-MetS results. Some studies have recently reported that Zn has been linked to improved diabetes through insulin resistance and blood sugar reduction<sup>(81-83)</sup>. Although not significant, Zn has also shown a relatively strong negative

correlation with MetS in our studies.

Some works from twin cohort studies and animal experiments indicated that MetS were linked to microbial diversity reduction<sup>(18,57,84)</sup>. Figure 2.4 also showed some elements could affect microbial diversity. Because Be and Tl were elements that were highly associated with MetS, the decrease in microbial diversity due to these elements might affect the MetS development. *Bifidobacterium* and *Akkermansia* are representative gut microbiota whose causality with MetS is being revealed most closely<sup>(31,85-88)</sup>. In our study, Ca and Be, which were highly associated with MetS, showed positive and negative correlation with two microorganisms, respectively. The result suggests that there could be interactions between the two elements, gut microbiota, and MetS. According to some recent studies, Ca supplementation has led to a significant decrease in body weight and adiposity, along with significant increases in *Bifidobacterium*, *Bacteroides*, and *Akkermansia*<sup>(89,90)</sup>. The result is consistent with our findings derived from human samples. Na, As and Cd may also affect intestinal microbial disturbance<sup>(46,48,53,55,91)</sup>. One study showed that high salts could lead to an automatic immunity caused by a decrease in *Lactobacillus*<sup>(55)</sup>. Although Na did not have a significant correlation with *Lactobacillus* in our study, *Bifidobacterium* showed a significant negative correlation with Na and grouped in an opposite cluster of Ca. There have been reports that Cd increases Bacteroidetes at the expense of *Firmicutes*, and similar aspects have been seen in our results. According to Figure 2.5, As did not show a high association with gut microbiota, which is attributed to the fact that our cohort did not originate from a cohort highly exposed to certain elements and belonged to population-wide study. In addition, we measure the total As

content in this study, which may have been difficult to analyze the exact effect of various As species, since the toxicity of As varies among As species such as arsenate and arsenite. the toxicity of As was dependent on the As species. Our mediation study indicated that Be and Ca had the different gut microbial mediation effects on MetS. The mediation effects of *Bifidobacterium* was greater in Be analysis compared to Ca analysis. This seems to be because Ca is more likely to act directly on the host than indirectly by microorganisms compared to Be.

When the microbial functions between high and low tertile of Be and Ca group were analyzed using PICRUSt, the energy metabolism, including pyruvate and methyl metabolism, were activated in the Be Low and Ca High groups. In our previous study<sup>(57)</sup>, it was a distinct function in the healthy group compared to MetS group, suggesting that Ca and Be could have conflicting effects on MetS. In Figure 2.8, the oxidative phosphorylation was the differentially abundant function in the Be high group. Considering that Be treatment could increase the ROS in cell experiments<sup>(92)</sup> and this ROS production could be generated by the process of oxidative phosphorylation<sup>(93)</sup>, our result seems to be reasonable. We performed the microbial function prediction using the primary metabolites profile obtained from the analysis of the fecal metabolites. This compound-based functionality prediction (Figure 2.10) was substantially consistent with the 16s microbiome-based functional prediction (Figure 2.9). Especially, Ca low group was abundant in acetate, and it showed a decreasing pattern in pyruvate, malate, and fumarate compared to Ca high group. These metabolic changes can be explained as an increase in the gut microbiota in relation to propionate cross-feeding, and the increases in the propionate-producing

bacteria such as *Akkermansia* and *Bifidobacterium* in Ca high group were linked to these changes<sup>(94)</sup>. The result underscores that convergence studies using several omics data may be important for the innovative data analysis with systemic perspectives as well as study validation. 16S microbial community analysis and whole genome sequencing are widely carried out using human feces<sup>(61,95-97)</sup>. Also, meta-transcriptomics and meta-proteomics have also been applied to analyze the microbial function from feces samples<sup>(98-102)</sup>. In this study, we have attempted to conduct a metallomics analysis to measure the fecal elements in a stool sample. Moreover, we could obtain the meaningful results for compounds-based microbial functional pathway by performing NMR-based metabolomics, which has been recently applied to analyze primary metabolites from human feces<sup>(62,103-105)</sup>. This approach could help acquire more information about the gut environment and broaden our knowledge by allowing us to analyze various omics data from excreted human feces.

In this study, we conducted a cross-sectional study using the feces samples from existing cohorts due to budget problems. Despite the limitations of the cross-sectional study, certain elements showed significant associations with MetS and gut microbiota, but the longitudinal studies are required for specific cohorts along with the large-scale element analysis of additional human feces samples in the future for further verification. In addition, our study has shown the importance of environmental factors such as fecal elements on the gut microbial composition and function. Considering that Ca and Be are the elements that exist at high concentration in the intestine, the several persistent organic pollutants including dioxins, polychlorinated biphenyls, and dichlorodiphenyltrichloroethane are likely to

disrupt gut microbiota. Therefore, further studies will be needed to analyze large quantities of persistent organic pollutants from human feces in the future.

In summary, we analyzed the association of fetal elements with MetS, and gut microbiota by measuring them from human feces. Ca and Be had a high correlation with MetS and two beneficial microbes, *Bifidobacterium* and *Akkermansia*, which is known to ameliorate metabolic abnormalities. In addition, by analyzing the microbial functions based on 16S rRNA gene sequences and fecal metabolites profiles, we confirmed that the microbial functions were differentially divided according to the fecal level of Ca and Be. Further research is required to demonstrate the causality between each element, gut microbiota, and MetS.

**CHAPTER III.**

**LOW DOSE OF BERYLLIUM INFLUENCES  
GUT MICROBIOTA PROMOTING  
METABOLIC SYNDROME**

## Introduction

The increasing prevalence of chronic metabolic syndrome (MetS) such as obesity and diabetes has been believed to be caused by excessive calorie intake and lack of physical activity in the last 30 years<sup>(14,106)</sup>. However, there is considerable evidence that other risk factors such as exposure to environmental pollutants and chemicals could be involved in MetS etiologies<sup>(107-109)</sup>. These chemicals that promote MetS have been functionally defined as obesogens and diabetogens because they can affect lipid accumulation and adipogenesis and also induce shifting energy balance, changing basal metabolic rates, and altering hormonal or neuronal control.

Heavy metals, along with environmental toxins and persistent organic pollutants, are one of the representative obesogens. Arsenic (As), cadmium (Cd), and lead (Pb) exposure have been associated with diabetes, cardiovascular disease, hypertension, and peripheral vascular disease<sup>(36,40,45,51)</sup>. In particular, it has been recently revealed that some heavy metals such as As, Cd, and Pb could affect the shift in the gut microbial community and this could occur at relatively low concentrations<sup>(48,53,91)</sup>. It was noteworthy that the patterns of microbial changes are very similar to the microbiome characteristics from obesity group including the decrease in the Bacteroidetes-to-Firmicutes ratio as well as the microbial diversity reduction<sup>(16,17)</sup>.

Beryllium (Be), the second lightest stable metal, is used as a material for leading-edge technologies, such as electronics, aerospace, weapons and nuclear, telecommunications, and medical specialty industries because of its unique physical and chemical properties<sup>(110)</sup>. Recently, the health risks of Be are being reported that the exposure to Be, even at very low concentrations,

can be associated with several adverse health outcomes including lung cancer as well as acute and chronic Be disease, a lung disorder with the abnormal release of inflammatory cytokine and granuloma formation<sup>(111)</sup>. The International Agency for Research on Cancer (IARC) lists Be and Be compounds as Category 1 carcinogens, and the Occupational Safety and Health Administration (OSHA) has designated a permissible exposure limit (PEL) in the workplace with a time-weighted average (TWA) 2  $\mu\text{g}/\text{m}^3$  (112,113).

As the toxicity of Be has been mostly reported about the respiratory tract, legal standards and regulations for Be have focused on exposure through inhalation. However, according to several studies on Be exposure, the estimated total daily Be intake of general population in the USA was 423 ng, with the largest contributions from drinking water (300 ng/day) and food (120 ng/day), with smaller contributions from air and dust (2.8 ng/day)<sup>(114,115)</sup>. The result underscores that more reliable and extensive investigations are required to analyze the occurrence and intake of Be from not only air but also food and drinking water.

In our previous study from Chapter II, the high level of Be in human feces was significantly associated with MetS status and the changes in the gut microbiome. However, few studies have ever been done to establish the relationship between the low dose of Be intake and MetS. Thus, we evaluated whether low dose Be exposure could affect gut microbial changes and promote MetS using *in vivo* mice model. Also, to assess the effect of Be exposure on the human gut microbiome, *in vitro* human feces cultivation was applied in this study.

### Materials and Methods

**Animals and exposure.** All animal experiments were conducted with the approval of the Institutional Animal Care and Use Committee of the Korean Institute of Science and Technology (No. 2018-036) and strictly followed National Institutes of Health guidelines for the use of live animals. Male C57BL/6 mice (5-weeks-old, 20-22 g; Central Lab. Animal Inc., Seoul, Korea) were housed in individually ventilated cages at  $23 \pm 0.5^\circ\text{C}$  and 10% humidity under a 12 hr-light-dark condition with access to feed and water ad libitum. All animals were acclimated for seven days and divided into 2-3 animals/cage, ensuring equal weight average. Be was administered to mice as beryllium sulfate tetrahydrate (Sigma-Aldrich Inc., St. Louis, MO, USA) in drinking water for 50 days. Freshly prepared Be-containing water (3 or 30 ppb) and feed were provided to mice twice a week, while control mice received a feed with water alone. Mice were randomly divided into three high fat diet (HFD) groups and two normal diet (ND) groups: (1) HFD (45% of total calories from fat; TD.06415, Harlan Laboratories) with water ( $n = 8$ ), (2) HFD with 3 ppb of Be water ( $n = 8$ ), (3) HFD with 30 ppb of Be water ( $n = 8$ ), (4) ND with water ( $n = 6$ ), and (5) ND with 30 ppb of Be water ( $n = 6$ ). Feed and water intake were recorded continuously once a week on the basis of cages, and the data were used for the calculation of average intake per mouse per week. The theoretical weekly Be exposure was calculated by multiplying the added Be concentration by the average weekly water intake. Body weight of each mouse was measured once a week.

**Sample collection.** The stool samples were collected once a week and immediately stored at  $-80^\circ\text{C}$  before further analysis. Animals were

euthanized by CO<sub>2</sub> inhalation at the beginning of the light cycle and after 16 h of food deprivation. Blood samples were collected by cardiac puncture in microtubes containing EDTA and centrifuged at 1,000 g and 4°C for 15 min to obtain the plasma, and stored at -80°C for subsequent biochemical measurements. Epididymal white adipose tissue (eWAT), cecum, and colon of each mouse were precisely dissected, weighed and collected for further analysis. All tissues were rinsed with saline and snap-frozen at -80°C.

**Biochemical measurements.** Plasma triglyceride (DoGEN Bio Co., Ltd, Seoul, Korea), glucose (Abcam, Cambridge, UK), insulin (Abcam), leptin (Abcam), and adiponectin (Abcam) concentration were measured using commercial ELISA kits according to the manufacturer's instructions. Lipopolysaccharide (LPS) was detected using an endpoint chromogenic endotoxin quantitative test (Signalway Antibody, College Park, MD, USA).

***In vitro* batch culture of human fecal microbiota.** *In vitro* colonic fermentation was performed according to Long's method with a slight modification<sup>(116)</sup>. Briefly, NaCl at 8 g/L, Na<sub>2</sub>HPO<sub>4</sub> at 1.15 g/L, L-cysteine at 0.5 g/L, KCl at 0.2 g/L, and KH<sub>2</sub>PO<sub>4</sub> at 0.2 g/L were dissolved in distilled water and autoclaved for PBS medium. Fecal samples were obtained from three healthy donors (age 20-30; mean BMI 22.3) who had taken no antibiotics or prebiotics for three months prior to the study. Written informed consent was obtained from donors, and the study was approved by the institutional review board of Korea Institute of Science and Technology (IRB No. 2015-003). 10% (w/v) fecal slurry was prepared by diluting and suspending the fecal samples with PBS medium in an anaerobic chamber

(Coy Laboratory Products Inc., Ann Arbor, MI, USA). The cultivation was started with 5% fecal inoculum by adding 0.9 mL of 10% fecal slurry into 0.9 mL of PBS medium (total volume: 20 mL) using 96 deep well plate. Cultures were performed with the various concentration of Be (3, 30, 300, and 3000 ppb) in an anaerobic jar (MGC, Japan) with AnaeroPack (MGC) at 37°C without stirring. Samples were collected after 24 hr and stored in the refrigerator (-20°C) for further analysis.

**16S rDNA amplicon sequence analysis.** DNA was extracted from cecum, stools, and *in vitro* batch culture samples using a QIAamp DNA Stool Mini Kit (QIAGEN, GmbH, Germany) with the additional bead-beating procedure to improve the DNA recovery for Gram-positive bacteria. The 16S rRNA genes were amplified using an improved dual-indexing amplification of the V3-V4 region (319F/806R) of the 16S rRNA gene with heterogeneity spacer<sup>(117)</sup>. PCR products were purified using AMPure XT beads (Beckman Coulter Genomics, Danvers, MA, USA) and quantified using a Qubit dsDNA high-sensitivity reagent (Invitrogen, Carlsbad, CA, USA). Sequencing was conducted on the MiSeq platform using a paired-end 2 × 300-bp reagent kit (Illumina, San Diego, CA, USA). The raw reads were demultiplexed, assembled, and quality-filtered in QIIME 2 (v2018.6), using default settings<sup>(118)</sup>. DADA2 was used to filter chimeric reads and artifacts commonly present in Illumina amplicon data<sup>(119)</sup>. To classify filtered reads to taxonomic groups, a Naive Bayes classifier was trained using the 16S rRNA region (V3-V4), the primer set and read length used (319F/806R, 469 bp), and the Greengenes 97% reference set (v13.5)<sup>(120-122)</sup>. This trained feature classifier was then used to assign taxonomy to each read using the

default settings in QIIME. Microbial composition at a certain level, and  $\alpha$ - and  $\beta$ -diversity was analyzed using MicrobiomeAnalyst<sup>(123)</sup>. Non-metric multidimensional scaling (NMDS) plots were generated from a Bray-Curtis distance matrix, and principal coordinate analysis (PCoA) plot was generated using unweighted Unifrac distances to represent microbiota compositional differences among groups visually. Random forest, a supervised learning method for the classification of human microbiome data<sup>(124)</sup>, was used to select subsets of taxa (genus level) that are highly discriminative of the type of community from Be-exposed mice. We measured feature importance as the mean decrease in model accuracy when that feature's values were permuted randomly using 500 trees and seven repetitions.

**Short chain fatty acids (SCFAs) measurements.** Cecal SCFAs content was determined by gas chromatography according to David's method<sup>(125)</sup>. Cecal contents (~80 mg) were homogenized in 500  $\mu$ L of deionized water. After that, the samples were acidified with 50  $\mu$ L of 50% sulfuric acid, followed by vortexing at room temperature for 5 min. After centrifugation at 14,000 g for 10 min, 400  $\mu$ L of the supernatant was moved to a new tube, and 40  $\mu$ L of the internal standard (1% 2-methyl pentanoic acid) and 400  $\mu$ L of anhydrous ethyl ether were added. The tube was vortexed for 1 min and then centrifuged at 14,000 g for 10 min. The upper ether layer was used for further analysis. Volatile Free Acid Mix (Sigma) was used as the SCFAs standard for the quantification of acetate, butyrate, isobutyrate, propionate, valerate, and isovalerate. GC-FID (GC 450, Bruker, USA) was used to analyze the SCFAs content with fused silica capillary columns (Nukol, 30 m

× 0.25 mm, 0.25 µm film thickness). The oven temperature was 170 °C, and the FID and injection ports were set to 225 °C. Nitrogen was used as the carrier gas, and the sample injection volume was 2 µL.

**RNA extraction and real-time PCR analysis.** Total RNA was extracted from colon tissues (~50 mg) using Trizol reagent (Thermo, South Logan, UT, USA) according to the manufacturer's instructions, followed by concentration measurement. cDNA was synthesized from 1 µg of total RNA using Superscript IV reverse transcriptase (Thermo). Real-time PCR was performed using the LightCycler 480 detection system (Roche Diagnostics, Mannheim, Germany) and LightCycler 480 SYBR Green I Master (For primer sequences, see Appendix E.). Samples were run in duplicate in a single 384-well reaction plate. Data were normalized to the housekeeping RPL19 gene and analyzed according to  $\Delta\Delta\text{CT}$  method.

**Cell culture.** The mouse macrophage cell line RAW264.7 was maintained in Dulbecco's modified Eagle's medium (Thermo) supplemented with 10% fetal bovine serum (Thermo) and 1% (v/v) penicillin (100 U/ml)-streptomycin (100 µg/ml) (Thermo). Cells were grown in 75 cm<sup>2</sup> tissue culture flask and incubated at 37 °C in 5% CO<sub>2</sub>. Cells were detached from the flask with a scraper and split 1:10 every five days. For nitrite measurement experiments, RAW264.7 cells ( $5 \times 10^4$  cells/well) were seeded in 24 well plates with one mL of medium per well. Cells were treated with LPS (100 ng/mL) as a positive control and a series of concentrations of Be (3, 30 and 100 ppb) after 24 h of inoculation. Fecal microbial supernatants and cell pellets from 1 mL of *in vitro* anaerobic culture with various

concentrations of Be (3, 30, and 100 ppb) were also treated on RAW264.7 cells.

**Determination of NO production.** The nitrite concentration in the culture medium was measured as an indicator of NO production using the Griess reaction. After incubation with test samples for 48 hr, supernatant from each well (50  $\mu$ L) was transferred to a fresh 96 well plate, and 25  $\mu$ L of 1% sulfanilamide plus 25  $\mu$ L of 0.1% naphthyl-ethylenediamine in 5% HCl was added. After 10 min incubation at room temperature, the absorbance of each well was measured at 540 nm using a Synergy HT microplate reader (Biotek, Winooski, VT, USA). Relative nitrite production was calculated from the comparison of each sample with LPS only treatment group.

**Statistical analysis.** All the grouped data were statistically performed with R software or GraphPad Prism 7. Significance was determined using two-tailed Student's *t* test, Mann Whitney test or one-way ANOVA corrected for multiple comparisons with a Sidak test compared to the control group. Microbial data processing and multivariate statistical analysis were performed using MicrobiomeAnalyst. Permutational multivariate analysis of variance (PERMANOVA) was performed to test for the association of microbiome composition with Be exposure based on NMDS.

## Results

### **Be promotes MetS in HFD mice.**

To determine the effect of Be exposure on adiposity and host metabolism, we first examined the body weight gain (%) and feed intake during seven weeks (Figure 3.1). In the ND group, there was no significant increase in body weight gain by 30 ppb of Be exposure and feed intake remained constant. (Figure 3.1A, C). However, in the HFD group, 30 ppb of Be exposure resulted in modest but significant gains in overall weight, indicating that Be might accelerate HFD-induced obesity. Although 3 ppb of Be did not show a significant weight gain in the overall seven weeks, there was a tendency to gain weight similar to 30 ppb of Be during the first two weeks (Figure 3.1B). Such an increase in body weight gain was linked to the upsurge of feed consumption in early breeding (Figure 3.1D). There was no significant difference in the intake of drinking water between all groups, regardless of ND or HFD (Figure 3.2). The theoretical average Be exposure was 43.84 ng/week, 300.50 ng/week, and 337.47 ng/week in HFD-Be3, ND-Be30, and HFD-Be30 groups, respectively.

Next, we investigated the possible causal relationship between Be exposure and host adiposity. In the ND group, the MetS-related biomarkers such as plasma concentration of TGs, glucose, insulin, leptin, and adiponectin did not show any significant difference due to Be exposure, whereas the eWAT weight was significantly higher than control when exposed to 30 ppb of Be (Figure 3.3). Similar to the results of body weight gain, Be exposure worsened the host adiposity in the HFD experiments (Figure 3.4). The plasma level of TGs, glucose, and insulin markedly increased in HFD-Be30. The adipokine leptin also increased with 30 ppb of

Be exposure, and in contrast, the adiponectin significantly decreased in both HFD-Be3 and HFD-Be30 group compared to control. We were unable to observe a considerable difference in eWAT weight in the three HFD groups, probably because the eWAT was almost saturated due to the high fat diet for seven weeks. Taken together, these findings indicate that long-term exposure to Be promotes the metabolic disorder in HFD mice.

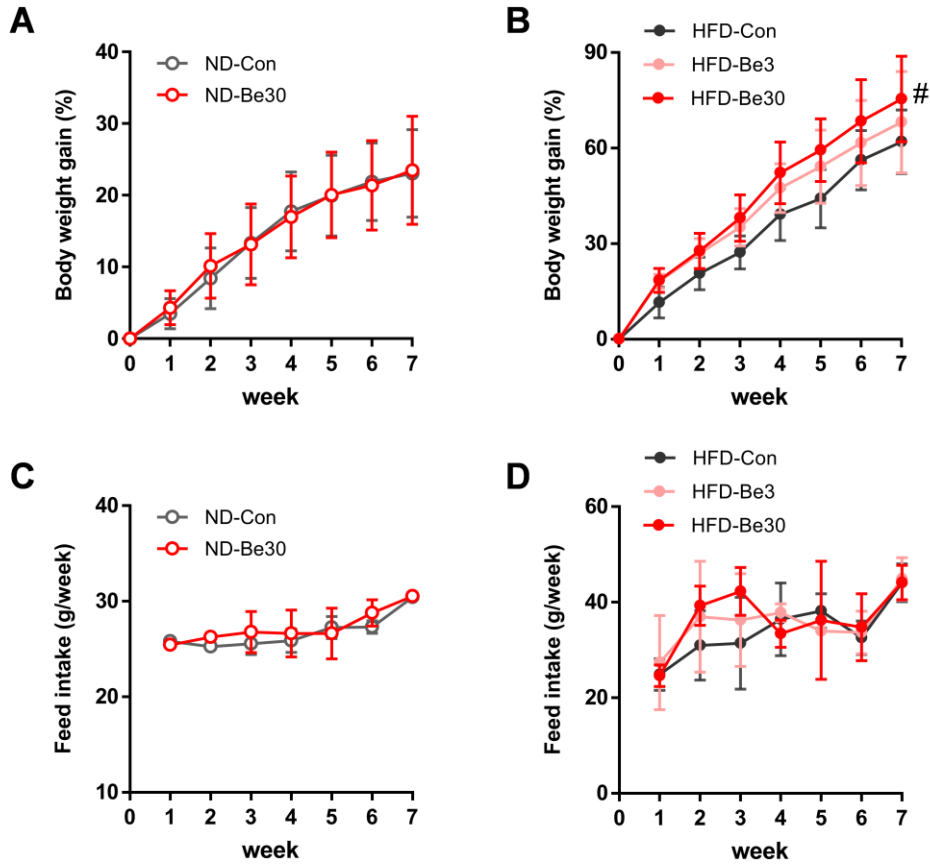


**Figure 3.1** Body weight gain (%) and feed intake over time in the control and Be-exposed mice.

Be groups were exposed to drinking water containing 3 ppb or 30 ppb of Be for 50 days. (A) Body weight gain (%) of normal diet mice (ND, N=6); (B) body weight gain (%) of high fat diet mice (HFD, N=8); (C) feed intake of normal diet mice; (D) feed intake of high fat diet mice. Data are the means  $\pm$  SEM. Significance was determined using two-way group ANOVA corrected for multiple comparisons with a Bonferroni test ( $\#P < 0.05$ ) compared to control group.

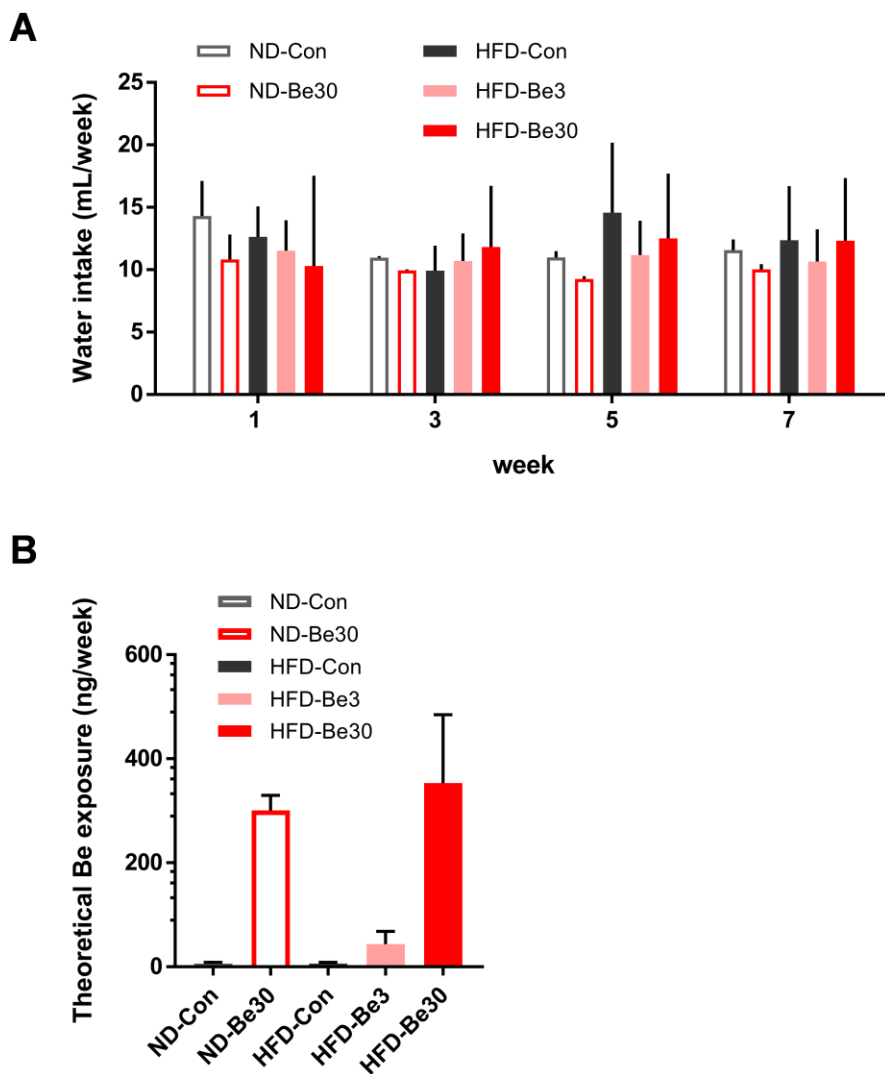


**Figure 3.2 Weekly water intake and Be exposure from drinking water in ND and HFD mice.**

(A) Water intakes at 1, 3, 5, and 7 weeks were represented and (B) the theoretical weekly Be exposure during Be exposure experiments was calculated. Data are the means  $\pm$  SEM.

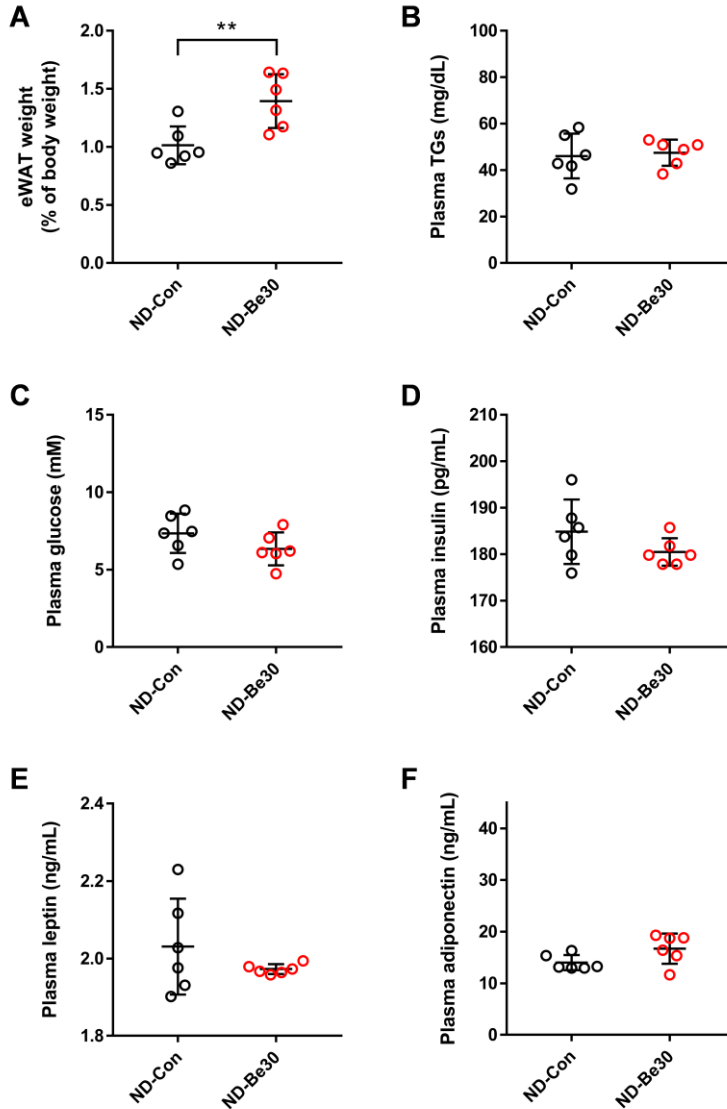


**Figure 3.3** Effect of Be exposure on host metabolism in ND mice.

(A) Epididymal white adipose tissue mass (eWAT); (B) plasma triglycerides (TGs); (C) plasma glucose; (D) plasma insulin; (E) plasma leptin; (F) plasma adiponectin in the control and Be treated mice (n = 6/group). Data are shown as mean ± SD. Significance was calculated using unpaired two-tailed Student's *t* test. \*\* $P < 0.01$ .

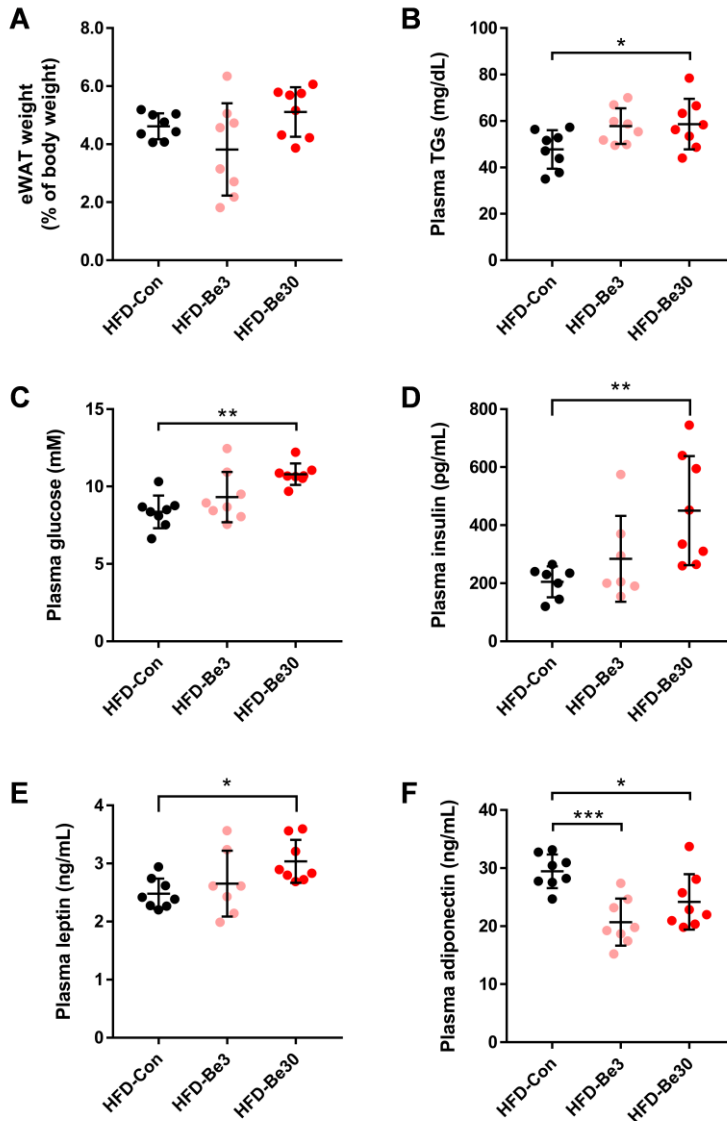


**Figure 3.4 Effect of Be exposure on host metabolism in HFD mice.**

(A) Epididymal white adipose tissue mass (eWAT); (B) plasma triglycerides (TGs); (C) plasma glucose; (D) plasma insulin; (E) plasma leptin; (F) plasma adiponectin in the control and Be treated mice ( $n = 8/\text{group}$ ). Data are shown as mean  $\pm$  SD. Significance was determined using one-way ANOVA corrected for multiple comparisons with a Sidak test compared to the control group. \* $P < 0.05$ , \*\* $P < 0.01$ , \*\*\* $P < 0.001$ .

### Be alters gut microbial composition in HFD mice

To determine whether the metabolic disorder shown by Be exposure is related to changes in microbial composition, we analyzed cecal microbiome. As compared to the cecal microbial profiles between ND and HFD groups, HFD group showed a tendency to increase in *Lachnospiraceae* and *Desulfovibrionaceae* with the decrease in *Bacteroidaceae* and *Prevotellaceae* (Figure 3.5). The result was consistent with the typical features of gut microbiota in HFD mice such as the increase in the Firmicutes to Bacteroidetes ratio and the increase in Proteobacteria phylum.

We then investigated the  $\alpha$ -diversity such as Chao1 richness, Simpson and Shannon diversity index to confirm whether the microbial diversity reduction of human feces samples with a high Be level in our previous study (Figure 2.4) could be reproduced by *in vivo* mice study (Figure 3.6). Similar to the human analysis results, Simpson and Shannon diversity index significantly decreased in HFD-Be groups. On the other hand, ND groups that did not show a significant change in adiposity by Be exposure indicated no significant reduction in microbial diversity. To compare the cecal microbial community shift between groups by Be manipulation, we conducted a  $\beta$ -diversity analysis. HFD-Be3 and HFD-Be30 showed marked microbial community changes compared to the control group, although the obvious microbial shift pattern was not shown in the ND groups. To further validate the change of gut microbial community due to Be exposure in HFD group, mice feces samples that collected over five weeks from the HFD group were used for fecal microbiome analysis (Figure 3.8). In 0 week, where the Be manipulation has not yet been started, three HFD groups were gathered in one cluster. However, in week 5, Be exposure groups appeared

to be moved to another cluster. Remarkably, these changes in microbial clusters occurred in a week. To assess gut microbiota variation between groups and identify features differentially abundant in HFD-Con and HFD-Be group, random forest, the machine-learning algorithm, was implemented (Figure 3.9). There were significant decreases in *Allobaculum* and *Akkermansia*, and increasing trends in *Lactobacillus* and *Oscillospira*. Only three microbiota from the ten most predictive genera were detected in human fecal samples with a relative abundance of not less than 0.1%.

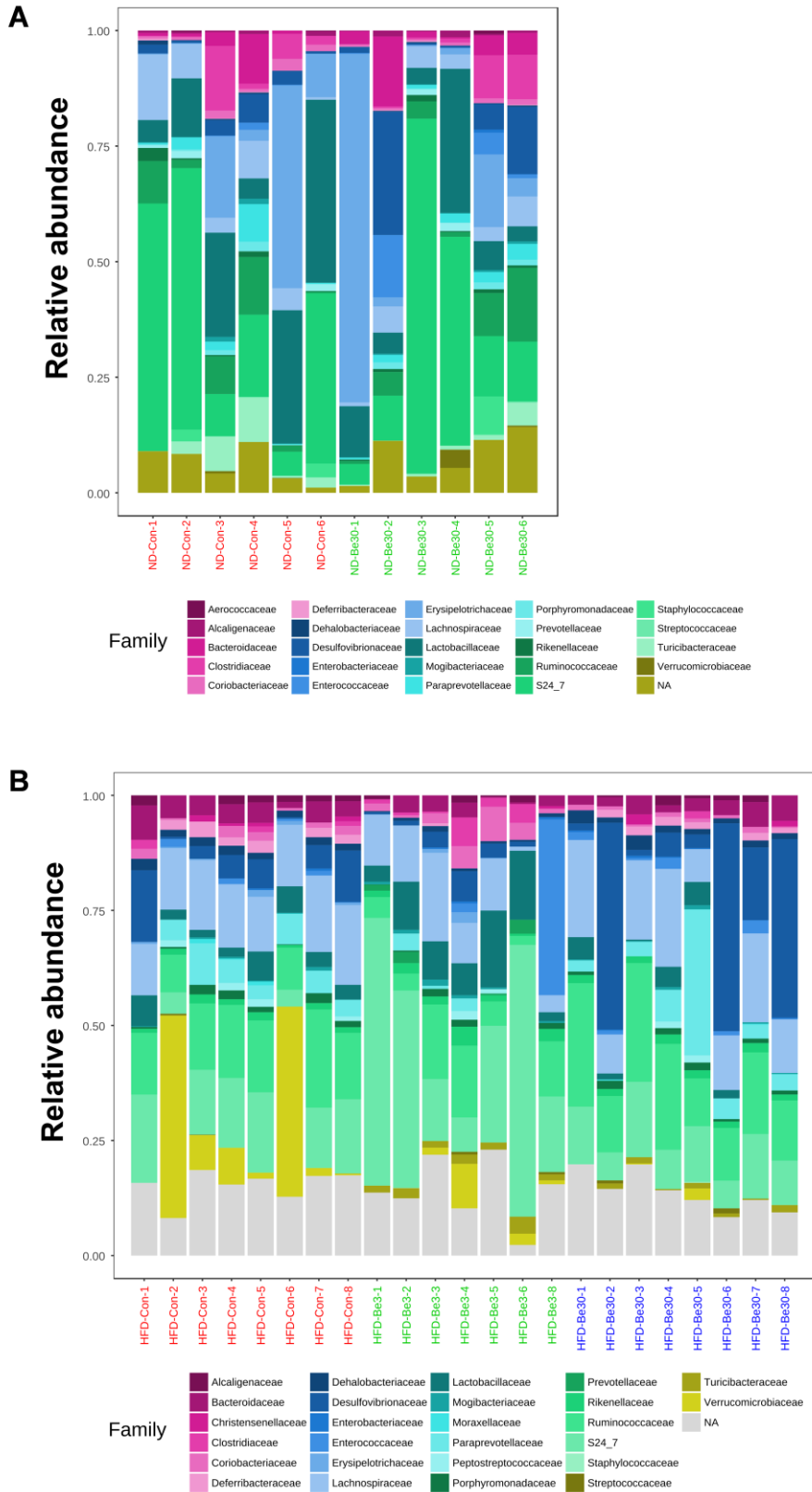


**Figure 3.5 The cecal microbiome composition profiles at the family level in the control and Be-exposed mice fed (A) ND or (B) HFD.**

Each color represents one bacterial family. Relative abundance of microbial taxa was determined by 16S rDNA sequencing.

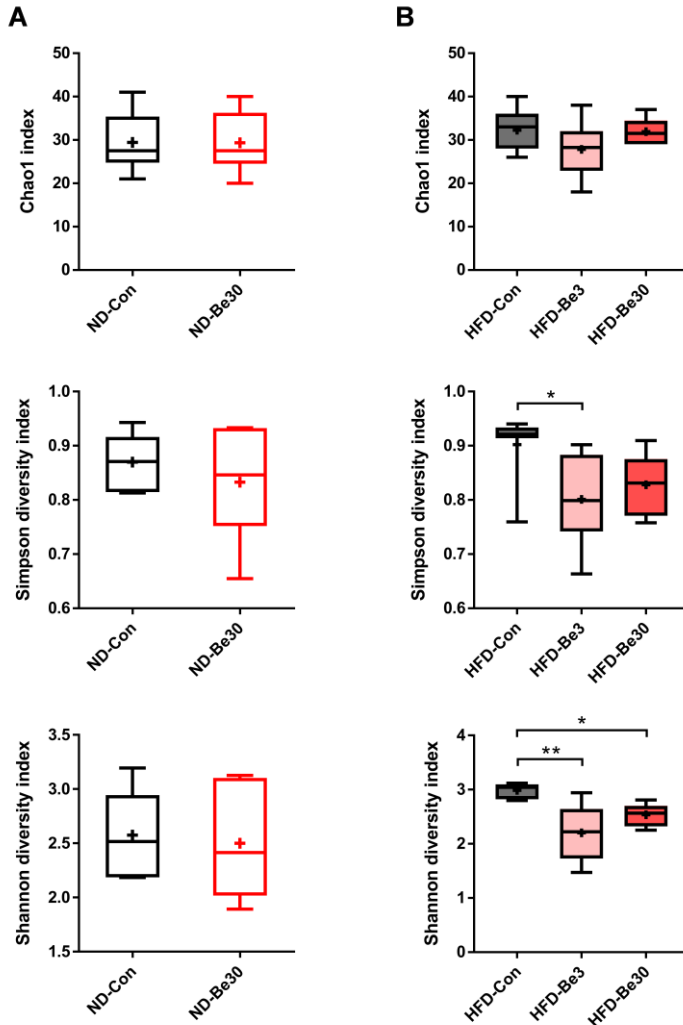


**Figure 3.6 Diversity analysis of the cecal microbial community based on Be exposure in (A) ND and (B) HFD.**

Chao1 species richness estimator, and Simpson and Shannon index values for microbial evenness were calculated to investigate the  $\alpha$ -diversity of each group. Box plots show median (horizontal line), mean (cross), and IQR, whiskers are minimum and maximum values. Significance was determined using unpaired two-tailed Student's *t* test or one-way ANOVA corrected for multiple comparisons with a Sidak test compared to the control group. \* $P < 0.05$ , \*\* $P < 0.01$ .

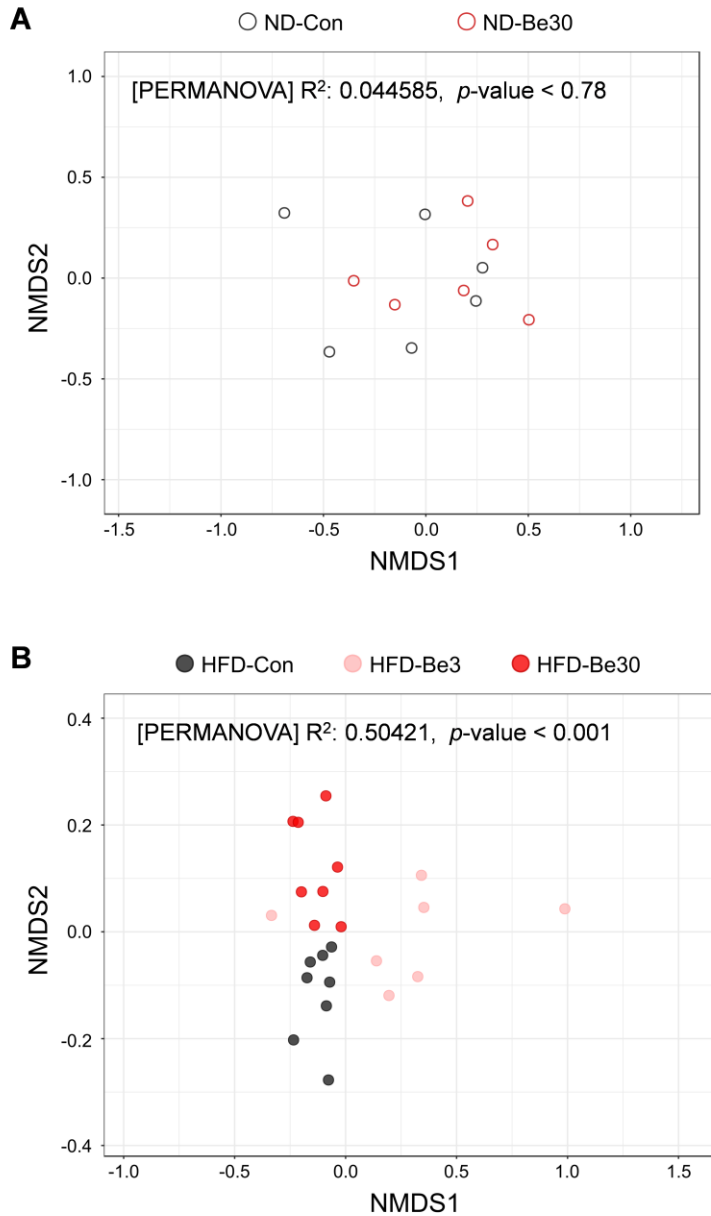


**Figure 3.7 Non-metric multidimensional scaling plots of cecal microbiota based on Be exposure in (A) ND and (B) HFD.**

Bray-Curtis distance matrix calculated from the genus-level relative abundance data were used. Significance was determined using PERMANOVA.

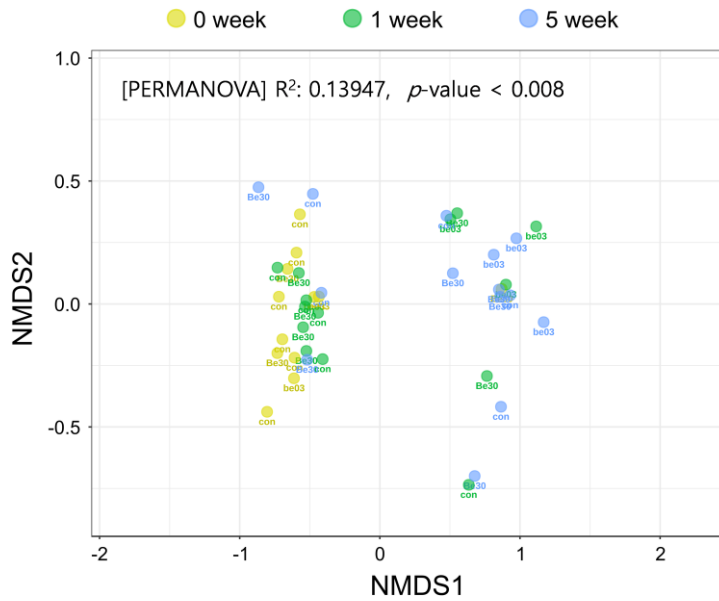
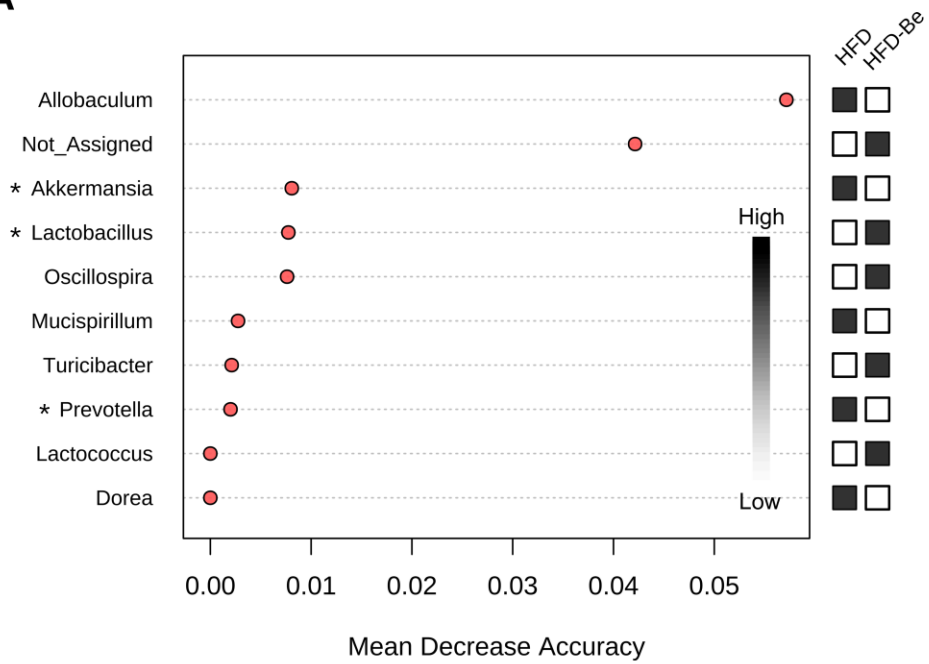


**Figure 3.8 Non-metric multidimensional scaling plot of fecal microbiota based on Be exposure over time in HFD mice.**

Stools were collected at three time points (0, 1, and 5 weeks) and analyzed for 16S rDNA sequencing. Bray-Curtis distance matrix calculated from the genus-level relative abundance data were used. Significance was determined using PERMANOVA.

**A**



**B**

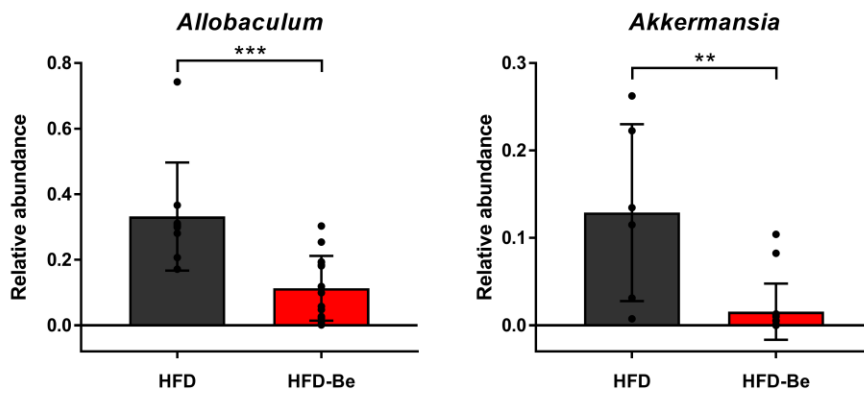


**Figure 3.9 Cecal microbiota perturbation and composition based on Be exposure.**

(A) Feature importance scores for the ten most predictive genera in the random forest classifier. Asterisk represents the microbial genera detected in human feces with over 0.1% of relative abundance in Figure 2.5. Feature importance was measured as the mean decrease in model accuracy when that feature's values were permuted randomly. (B) Relative abundances for two discriminative taxa: *Allobaculum* and *Akkermansia*. Data are shown as mean  $\pm$  SD. Significance was determined using Mann Whitney test compared to HFD control group. \*\* $P < 0.01$ , \*\*\* $P < 0.001$ .

**Be induces gut microbiome changes from *in vitro* cultured human feces.**

We carried out *in vitro* anaerobic colonic culture using human feces to check the impact of Be exposure on the human microbiome, not mice, and to evaluate the direct relationship between Be and gut microbiota excluding host effect (Figure 3.10). After 24 hours of *in vitro* cultivation, the microbial composition was maintained almost identical to the original human feces samples except for the slight reduction of *Bacteroides* and *Dialisters*. Notably, Be treatment has greatly changed the microbial composition. Similar to the results from the human study and *in vivo* HFD experiments group, microbial diversity showed a tendency to reduce during the *in vitro* culture with Be (Figure 3.11A). Also, the Be treatment groups were clearly distinguished from the Be untreated group, suggesting that exposure to Be could directly alter the microbial community (Figure 3.11B). In particular, there was a significant reduction in *Coprococcus*, *Bifidobacterium*, *Ruminococcus*, and *Roseburia*, and *Bilophila* significantly increased in Be exposure groups compared to the control group (Figure 3.12). In contrast to the mice experiments, eight of the ten most predictive genera were the microbiota that were also detected in human feces (> 0.1% of relative abundance).

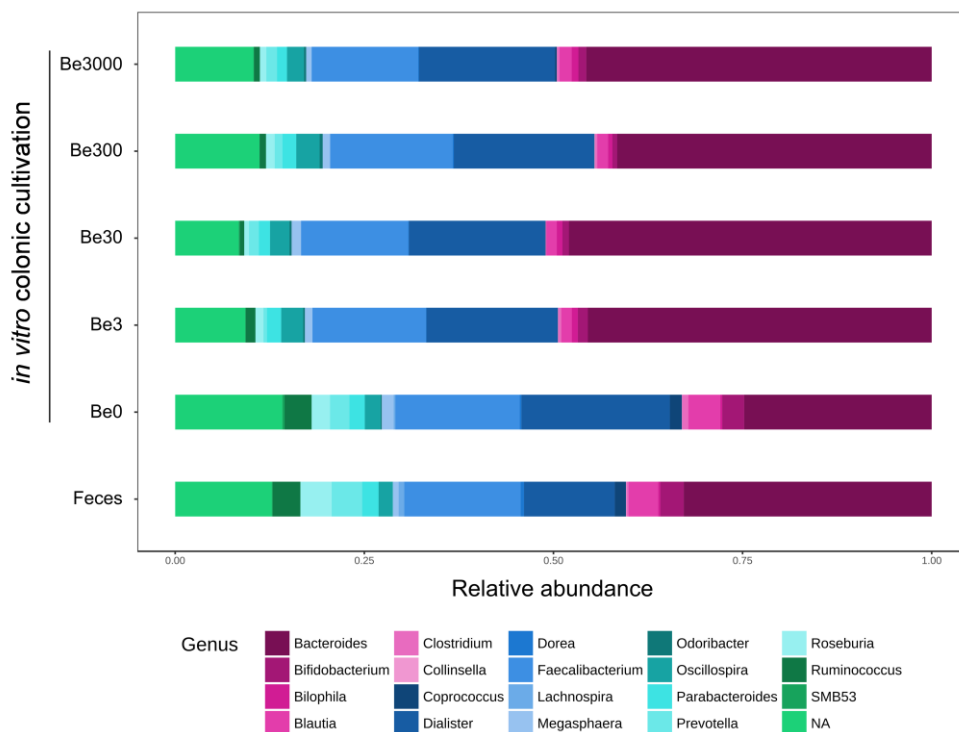
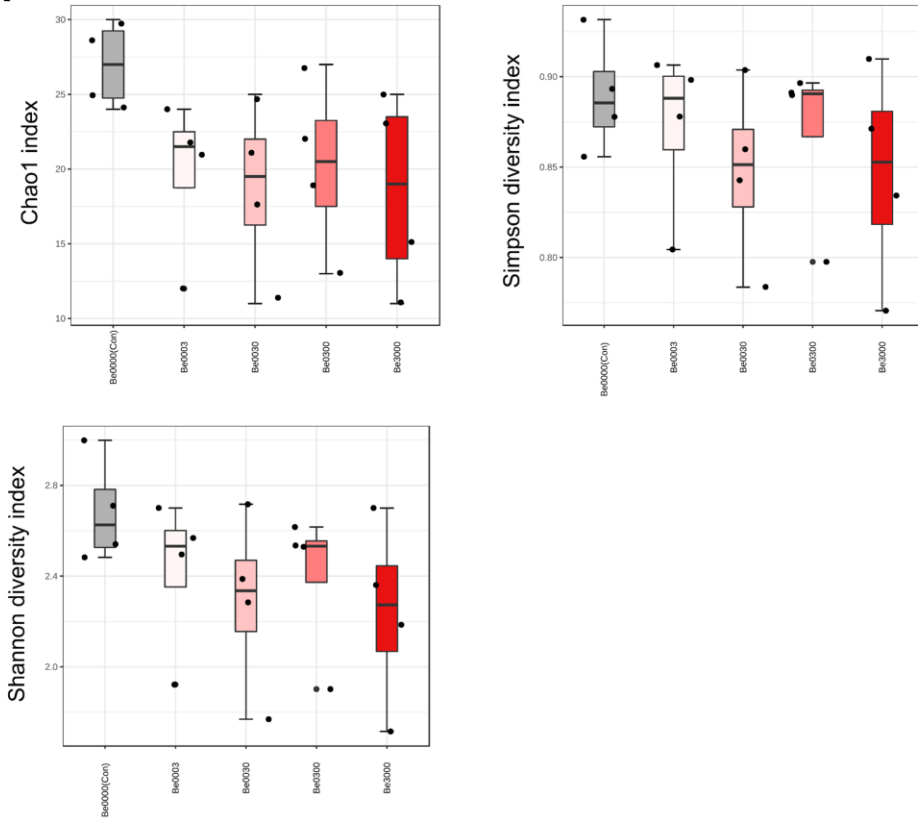


**Figure 3.10 The cultured human fecal microbiome composition profiles at the genus level based on Be concentration.**

Human feces were collected from three healthy volunteers and cultured in anaerobic condition with different Be concentration for 24 hr. The microbial pellet was used for 16S rDNA sequencing. Each color represents one bacterial family. Relative abundance of microbial taxa was determined by 16S rDNA sequencing.

**A**



**B**

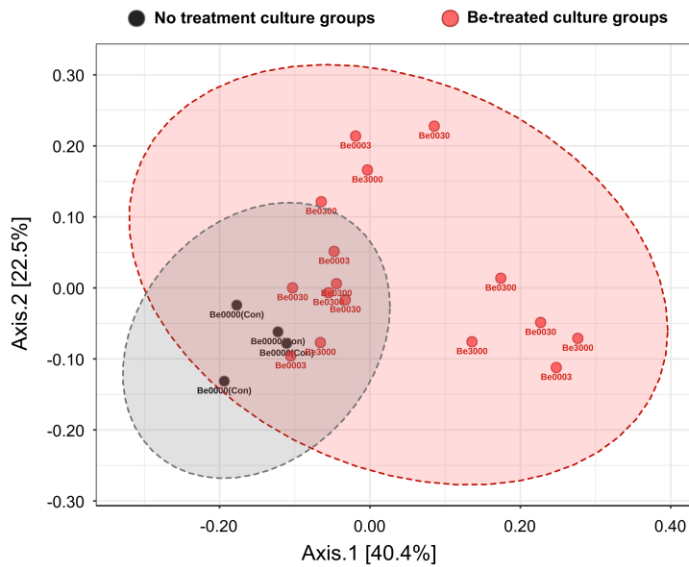
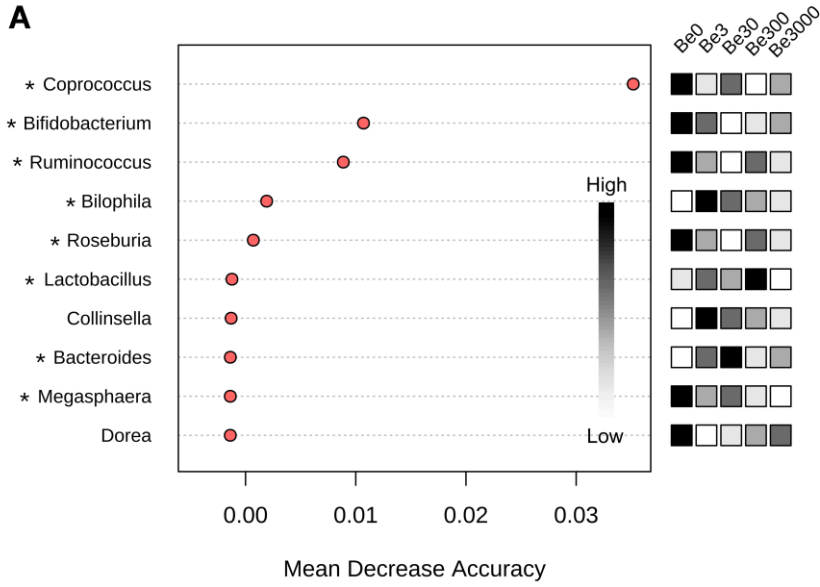


**Figure 3.11 Diversity analysis of the cultured human fecal microbial community based on Be concentration.**

(A) Chao1 species richness estimator, and Simpson and Shannon index values for microbial evenness were calculated to investigate the  $\alpha$ -diversity of each group. Box plots show median (horizontal line) and IQR; whiskers are  $1.5 \times$  IQR. (B) PCoA score plot with 95% confidence ellipse based on unweighted UniFrac metrics was analyzed to investigate the  $\beta$ -diversity of the community.

**A**



**B**

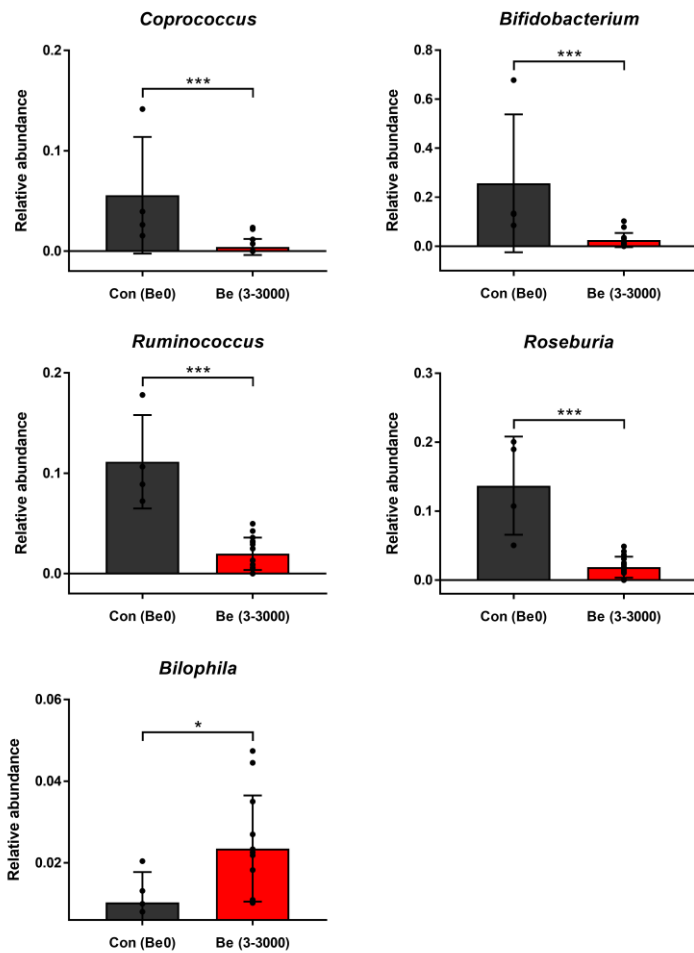


**Figure 3.12 Cultured human fecal microbiota perturbation and composition based on different Be concentration.**

(A) Feature importance scores for the ten most predictive genera in the random forest classifier. Asterisk represents the microbial genera detected in human feces with over 0.1% of relative abundance in Figure 2.5. Feature importance was measured as the mean decrease in model accuracy when that feature's values were permuted randomly. (B) Relative abundances for five discriminative taxa: *Coprococcus*, *Bifidobacterium*, *Ruminococcus*, *Roseburia*, and *Bilophila*. Data are shown as mean  $\pm$  SD. Significance was determined using Mann Whitney test compared to control (Be0) group. \* $P < 0.05$ , \*\*\* $P < 0.001$ .

**Be affects cecal SCFAs, colonic functions, and inflammation.**

We evaluated whether the exposure to Be could affect the production of SCFAs, the major microorganism-derived metabolites (Figure 3.13). The content of total SCFAs from cecum was not significantly different between the groups. However, there were significant changes in the ratio of acetate, propionate, and butyrate, the three major SCFAs. Acetate increased with Be exposure in the HFD group, while propionate and butyrate decreased significantly. Such a result was reasonable because *Akkermansia*, *Coprococcus*, and *Bifidobacterium*, which were reduced by exposure to Be, were the representatives of propionate producer, butyrate producer, and the microorganism that have a strong butyrogenic effect, respectively.

The Be exposure also affected the colonic mRNA expression in mice fed HFD (Figure 3.14). The inflammation-related genes including inducible nitric oxide synthase (Nos2) and interleukin (IL)1 $\beta$ , were highly expressed in Be groups, whereas the expression of IL-10, which was associated with the regulation of the inflammation, was inhibited. Also, Be exposure has markedly increased the expression of mucin (Muc)2 gene which was associated with gel-forming mucin production. The expression of occludin (Occl) and zonula occludens (Zo)-1 related to the intestinal cell integrity was not significantly affected. Notably, there has been a significant decrease in the peptide YY (PYY), the anorexigenic hormone.

We compared the ratio of Gram-positive (G<sup>+</sup>) to Gram-negative (G<sup>-</sup>) bacteria between groups to determine whether the metabolic abnormalities was induced by low-grade inflammation with metabolic endotoxemia. Although there was not a clear decrease in G<sup>+</sup>/G<sup>-</sup> ratio in HFD-Be groups (Figure 3.15A) and during *in vitro* anaerobic culture (Figure 3.15B), there

was a tendency to decrease depending on the Ca concentration. We then measured the plasma LPS levels to ensure that the LPS from G- bacteria spilled into the systemic circulation and caused metabolic endotoxemia (Figure 3.15C). The increase in Be exposure did not lead to a significant increase in plasma LPS levels, although there were slight increases. However, the plasma LPS levels in HFD groups were higher than ND groups, and HFD-Be3 and HFD-Be30 showed significant increases compared with ND-Con group, implying that the combination of HFD and Be exposure may lead to more endotoxemia.

To ensure whether the combinatory increase of Be and LPS, which might have been originated from the mucosal barrier disintegration by HFD, could be linked to the induction of inflammatory response, we performed *in vitro* cell experiment using mouse macrophage-like RAW264.7 cells. First, the microbial pellets and supernatants which were collected from the *in vitro* human feces cultivation with various concentrations of Be (3, 30, and 100 ppb) were treated on RAW264.7 cells. (Figure 3.16A). The relative nitrite production was upsurged in the pellet treatment groups, showing that the gut microbial cells might be a source of the inflammation increase. However, the effects of Be on the shifts in inflammation-related microbial composition were not strong because there were no noticeable nitrite changes in proportion to Be concentrations compared to control (cell pellets without Be). We then carried out the treatment of Be with or without LPS to assess the combinatory effects of Be and LPS (Figure 3.16B). Notably, the combination of Be and LPS significantly increased nitrite production compared to the LPS only treatment group, whereas the treatments of Be alone could not increase nitrite production.

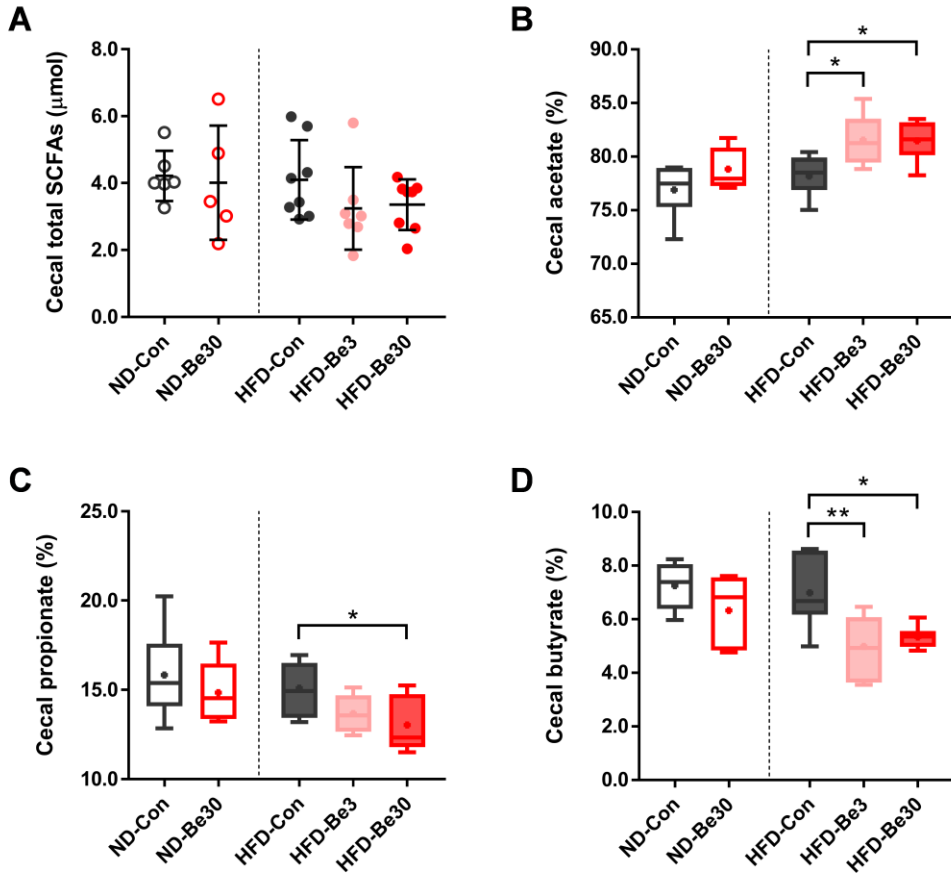


**Figure 3.13** Cecal SCFAs profiles based on Be exposure in ND and HFD mice.

(A) Cecal total SCFAs content; (B) cecal acetate ratio; (C) cecal propionate ratio; (D) cecal butyrate ratio. Box plots show median (horizontal line), mean (cross), and IQR, whiskers are minimum and maximum values. Significance was determined using two-tailed Student's *t* test or one-way ANOVA corrected for multiple comparisons with a Sidak test compared to each control group. \* $P < 0.05$ , \*\* $P < 0.01$ .

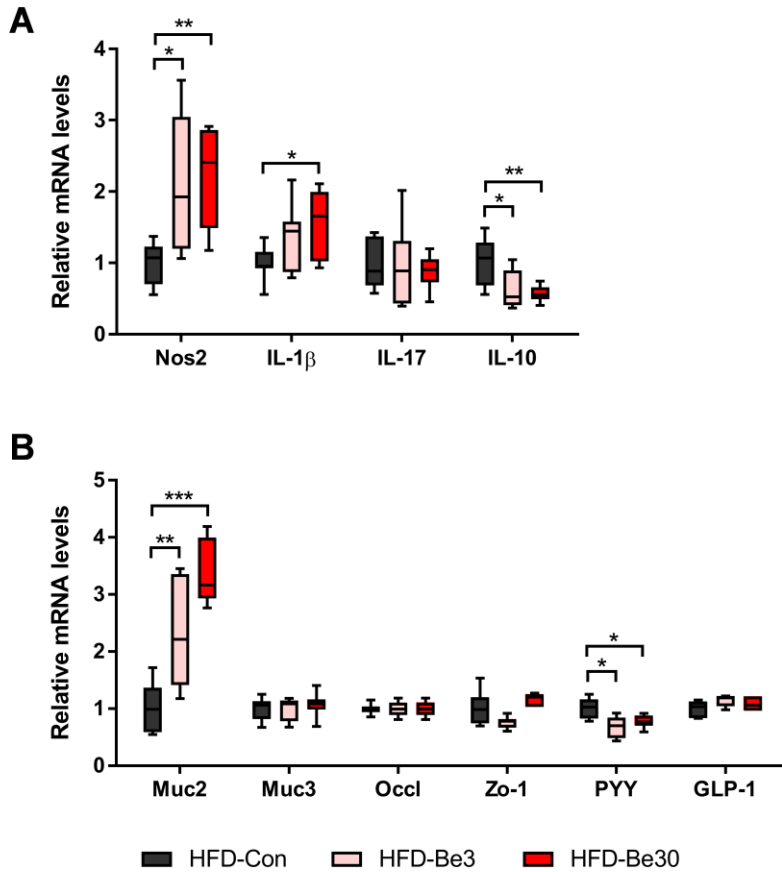


**Figure 3.14** mRNA levels of the indicated genes in proximal colons based on Be exposure in HFD mice.

(A) Inflammation and (B) mucin production (Muc2 and Muc3), tight junction (Occl and Zo-1), and appetite suppression-related genes (PYY and GLP-1) were investigated for their mRNA expression. Box plots show median (horizontal line) and IQR; whiskers are minimum and maximum values. Significance was determined using one-way ANOVA corrected for multiple comparisons with a Sidak test compared to the control group. \* $P < 0.05$ , \*\* $P < 0.01$ , \*\*\* $P < 0.001$ .

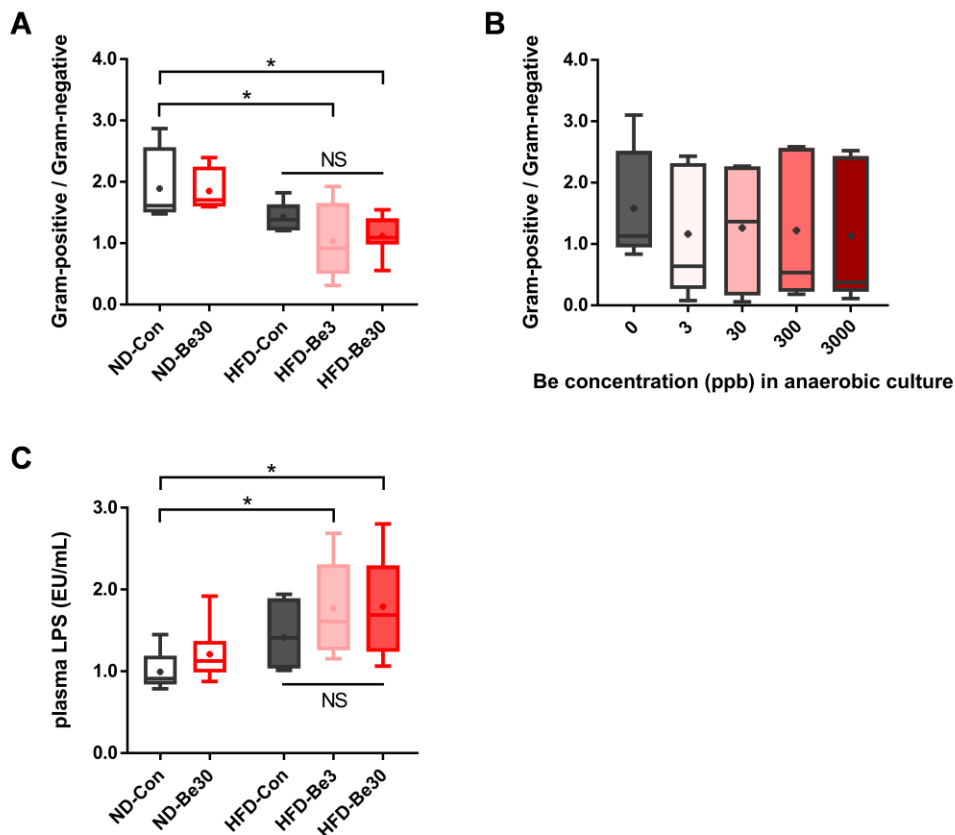


**Figure 3.15** The ratios of Gram-positive / Gram-negative bacteria in (A) *in vivo* mice experiments and (B) *in vitro* anaerobic cultivation, and the plasma LPS level based on Be exposure.

Box plots show median (horizontal line), mean (cross) and IQR; whiskers are minimum and maximum values. Significance was determined using two-tailed Student's *t* test or one-way ANOVA corrected for multiple comparisons with a Sidak test compared to ND-Con or HFD-Con group. NS represents no significant difference.

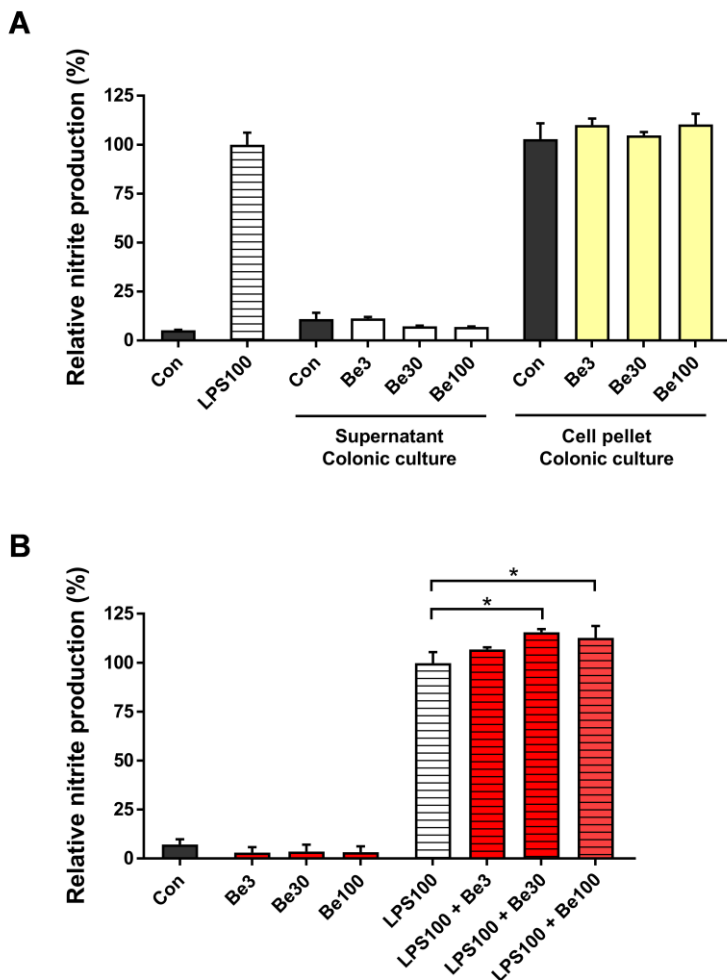


**Figure 3.16 Effect of Be and colonic culture with Be on nitrite level.**

(A) Fecal microbial supernatants and cell pellets from *in vitro* colonic culture with various Be concentrations (3, 30 and 100 ppb) were treated on RAW264.7 cells for 48 hr, and nitrite level was determined by a Griess assay. (B) Different concentrations of Be with or without LPS (100 ng/mL) were also treated on RAW264.7 cells. LPS (100 ng/mL) was used as a positive control. Data are shown as mean  $\pm$  SEM. Significance was calculated using one-way repeated measures ANOVA corrected for multiple comparisons with a Sidak test compared to positive control. \* $P < 0.05$ .

## Discussion

In this work, we used 3 ppb and 30 ppb of Be in drinking water to evaluate the effect of low dose of Be exposure on the metabolic homeostasis in HFD mice. The daily Be intake level of mice exposed to 30 ppb of Be water was equivalent  $\sim 1.7 \mu\text{g}/\text{kg}/\text{day}$  estimated from the consumption of drinking water, which closely corresponded to the Tolerable Daily Intake (TDI),  $2 \mu\text{g}/\text{kg}/\text{day}$ , and was much less than the commonly known No Observed Adverse Effect Level (NOAEL) of Be,  $0.1 \text{ mg}/\text{kg}/\text{day}$ <sup>(126)</sup>. Such a low dose of Be was still found to affect body weight gain and worsening MetS symptoms in HFD mice. In particular, analysis of gut microbiome and colonic mRNA expression revealed that exposure to not only 30 ppb but also 3 ppb of Be could disturb the microbial community and the expression of MetS-related genes in HFD mice, implying a possible low dose effect of Be. Considering that the present drinking water standard for Be established in 1992 by the Environmental Protection Agency (USEPA, 1992) is 4 ppb, and recent WHO report determined that it was not considered necessary to set a formal guideline value for Be in drinking water because Be rarely is found in drinking water at concentrations of health concern<sup>(114,127)</sup>, our findings may draw attention to the importance the current water standard for Be need to be strengthened.

The exposure to Be affected changes in gut microbiota, which was noteworthy that the significantly changed microorganisms included *Akkermansia* and *Bifidobacterium* (Figure 3.9; Figure 3.12), which have been heavily studied for their effects on MetS suppression<sup>(31,85-88)</sup>. Also, as is commonly found in MetS patients<sup>(18,57,84)</sup>, increased Be exposure has reduced microbial diversity (Figure 3.6; Figure 3.11). The result was the

same as the results of our human feces analysis in Chapter II. Among *Akkermansia*, *Allobaculum*, *Bifidobacterium*, *Coprococcus*, and *Ruminococcus*, which were significantly reduced in Be exposure, most microbes were G<sup>+</sup> bacteria except *Akkermansia* (Figure 3.9; Figure 3.12). The results of a significant reduction in the Gram-positive microorganisms such as *Coprococcus*, *Bifidobacterium*, *Ruminococcus*, and *Roseburia* were also found in the *in vitro* human feces culture, which shows the direct effects of Be on the gut microbiota. Gram-positive bacteria have a different cell structure compared to Gram-negative bacteria and are characterized by a thick peptidoglycan layer. These peptidoglycans have the metal-binding sites for magnesium and calcium, which may have been disrupted by Be<sup>(128)</sup>. When comparing the ratio of G<sup>+</sup> / G<sup>-</sup> bacteria considering all microbial component, there was no obvious difference in the ratio due to Be exposure in both mice study and *in vitro* colonic experiment (Figure 3.15A, B). Therefore, an accurate mechanism on how Be disrupt gut microbiota needs to be revealed through further study.

Although the *in vitro* colonic culture experiment was close to the ND, not the HFD condition, it showed a clear gut microbial clustering based on various Be concentrations. Probably, this is because the dynamic Be intake and excretion of *in vivo* mice model cannot be reproduced during *in vitro* experiment, and the cultivation was performed with static Be exposure for a long time. Despite the mechanical limitations of the *in vitro* experiment, the outputs were similar to the results from human data in Chapter II. In particular, the proportion of the human-specific genera, which were detected in human feces with over 0.1% of relative abundance in Chapter II, in the ten differentially different genera between groups were higher in our *in vitro*

colonic experiment (8 of 10) compared to the *in vivo* mice study (3 of 10). These results suggest that *in vivo* mice study may need to be combined with *in vitro* human feces culture experiments to explain the possible effects on humans better.

The Be exposure group showed noticeable differences in the profiles of SCFAs, which are the major microbial metabolites [Figure 3.13]. Several studies have shown that SCFAs play the pivotal role in linking gut microbiota and MetS. Butyrate and propionate are reported to be predominantly anti-obesogenic, inducing the secretion of anorexigenic hormones such as PYY and glucagon-like peptide (GLP)-1 for the appetite regulation<sup>(129-131)</sup>. On the contrary, since much of acetate is absorbed into the body and it acts as a substrate for hepatic and adipocyte lipogenesis, acetate is believed to have more obesogenic potentials than propionate and butyrate<sup>(131-134)</sup>. Also, a recent study has shown that the high level of plasma acetate originated from gut microbial dysbiosis could increase glucose-induced insulin secretion to promote the release of ghrelin, the orexigenic hormone, which can lead to metabolic disease through parasympathetic activation<sup>(135)</sup>. In this study, the ratio of acetate markedly increased in HFD-Be groups with a temporary increase in feed consumption (Figure 3.13B; Figure 3.1D). Furthermore, Be exposure significantly decreased the production of propionate and butyrate, and the anorexigenic PYY expression (Figure 3.13C, D; Figure 3.14B). Thus, we concluded that exposure to Be might have led to worsening MetS through parasympathetic activation.

The most plausible reason for a causal relationship of gut microbiota with MetS is low-grade inflammation induced by gut microbial dysbiosis.

The HFD increased Gram-negative bacteria and mucosal barrier disintegration, and then LPS spills into the systemic circulation, causing metabolic endotoxemia with low-grade inflammation<sup>(136-139)</sup>. In our study, the expression of inflammation-related genes was strongly affected by Be exposure (Figure 3.14A). The pro-inflammatory markers such as Nos2 and IL1 $\beta$  were highly expressed due to Be exposure, whereas the expression of IL-10, which is an anti-inflammatory cytokine related to inflammation regulation, was significantly reduced, indicating that the colonic inflammation condition became worse. These results were consistent with other studies<sup>(140,141)</sup>. In addition, HFD-Be groups indicated significant increases in plasma LPS levels compared to ND-Con group (Figure 3.15C]. These results show that the metabolic endotoxemia and intestinal inflammation have noticeably increased by HFD and Be. What's unusual is that the hyper-expression of Muc2 gene related to the release of the gel-forming mucin was observed (Figure 3.14B). According to another study, if the pro-inflammatory cytokines were increased, the expression of Muc2, Muc1, and Muc4 was increased from the goblet cell, and then the continuous Muc1 and Muc4 expression finally promoted cancer development<sup>(142)</sup>. Given that Be is one of the most toxic metals, the hyper-expression of Muc2 might be due to the compensatory host defense response against Be exposure to prevent the impairment of the mucus barrier<sup>(143)</sup>.

Some studies were conducted to evaluate the risk of Be through the oral intake<sup>(144-146)</sup>. Unlike our results, most of them have shown less than 10 percent body weight loss in animal studies. Perhaps, this is because the experimental conditions are different from our study. First, that studies

focused on the risk of cancer of Be, and therefore tested at a concentration of more than 5 ppm of Be, which was approximately 150 times higher than the maximum concentration (30 ppb) we used. The second reason is that most studies evaluated Be risk with ND condition, whereas the low dose of Be exposure increased the risk under HFD conditions in our study. Notably, some of the preceding studies have found that Be exposure increased in the body weight and feed intake up to early 30 days<sup>(147,148)</sup>. The results were consistent with our results of increased feed intake at the beginning stage of the experiment. Also, our cell experiments showed the combinatory effects of Be and LPS on the increase in inflammation, suggesting that low dose of Be could be toxic under certain conditions (Figure 3.16B). There was a relating report that the co-treatment with LPS and 100  $\mu$ M of Be sulfate, equivalent to 900 ppb of Be, significantly increased IL1 $\beta$  with the significant decrease in IL-10 compared to LPS only treatment<sup>(140)</sup>. The result was consistent with our findings, and even our results could be obtained from the low dose of Be treatment that was about 30 times less than the test. Considering the results of our study comprehensively, the risk of Be may become more severe when the mucosal barrier functions are incomplete, such as HFD or early development stages. In addition, Be can worsen the intestinal environment by changing the gut microbial composition and their functionality. Verification studies through *in vitro* cell experiments are needed to further study the effects of Be directly on hosts. Also, the effects of Be on the gut microbial dysbiosis should be assessed from a systemic perspective by providing an accurate picture of the disturbance mechanism. Thus, further studies are required to demonstrate the risk of Be under various experimental conditions. Figure 3.17 indicates the possible

mechanisms explaining the overall effects of a low dose of Be on gut microbiota and MetS.

In conclusion, we redefined the risk of a low dose of Be to MetS. Exposure to Be along with HFD led to worsening MetS by the changes in gut microbiota and mucosal barrier dysfunction. Our study is of great significance because it first suggested that the global legal standards for the Be content of drinking water might be at a dangerous level. The human risks of Be and its accurate mechanisms of action are expected to be verified by further studies.

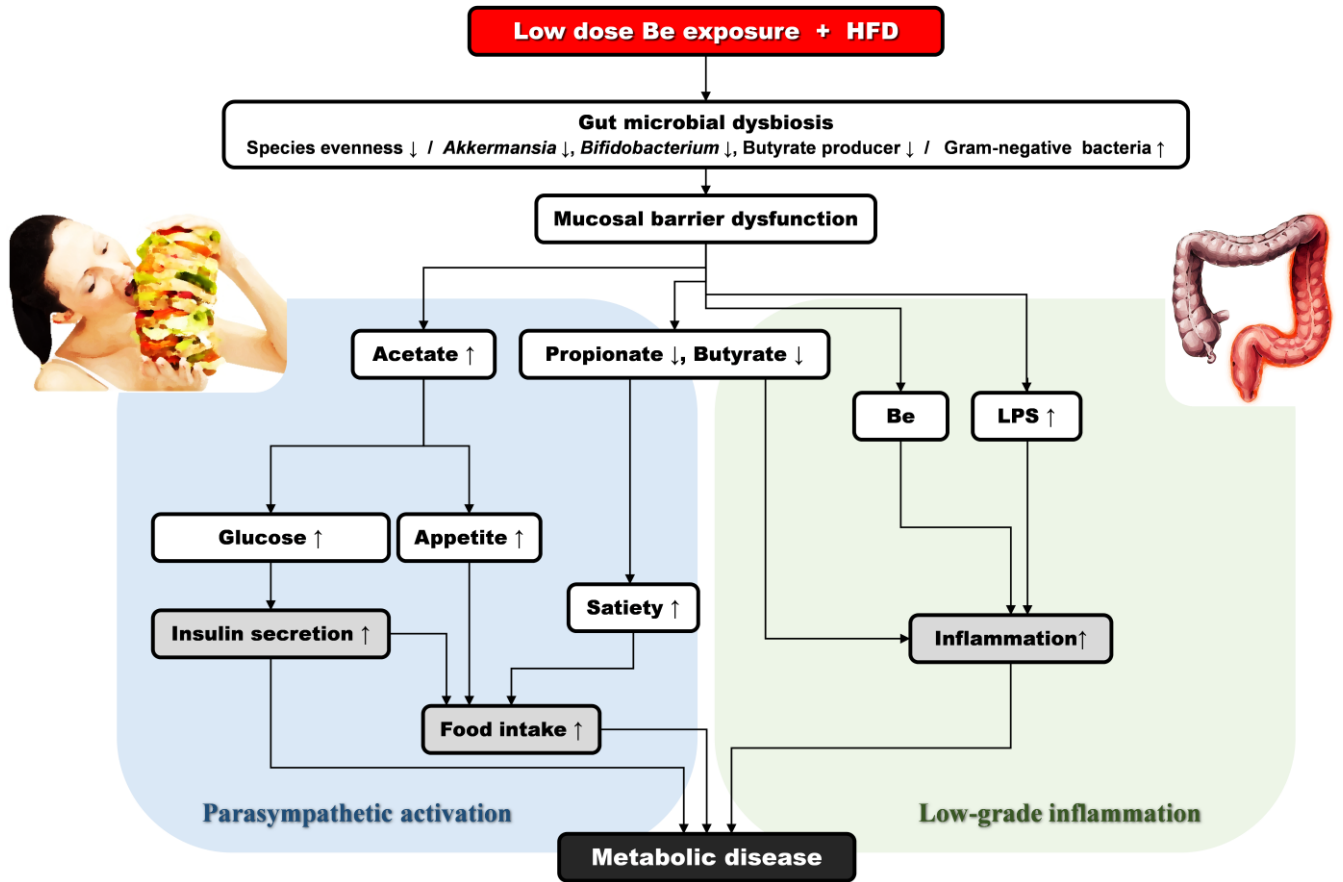


Figure 3.17 Possible mechanisms explaining the effects of Be on gut microbiota and MetS.

**CHAPTER IV.**

**CALCIUM SUPPLEMENTS IMPROVE  
HOST METABOLIC HOMEOSTASIS IN  
HIGH FAT DIET MICE WITH CHANGES IN  
GUT MICROBIOTA**

### **Introduction**

Metabolic syndrome (MetS), one of the major global public health concerns, is defined by a cluster of metabolic disorders including obesity, insulin resistance, dyslipidemia, and hypertension<sup>(12,13)</sup>. The high incidence of MetS is associated with excessive energy intake, low physical activity, genetics, and environmental factors<sup>(14,20,21,49,50,106)</sup>. Recent studies suggest a possible role of gut microbiota in MetS<sup>(16-19)</sup>. Microbial alteration could not only affect energy intake by changing the digestive capacity and increasing lipid absorption but also induce metabolic endotoxemia that can trigger weight gain and insulinemia through low-grade chronic inflammation<sup>(149)</sup>. Also, short chain fatty acids (SCFAs), the major colonic fermentation products of dietary fiber, could contribute to energy homeostasis via appetite regulation<sup>(150,151)</sup>.

Epidemiologic studies suggest that dietary calcium (Ca) intake has been inversely linked to MetS<sup>(152-156)</sup>. Ca intake was lower than recommended for a majority of MetS individuals and Ca supplementation could improve the metabolic abnormalities by changing lipid profiles, decreasing fat accumulation, and increasing fecal fat excretion<sup>(157-159)</sup>. However, not all studies have shown consistent results<sup>(160,161)</sup>, probably due to differences in the concentration, treatment duration, and form of Ca used in the experiment. For example, Ca-carbonate and Ca-citrate, the two most commonly used Ca supplements, can result in different effects on MetS, because Ca-citrate has been reported as having higher bioavailability than Ca-carbonate<sup>(162-164)</sup>.

Despite the emphasis on the relationships between MetS and gut microbiota, most Ca studies so far have been conducted without taking into account the factor of gut microbiota. There are several influential papers

considering these relationships, but these studies have some limitations<sup>(89,90)</sup>. They performed a targeted bacterial profiling instead of 16s amplicon sequencing which can analyze the entire microbial community, or the analysis of microbial metabolites such as SCFAs was not applied despite the growing evidence that SCFAs can be involved in appetite control.

In this study, we assessed and compared the effects of two different Ca supplements, Ca-carbonate and Ca-citrate, on the improvement of host metabolic homeostasis in high fat diet mice. Furthermore, we analyzed the cecal microbiome, SCFAs production, and the expression of MetS-related genes to gain deeper insight into the Ca mechanism.

### **Materials and Methods**

**Animals and exposure.** All animal protocols were approved by the Institutional Animal Care and Use Committee of the Korean Institute of Science and Technology (No. 2018-036) and strictly followed National Institutes of Health guidelines. Male C57BL/6 mice (5-weeks-old, 20-22 g; Central Lab. Animal Inc., Seoul, Korea) were housed in individually ventilated cages at  $23 \pm 0.5^\circ\text{C}$  and 10% humidity under a 12 hr-light-dark condition with access to feed and water ad libitum. All animals were acclimated for seven days and divided into 2-3 animals/cage, ensuring equal weight average. Feeds containing two different Ca supplements (Ca-carbonate or Ca-citrate) were prepared with two concentrations of Ca (4 g/kg and 12 g/kg) by Dooyeol Biotech (Seoul, Korea) and presented as pellets to the mice. In total, four diets contained 4.6 kcal/g, 45% of energy content as fat and 21% as protein with each different Ca supplement: (1) Ca-carbonate 0.4% (n = 8), (2) Ca-carbonate 1.2% (n = 8), (3) Ca-citrate 0.4% (n = 8), and (4) Ca-citrate 1.2% (n=8). The feed was changed twice a week. Feed and water intake were recorded continuously once a week on the basis of cages and was calculated as average food intake per mouse per week. Body weight of each mouse was measured once a week.

**Sample collection.** The stool samples were collected once a week and immediately stored at  $-80^\circ\text{C}$  before further analysis. Animals were euthanized by  $\text{CO}_2$  inhalation at the beginning of the light cycle and after 16 h of food deprivation. Blood samples were collected by cardiac puncture in microtubes containing EDTA and centrifuged at 1,000 g and  $4^\circ\text{C}$  for 15 min to obtain the plasma, and stored at  $-80^\circ\text{C}$  for subsequent biochemical

measurements. Epididymal white adipose tissue (eWAT), cecum, and colon of each mouse were precisely dissected, weighed and collected for further analysis. All tissues were rinsed with saline and snap-frozen at -80°C.

**Biochemical measurements.** Plasma triglyceride (DoGEN Bio Co., Ltd, Seoul, Korea), glucose (Abcam, Cambridge, UK), insulin (Abcam), leptin (Abcam), and adiponectin (Abcam) concentration were measured using commercial ELISA kits according to the manufacturer's instructions. Lipopolysaccharide (LPS) was detected using an endpoint chromogenic endotoxin quantitative test (Signalway Antibody, College Park, MD, USA). To measure the cecal Ca content, a colorimetric Ca Detection Kit (Abcam) was used.

**16S rDNA amplicon sequence analysis.** DNA was extracted from cecum, stools, and *in vitro* batch culture samples using a QIAamp DNA Stool Mini Kit (QIAGEN, USA) with the additional bead-beating procedure to improve the DNA recovery for Gram-positive bacteria. The 16S rRNA genes were amplified using an improved dual-indexing amplification of the V3-V4 region (319F/806R) of the 16S rRNA gene with heterogeneity spacer [Fadrosh, 2014]. PCR products were purified using AMPure XT beads (Beckman Coulter Genomics, Danvers, MA, USA) and quantified using a Qubit dsDNA high-sensitivity reagent (Invitrogen, Carlsbad, CA, USA). Sequencing was conducted on the MiSeq platform using a paired-end 2 × 300-bp reagent kit (Illumina, San Diego, CA, USA). The raw reads were demultiplexed, assembled, and quality-filtered in QIIME 2 (v2018.6), using default settings<sup>(118)</sup>. DADA2 was used to filter chimeric reads and artifacts

commonly present in Illumina amplicon data<sup>(119)</sup>. To classify filtered reads to taxonomic groups, a Naive Bayes classifier was trained using the 16S rRNA region (V3-V4), the primer set and read length used (319F/806R, 469 bp), and the Greengenes 97% reference set (v13.5)<sup>(120-122)</sup>. This trained feature classifier was then used to assign taxonomy to each read using the default settings in QIIME. Microbial composition at a certain level, and  $\alpha$ - and  $\beta$ -diversity was analyzed using MicrobiomeAnalyst<sup>(123)</sup>. Principal coordinate analysis (PCoA) plot was generated using unweighted Unifrac distances to represent microbiota compositional differences among groups visually. Random forest, a supervised learning method for the classification of human microbiome data<sup>(124)</sup>, was used to select subsets of taxa (genus level) that are highly discriminative of the type of community from Ca-treated mice. We measured feature importance as the mean decrease in model accuracy when that feature's values were permuted randomly using 500 trees and seven repetitions.

**Short chain fatty acids (SCFAs) measurements.** Cecal SCFAs content was determined by gas chromatography according to David's method<sup>(125)</sup>. Cecal contents (~80 mg) were homogenized in 500  $\mu$ L of deionized water. After that, the samples were acidified with 50  $\mu$ L of 50% sulfuric acid, followed by vortexing at room temperature for 5 min. After centrifugation at 14,000 g for 10 min, 400  $\mu$ L of the supernatant was moved to a new tube, and 40  $\mu$ L of the internal standard (1% 2-methyl pentanoic acid) and 400  $\mu$ L of anhydrous ethyl ether were added. The tube was vortexed for 1 min and then centrifuged at 14,000 g for 10 min. The upper ether layer was used for further analysis. Volatile Free Acid Mix (Sigma) was used as the SCFAs

standard for the quantification of acetate, butyrate, isobutyrate, propionate, valerate, and isovalerate. GC-FID (GC 450, Bruker, USA) was used to analyze the SCFAs content with fused silica capillary columns (Nukol, 30 m × 0.25 mm, 0.25 µm film thickness). The oven temperature was 170 °C, and the FID and injection ports were set to 225 °C. Nitrogen was used as the carrier gas, and the sample injection volume was 2 µL.

**RNA extraction and real-time PCR analysis.** Total RNA was extracted from colon tissues (~50 mg) using Trizol reagent (Thermo, South Logan, UT, USA) according to the manufacturer's instructions, followed by concentration measurement. cDNA was synthesized from 1 µg of total RNA using Superscript IV reverse transcriptase (Thermo). Real-time PCR was performed using the LightCycler 480 detection system (Roche Diagnostics, Mannheim, Germany) and LightCycler 480 SYBR Green I Master (For primer sequences, see Appendix E.). Samples were run in duplicate in a single 384-well reaction plate. Data were normalized to the housekeeping RPL19 gene and analyzed according to  $\Delta\Delta CT$  method.

**Statistical analysis.** All the grouped data were statistically performed with R software or GraphPad Prism 7. Significance was determined using Student's *t* test, Mann Whitney test or one-way ANOVA corrected for multiple comparisons with a Sidak test compared to each control group. Microbial data processing were performed by MicrobiomeAnalyst.

### **Results**

#### **Effects of Ca supplementations on the suppression of metabolic syndrome in high fat diet mice**

To determine whether Ca intake could reduce metabolic features associated with a HFD, we fed mice the feeds containing 0.4% of Ca as the recommended Ca level, and 1.2% of Ca as the high Ca intake group. Also, we conducted the comparison study between Ca-carbonate and Ca-citrate to check if there was a difference in efficacy according to the type of Ca supplements. According to Figure 4.1, the Ca-carbonate group did not show a distinct body weight change due to Ca concentration, and the consumption of feed maintained constant between 0.4% and 1.2% of Ca-carbonate groups. On the other hand, there was a significant body weight decrease at 1.2% of Ca-citrate group compared to the control group. Notably, the feed intake was significantly decreased in the 1.2% of Ca-citrate group.

To further investigate the effects of Ca on the adiposity and host metabolism induced by HFD, we measured eWAT weight and the plasma level of MetS biomarkers (Figure 4.2). Similar to the body weight gain results, only Ca-citrate between the two Ca supplements showed a weight loss of eWAT due to increased Ca concentration. Although the plasma concentrations of TGs, insulin, and adiponectin were not significantly different between the groups, the plasma level of glucose and leptin was all reduced in both high Ca-carbonate and high Ca-citrate group, indicating that Ca-carbonate, as well as Ca-citrate, can improve metabolic disorder induced by HFD.

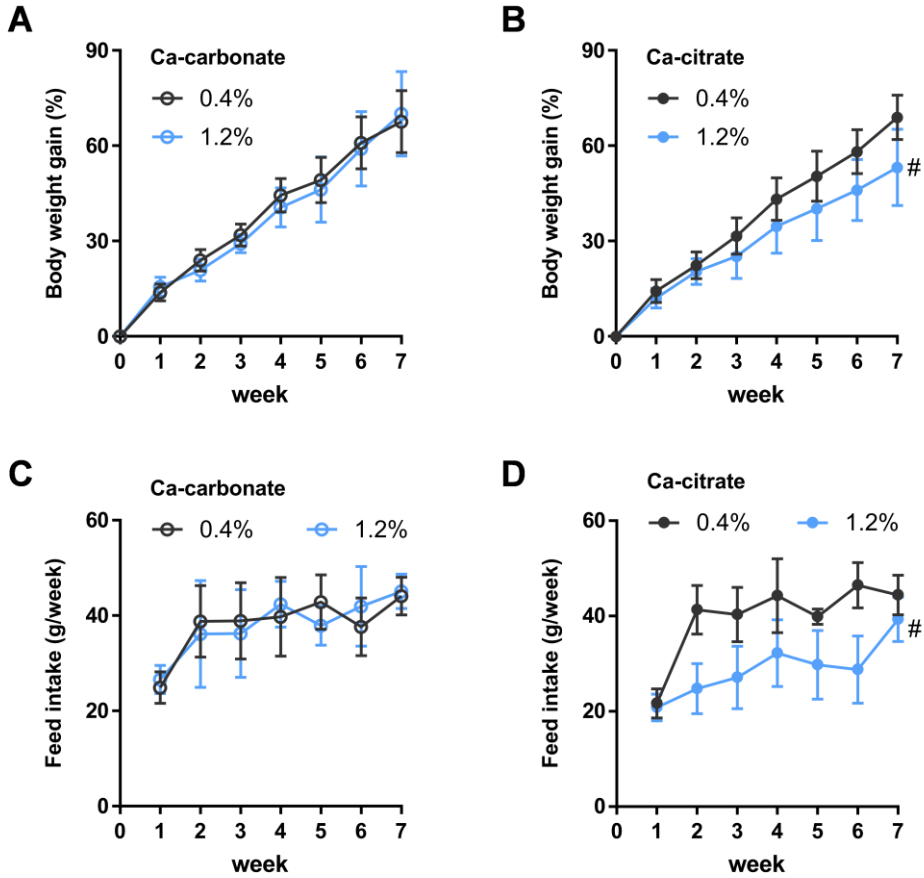


**Figure 4.1 Body weight gain (%) and feed intake over time in the control (0.4% Ca) groups and Ca supplementation groups (1.2% Ca) under a high fat diet (N=8).**

Two types of Ca (Ca-carbonate and Ca-citrate) were prepared and presented as pellets to the mice. (A) Body weight gain (%) of Ca-carbonate group; (B) body weight gain (%) of Ca-citrate group; (C) feed intake of Ca-carbonate group; (D) feed intake of Ca-citrate group. Data are the means  $\pm$  SEM. Significance was determined using two-way group ANOVA corrected for multiple comparisons with a Bonferroni test (# $P < 0.05$ ) compared to control group (black color).

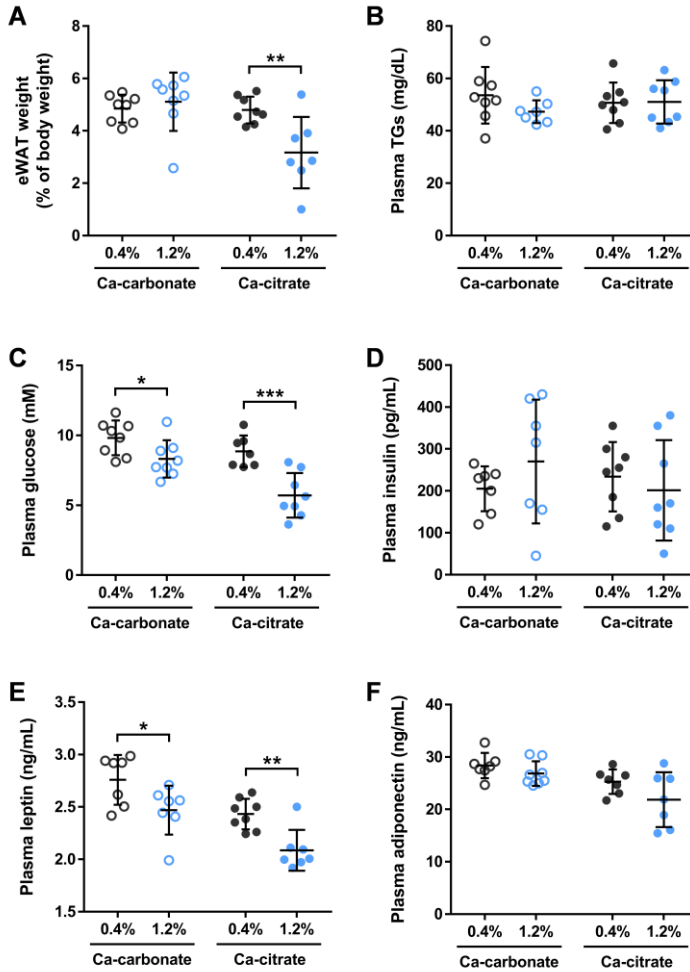


**Figure 4.2 Effect of Ca-carbonate and Ca-citrate supplementation on host metabolism under a high fat diet.**

(A) Epididymal white adipose tissue mass (eWAT); (B) plasma triglycerides (TGs); (C) plasma glucose; (D) plasma insulin; (E) plasma leptin; (F) plasma adiponectin in the control and each Ca supplementation group (n = 8/group). Data are shown as mean ± SD. Significance was determined using two-tailed Student's *t* test. \* $P < 0.05$ , \*\* $P < 0.01$ , \*\*\* $P < 0.001$ .

### Effects of Ca supplementations on alterations of gut microbiota in high fat diet mice

Next, we performed the microbiome analysis from mice cecum to evaluate whether the increase in Ca intake could affect the microbial composition change (Figure 4.3). When performing an  $\alpha$ -diversity analysis, both Ca-carbonate and Ca-citrate significantly increased the Chao1 index, which is related to species richness (Figure 4.4), whereas Simpson and Shannon diversity index, which accounts for both abundance and evenness of the species, did not show any significant differences between the groups.

We then performed a PCoA analysis to check the difference in the microbial clusters among the groups (Figure 4.5). There was a clear clustering between 0.4% of Ca (black color) and 1.2% of Ca (blue color). On the contrary, Ca-carbonate (blank circles) and Ca-citrate (filled circles) did not show a clear cluster separation, suggesting that the Ca concentration is more important than Ca supplements type in the microbial community shift. We identified the differentially abundant gut microbiota between 0.4% and 1.2% Ca group using the random forest analysis. *Akkermansia*, known for improving glucose homeostasis<sup>(31-33,101)</sup>, significantly increased in the high Ca group. *Acinetobacter*, SMB53, and *Klebsiella* also showed an increasing trend (Figure 4.6). Figure 4.6B indicates that the increase in *Akkermansia* is seen in both high Ca-carbonate and high Ca-citrate group. When we evaluated whether Ca concentration could affect the Gram-positive to Gram-negative ratio, there was an increasing tendency based on Ca-citrate concentration, but it was not statistically significant (Figure 4.7).

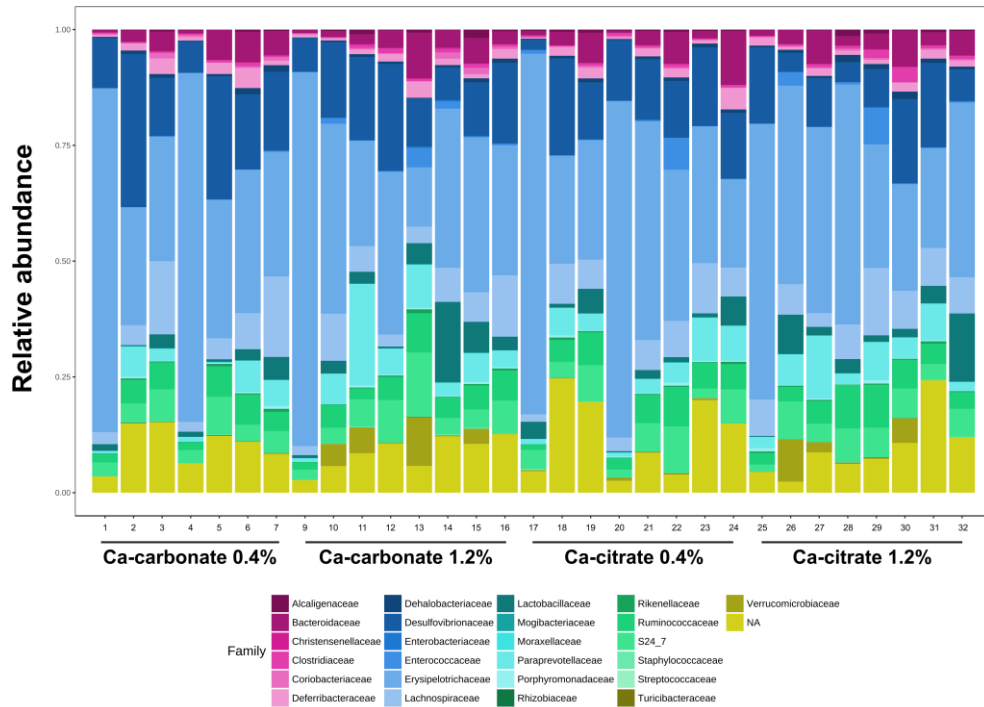


**Figure 4.3** The cecal microbiome composition profiles at the family level with Ca supplementations under a high fat diet.

Each color represents one bacterial family. Relative abundance of microbial taxa was determined by 16S rDNA sequencing.

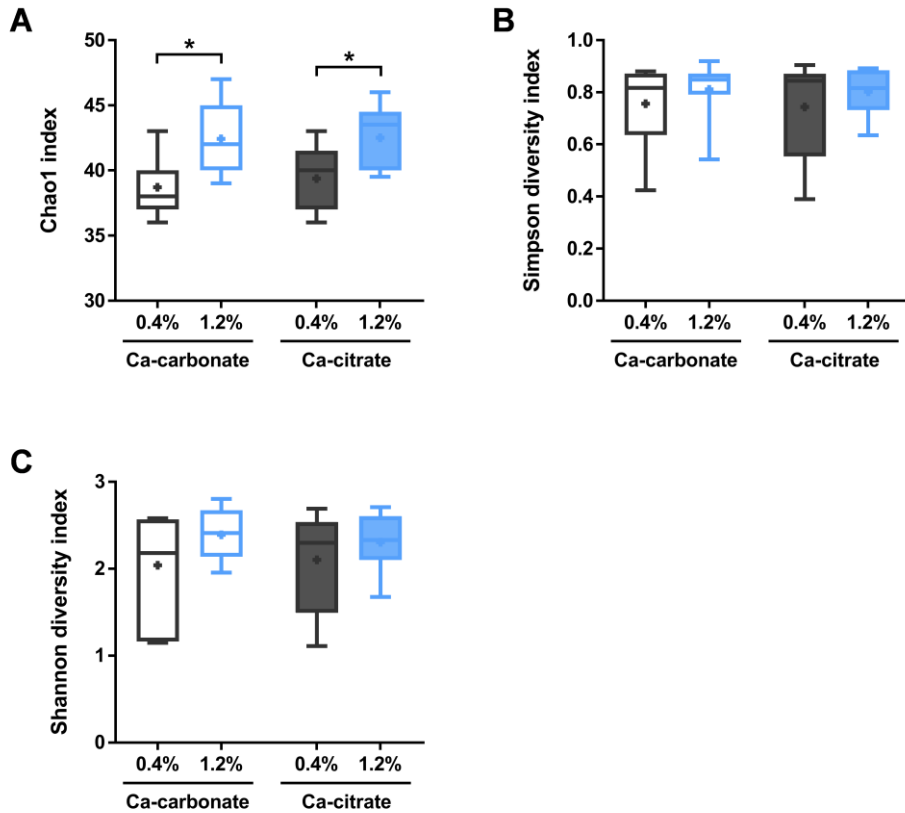
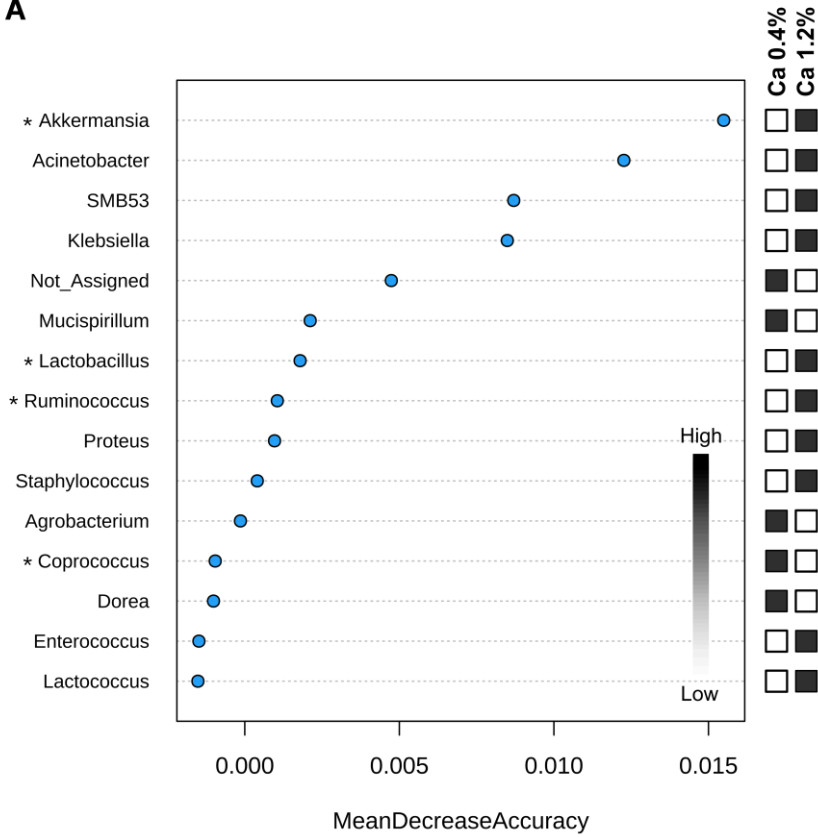


**Figure 4.4**  $\alpha$ -Diversity analysis of the cecal microbial community based on Ca supplementations.

Chao1 species richness estimator, and Simpson and Shannon index values for microbial evenness were calculated to investigate the  $\alpha$ -diversity of each group. Box plots show median (horizontal line), mean (cross), and IQR, whiskers are minimum and maximum values. Significance was determined using two-tailed Student's *t* test. \* $P < 0.05$ .



A



B

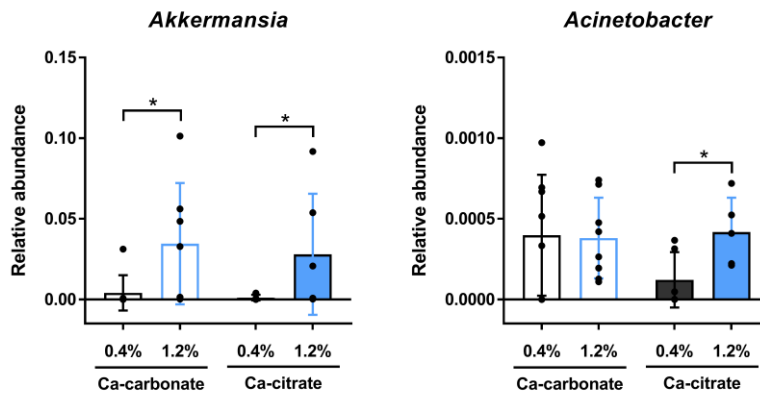


### **Figure 4.6 Cecal microbiota changes and composition based on Ca supplementations.**

(A) Feature importance scores for the 15 most predictive genera in the random forest classifier. Asterisk represents the microbial genera detected in human feces with over 0.1% of relative abundance in Figure 2.5. Feature importance was measured as the mean decrease in model accuracy when that feature's values were permuted randomly. (B) Relative abundances for two discriminative taxa: *Akkermansia* and *Acinetobacter*. Data are shown as mean  $\pm$  SD. Significance was determined using Mann Whitney test compared to HFD control group. \* $P < 0.05$ .

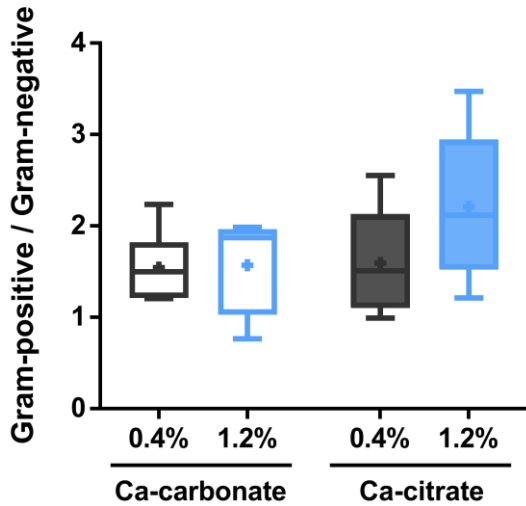


**Figure 4.7 The ratios of Gram-positive/Gram-negative bacteria based on Ca supplementations.**

Box plots show median (horizontal line), mean (cross), and IQR, whiskers are minimum and maximum values. Significance was determined using two-tailed Student's *t* test.

### **Effects of Ca supplementations on microbial SCFAs production and MetS-related gene expression**

To evaluate the effects of Ca supplementations on metabolic functions of gut microbiota, we analyzed the cecal SCFAs production from each group (Figure 4.8). Regardless of the types or concentrations of Ca supplements, the total SCFAs content did not show any significant differences between groups. However, the ratio of each SCFA was significantly different. Notably, both 1.2% of Ca-carbonate and 1.2% of Ca-citrate groups showed a significant decrease in acetate ratio compared to each control group. On the other hand, the ratio of propionate markedly increased in the Ca treatments with high concentration, and 1.2% of Ca-citrate showed a higher increase. There was no significant difference in butyrate ratio between groups.

We then determined whether Ca supplements could affect colonic gene expression (Figure 4.9). First, we assessed the expression of appetite suppressing genes including peptide YY (PYY) and glucagon-like peptide-1 (GLP-1) from proximal colons. Although PYY maintained constant, the expression of GLP-1 significantly increased with the Ca supplementations. Compared to 1.2% of Ca-carbonate, 1.2% of Ca-citrate showed a higher increase in GLP-1 expression. Between two Ca supplements, only 1.2% of Ca-citrate supplementation led to significant decreases in the expression of the inflammatory markers such as tumor necrosis factor (TNF) $\alpha$  and interleukin (IL)17. To further investigate whether Ca supplementations could influence mucosal barrier function, we evaluated the expression of mucin glycoprotein and tight junction-related genes. Although there were no differences in mucin (Muc)3 and zonula occludens (Zo)1 expression, the

expression of occludin (Occl) significantly increased with 1.2 % of Ca-citrate treatment. Notably, the Muc2 gene was highly expressed in both 1.2% of Ca-carbonate and 1.2% of Ca-citrate. To determine whether the increase in the expression of mucosal barrier function-related genes such as Muc2 and Occl attenuated the HFD-induced endotoxemia, we analyzed plasma LPS level. In Ca-citrate group, the high concentration of Ca supplementation markedly decreased plasma LPS level, whereas 1.2% of Ca-carbonate did not show a significant reduction in plasma LPS level, although a slight decreasing pattern was seen.

In Figure 4.9C, the supplementation with 0.4% of Ca-citrate showed the significantly higher basal expression of Muc2 compared to Ca-carbonate control group, suggesting that the difference in bioavailability between the Ca supplements might have resulted in this result. Thus, to determine whether there was a difference in bioavailability of the two Ca supplements, we compared cecal Ca content between groups (Figure 4.10). Although there was no difference in feed intake between each control group of Ca-carbonate and Ca-citrate (Figure 4.1C, D), the cecal Ca content of Ca-citrate 0.4% group was significantly lower than that of Ca-carbonate 0.4% group, implying that the Ca from Ca-citrate have been better absorbed through the gastrointestinal tract. We were able to confirm that the two groups of Ca levels had increased to a similar level with the high concentration of Ca supplementations.

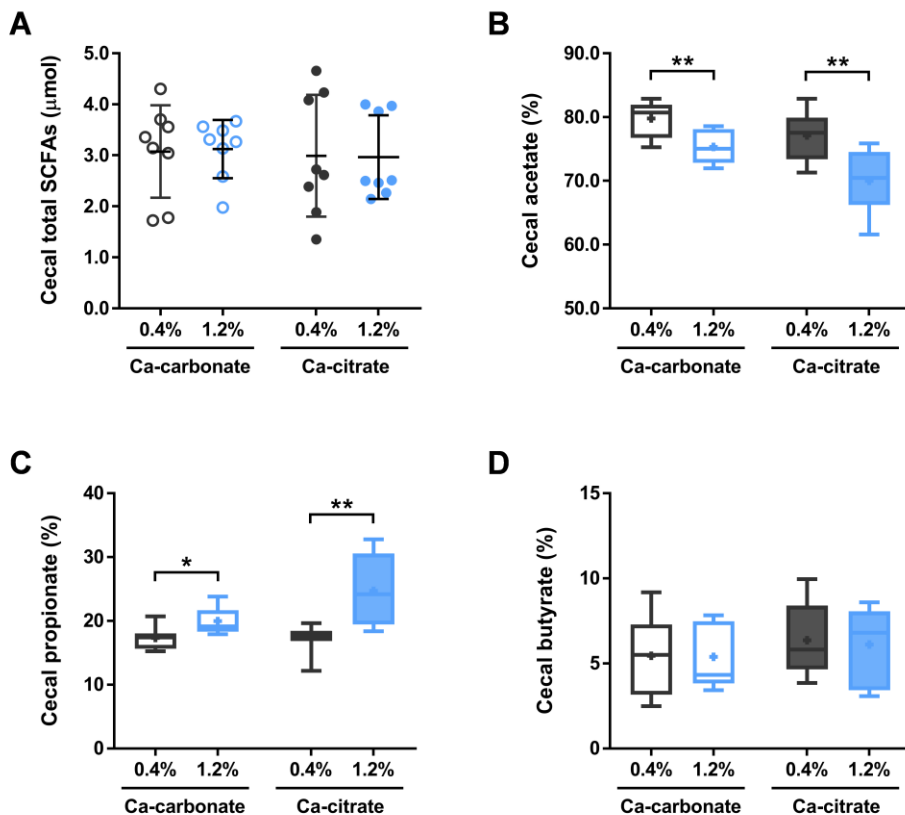


**Figure 4.8** Cecal SCFAs profiles based on Ca supplementations.

(A) Cecal total SCFAs content; (B) cecal acetate ratio; (C) cecal propionate ratio; (D) cecal butyrate ratio. Box plots show median (horizontal line), mean (cross), and IQR, whiskers are minimum and maximum values. Significance was determined using two-tailed Student's *t* test. \* $P < 0.05$ , \*\* $P < 0.01$ .

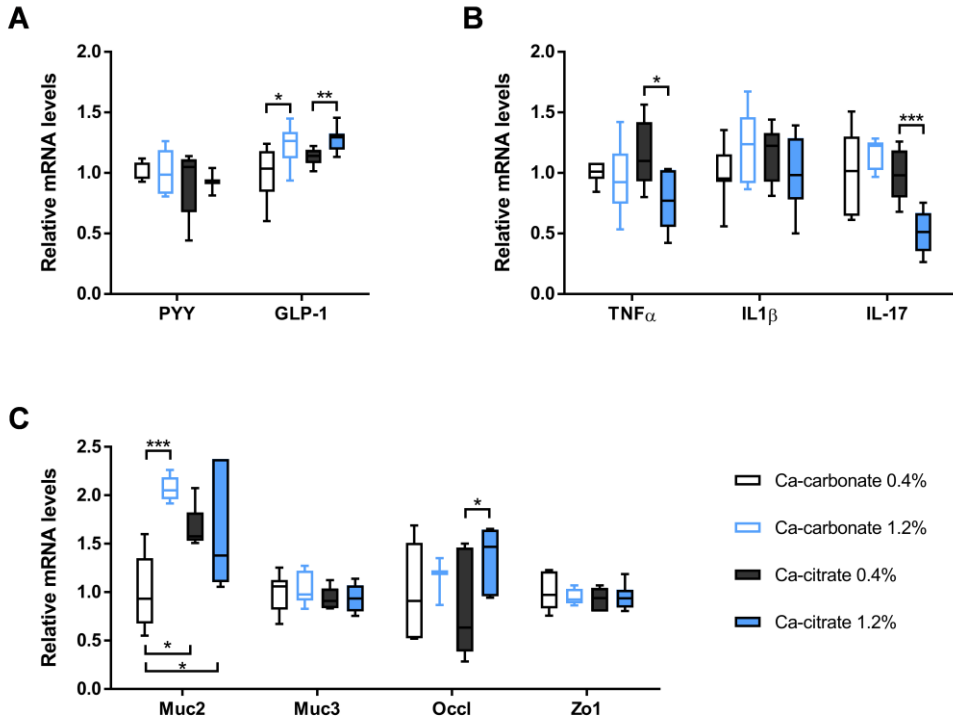


**Figure 4.9 Gene expression for (A) appetite suppression, (B) inflammation, and (C) mucosal barrier function in proximal colons based on Ca supplementations.**

Box plots show median (horizontal line) and IQR; whiskers are minimum and maximum values. Significance was determined using two-tailed Student's *t* test. \* $P < 0.05$ , \*\* $P < 0.01$ , \*\*\* $P < 0.001$ .

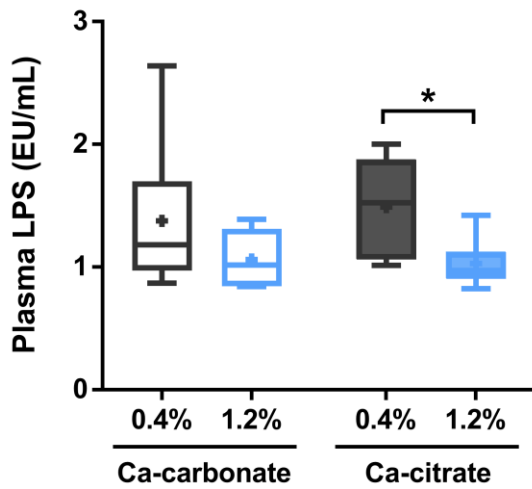


**Figure 4.10 Plasma LPS level based on Ca supplementation.**

Box plots show median (horizontal line), mean (cross), and IQR, whiskers are minimum and maximum values. Significance was determined using two-tailed Student's *t* test. \* $P < 0.05$ .

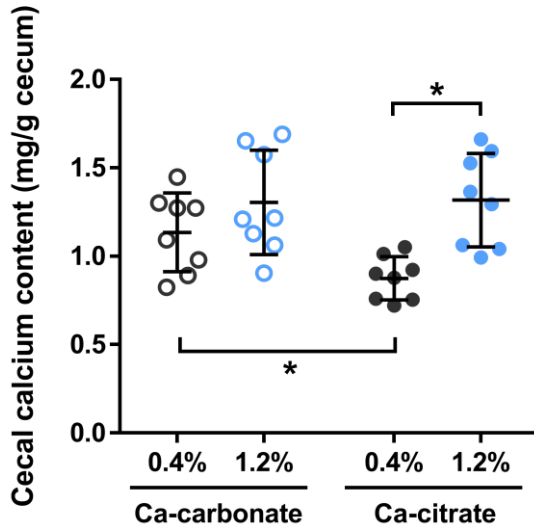


**Figure 4.11 Comparison of cecal Ca content between Ca-carbonate and Ca-citrate based on Ca supplementations.**

Data are shown as mean  $\pm$  SD. Significance was determined using two-tailed Student's *t* test. \* $P < 0.05$ .

### **Discussion**

The epidemiologic studies on the relationship between Ca intake and MetS have led to many subsequent works trying to prove the causality of Ca intake for improvement of metabolic disorders. However, some works did not result in clear outputs<sup>(160,161)</sup>, indicating that increasing Ca intake from diet might not confer significant cardiovascular benefits, while Ca supplement might raise myocardial infarction risk<sup>(165)</sup>. Ca can increase production of the ROS, and ROS can significantly affect Ca influx into the cell and intracellular Ca stores, which results in the dysfunction of the Ca-ROS balance and the onset of various diseases<sup>(166)</sup>. Because the increased serum Ca levels are significantly associated with metabolic disorders through increased oxidative stress, there has been a lot of controversy over the benefits of calcium supplement<sup>(167)</sup>. Despite some conflicting studies, a recent meta-analysis of the Ca supplement indicated that it had a significant effect on body weight loss<sup>(43)</sup>. Furthermore, a study indicated that Ca plus vitamin D supplementation could reduce inflammation including serum high-sensitivity C-reactive protein and plasma malondialdehyde concentration with a significant increase in plasma total antioxidant capacity and glutathione levels<sup>(168)</sup>. The results from many Ca study seemed to differ slightly because the age, sex, and health status of the cohort were different, and the type and intake periods of Ca supplement were not similar.

In our study, we used Ca-carbonate and Ca-citrate, the most widely used Ca supplement. According to Figure 4.1 and 4.2 in this study, the two different types of Ca had distinctive effects on body weight loss and adiposity reduction. Ca-citrate showed a clearer MetS improvement than Ca-carbonate, although Ca-carbonate supplementation also had some effects

on ameliorating the disease. The result indicates that the type of Ca supplements can act as an important factor in preventing MetS. Many studies demonstrated that Ca-citrate provides a more optimum Ca bioavailability than Ca-carbonate by approximately 20% to 30%, implying that Ca-citrate may offer significant advantages as a dietary Ca supplement<sup>(162-164,169,170)</sup>. Our study also indirectly demonstrated the better bioavailability of Ca-citrate by evaluating that Ca-citrate remained in cecum less than Ca-carbonate when the recommended amount (0.4%) was taken (Figure 4.11). Thus, the different effects of the two Ca supplements may have been attributed to the dissimilarity in their bioavailability.

As the interplay between MetS and gut microbiota became important, some studies were conducted to analyze the changes in microbial composition during Ca supplementation. According to the reports, *Bifidobacterium*, *Lactobacillus*, and *Akkermansia* significantly increased when high concentrations of Ca were ingested<sup>(89,90)</sup>. These results were in line with our findings showing a significant increase in *Akkermansia*. Nadeem also showed a significant reduction in serum proinflammatory cytokines such as TNF $\alpha$  with a slight increase in Shannon diversity index by Ca treatment<sup>(90)</sup>. In our study, there was no significant difference in  $\alpha$ -diversity of the gut microbiota in the high level Ca group. This difference may have been due to Nadeem's study using ten times more than the Ca concentration compared to the typical Ca ingestion concentration, whereas we used three times the Ca concentration. In this study, both 1.2% of Ca-carbonate and 1.2% of Ca-citrate supplementations caused an increase in *Akkermansia* known as a propionate-producing bacteria, and the cecal propionate also increased significantly to make sense. There was no

microbial SCFA measurement in several Ca studies which were performed to confirm whether Ca could shape the gut microbiota (85, 86). Our study is meaningful because it has demonstrated that Ca supplement can not only improve the gut microbial composition changed by an HFD but also affect the formation of SCFAs, the major microbial metabolites.

Recent studies have demonstrated that colonic propionate could contribute to intestinal gluconeogenesis and prevent body weight gain, increasing anorectic hormones such as GLP-1 and PYY<sup>(150,171,172)</sup>.

According to Figure 4.9, the high concentration of two Ca-supplemented diets effectively increased the GLP-1 expression, although the expression level of PYY was constant regardless of each Ca group. These results suggest that intestinal Ca levels, regardless of the Ca types, are an important factor in the appetite regulation by gut microbiota and can affect the host metabolism. The results of several papers support this Ca-specific appetite control hypothesis<sup>(152,173-175)</sup>. Unlike 1.2% of Ca-citrate group, where the feed intake decreased notably due to the increase in GLP-1, the reduction in feed intake was not noticeable in 1.2% of Ca-carbonate group. Probably this is because the Ca-carbonate group had a relatively small increase in GLP-1 and leptin expression compared to the Ca-citrate group. The G-protein-coupled free fatty acid receptor (FFAR)2 and FFAR3 are known as SCFA receptors, and propionate stimulates GLP-1 secretion via FFAR2<sup>(151)</sup>. In this study, whether FFAR2 could be altered by propionate increase to trigger the release of anorectic hormones remained to be determined. Moreover, since GLP-1, PYY, and leptin are not the only ones involved in appetite regulation, further studies should reveal the detailed mechanism of appetite control by Ca.

Metabolic endotoxemia due to gut microbial dysbiosis is a primary contributor to the chronic low-grade inflammation, responsible for the development of MetS<sup>(136,137)</sup>. It is characterized by increased plasma LPS levels, which are considered originating from Gram-negative bacteria that come into the systemic circulation because of mucosal barrier disintegration<sup>(138)</sup>. HFD can be a crucial source in the perturbation of gut microbiota and the formation of defective mucosal barrier<sup>(139)</sup>. In our study, the high concentration of Ca-citrate supplementation could increase the expression of mucosal barrier function-related genes (Muc2 and Occl) and some pro-inflammatory cytokines (TNF $\alpha$  and IL-17), suggesting that Ca-citrate might be beneficial to ameliorate the low-grade inflammation induced by HFD. Lower plasma LPS levels in Ca-citrate group (Figure 4.10) can also be decisive evidence of the decreased metabolic endotoxemia. Some studies demonstrated that the intracellular Ca played a pivotal role in tight junction biogenesis, and the Ca treatment improved gut epithelial integrity in the cell model<sup>(176,177)</sup>. Thus, we can infer that the superiority of Ca-citrate might be caused by the gut microbial factor as well as a direct host effect of Ca, considering the better bioavailability of Ca-citrate compared to Ca-carbonate as mentioned earlier. In this study, we identified the effects of Ca supplement only in high-fat diet groups, not in the normal-diet group. A follow-up study is needed to confirm whether Ca-citrate can better induce the changes in the gut microbial composition and the enhancement of the functional properties of the intestinal immune system in normal diet condition. Figure 4.12 indicates the possible mechanisms explaining the effects of two Ca supplements on gut microbiota and MetS.

In conclusion, we evaluated the effects of two different Ca supplements

on the amelioration of host metabolic disorder caused by HFD. Ca supplementations could affect the shift in the gut microbial community and help to recover the normal metabolic homeostasis in HFD mice. Furthermore, we demonstrated that the bioavailability of Ca supplements could be a key factor in improving MetS. However, to understand the more detailed molecular mechanism, further studies using knock-out mice or germ-free mice model will be required, and the effect of Ca on MetS should be verified against humans.

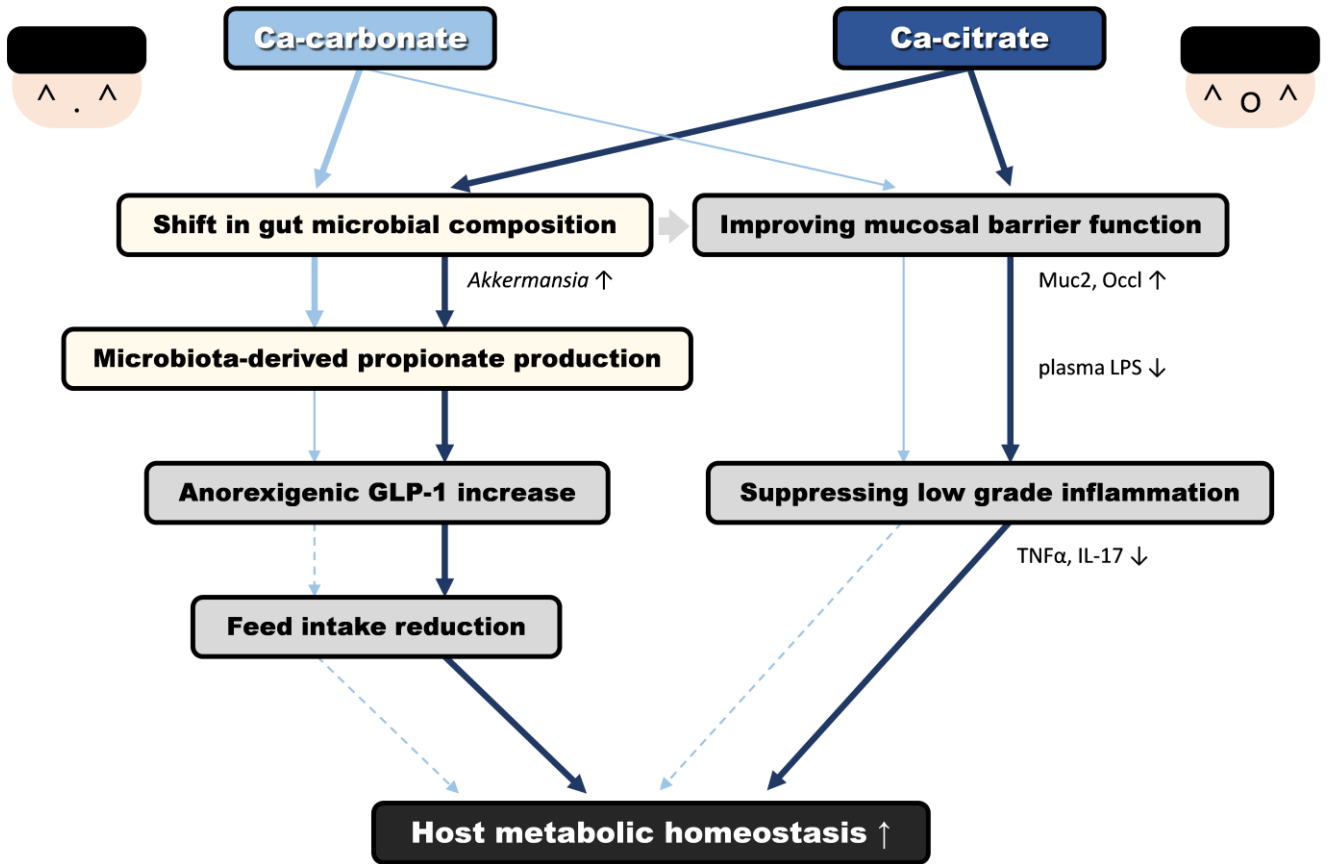


Figure 4.12 Possible mechanisms explaining the effects of two different Ca supplements on gut microbiota (light yellow color) and MetS (gray color).

**CHAPTER V.**

**CONCLUSIONS**

## Summary and Conclusions

Recent studies suggest a possible role of gut microbiota in MetS, demonstrating that microbial alteration could affect energy intake as well as induce low-grade inflammation by metabolic endotoxemia. There has also been considerable evidence that exposure to environmental chemicals could be linked with MetS. In particular, the elements including essential minerals and metals play a pivotal role in host metabolic homeostasis. Most elements studies on MetS were performed on the host side without considering the role of gut microbiota, and have only been done with a few elements such as As and Cd. Thus, this thesis aims to demonstrate the relationships of fecal elements with gut microbiota and MetS.

**First, we evaluated the association of various fecal elements with human gut microbiome and MetS status.** Among 29 fecal elements, Be showed the most positive correlation with MetS status, whereas Ca had the significant negative association with MetS. Be and Tl also had the high relationships with the reduction of microbial diversity. Besides, Be and Ca showed conflicting associations with MetS-related gut microbiota, *Akkermansia* and *Bifidobacterium*. Two elements also had a link with gut microbial functions in the analysis of metagenomics-based or metabolomics-based function predictions.

**Second, we assessed whether a low dose of Be exposure could influence gut microbial changes and worsen MetS.** In HFD mice, 30 ppb of Be exposure resulted in significant body weight gain as well as adiposity increase, but these increasing effects were not shown in normal diet groups. The shifts in the gut microbial community were caused by the exposure to

both 3 ppb and 30 ppb of Be in HFD groups, with the microbial diversity reduction and the significant decrease of *Akkermansia*. *In vitro* human feces culture also indicated the reduction of species evenness and Mets-related *Bifidobacterium* due to a low dose of Be. The increase in acetate and the decrease in propionate and butyrate were observed in HFD groups. The expression of inflammatory genes and plasma LPS levels significantly increased in HFD groups, showing the evidence of metabolic endotoxemia and low-grade inflammation.

**Third, we verified and compared the effects of two different Ca supplements on the improvement of host metabolic homeostasis in HFD mice.** High concentration of Ca-citrate supplementation showed significant decreases in body weight gain and MetS-related plasma biomarkers compared to Ca-carbonate groups. Both Ca-carbonate and Ca-citrate supplementation led to similar changes in gut microbial composition. However, Ca-citrate groups showed more significant differences in the propionate production, with the increase of anorexigenic GLP-1 gene expression. Also, Ca-citrate groups significantly reduced the expression of inflammatory cytokines, with the increases in the expression of the mucosal barrier function-related genes.

These studies have several significances. The analysis of fecal elements and metabolites could provide the information on the environmental factors including human exposure level to various elements and nutrients. Certain gut microbiota showed the strong correlation with fecal elements, showing the need for follow-up elements research to reveal the interaction mechanism between elements, gut microbiota, and diseases. In particular, we found out for the first time that the low dose of Be, almost identical to

the current global standard levels for drinking water, could be an important cause of MetS by disturbing gut microbiota and inducing inflammation responses.

Overall, this study indicated that fecal elements were highly associated with gut microbiota and MetS. Exposure to Be could affect the changes in gut microbial composition and worsen MetS even at very low concentrations. Ca supplementations effectively helped attenuate MetS with the increase in MetS-suppressing microbiota, and Ca-citrate showed greater improvement in MetS compared to Ca-carbonate. These data suggest that fecal elements analysis will provide important information to understand the association between gut microbiota and diseases and further research will be required in the future.

---

## REFERENCES

- 1 de Vos, W. M. & de Vos, E. A. **Role of the intestinal microbiome in health and disease: from correlation to causation.** *Nutr Rev* 70 Suppl 1, S45-56 (2012).
- 2 Kau, A. L. *et al.* **Human nutrition, the gut microbiome and the immune system.** *Nature* 474, 327-336 (2011).
- 3 Tremaroli, V. & Backhed, F. **Functional interactions between the gut microbiota and host metabolism.** *Nature* 489, 242-249 (2012).
- 4 Gill, S. R. *et al.* **Metagenomic analysis of the human distal gut microbiome.** *Science* 312, 1355-1359 (2006).
- 5 Lee, D. K. *et al.* **Anti-proliferative effects of *Bifidobacterium adolescentis* SPM0212 extract on human colon cancer cell lines.** *BMC Cancer* 8, 310 (2008).
- 6 Hidalgo-Cantabrana, C. *et al.* **Genomic overview and biological functions of exopolysaccharide biosynthesis in *Bifidobacterium* spp.** *Appl Environ Microbiol* 80, 9-18 (2014).
- 7 Gomes, A. C., Hoffmann, C. & Mota, J. F. **The human gut microbiota: Metabolism and perspective in obesity.** *Gut Microbes*, 1-18 (2018).
- 8 Panzer, A. R. & Lynch, S. V. **Influence and effect of the human microbiome in allergy and asthma.** *Curr Opin Rheumatol* 27, 373-380 (2015).
- 9 Gevers, D. *et al.* **A microbiome foundation for the study of Crohn's disease.** *Cell Host Microbe* 21, 301-304 (2017).
- 10 Huttenhower, C. *et al.* **Advancing the microbiome research**

- community.** *Cell* 159, 227-230 (2014).
- 11 Gonzalez-Muniesa, P. *et al.* **Obesity.** *Nat Rev Dis Primers* 3, 17034 (2017).
- 12 Grundy, S. M. **Metabolic syndrome pandemic.** *Arterioscler Thromb Vasc Biol* 28, 629-636 (2008).
- 13 Wilson, P. W. *et al.* **Metabolic syndrome as a precursor of cardiovascular disease and type 2 diabetes mellitus.** *Circulation* 112, 3066-3072 (2005).
- 14 Hotamisligil, G. S. & Erbay, E. **Nutrient sensing and inflammation in metabolic diseases.** *Nat Rev Immunol* 8, 923-934 (2008).
- 15 Kaur, J. **A comprehensive review on metabolic syndrome.** *Cardiol Res Pract* 2014, 943162 (2014).
- 16 Ley, R. E. *et al.* **Obesity alters gut microbial ecology.** *Proc Natl Acad Sci U S A* 102, 11070-11075 (2005).
- 17 Turnbaugh, P. J. *et al.* **An obesity-associated gut microbiome with increased capacity for energy harvest.** *Nature* 444, 1027-1031 (2006).
- 18 Turnbaugh, P. J. *et al.* **A core gut microbiome in obese and lean twins.** *Nature* 457, 480-484 (2009).
- 19 Ridaura, V. K. *et al.* **Gut microbiota from twins discordant for obesity modulate metabolism in mice.** *Science* 341, 1241214 (2013).
- 20 Chu, H. *et al.* **Gene-microbiota interactions contribute to the pathogenesis of inflammatory bowel disease.** *Science* 352, 1116-1120 (2016).
- 21 Thaiss, C. A. *et al.* **The microbiome and innate immunity.** *Nature* 535,

- 65-74 (2016).
- 22 Ley, R. E. *et al.* **Microbial ecology: human gut microbes associated with obesity.** *Nature* 444, 1022-1023 (2006).
- 23 Ley, R. E. **Obesity and the human microbiome.** *Curr Opin Gastroenterol* 26, 5-11 (2010).
- 24 Backhed, F. *et al.* **Mechanisms underlying the resistance to diet-induced obesity in germ-free mice.** *Proc Natl Acad Sci U S A* 104, 979-984 (2007).
- 25 Rabot, S. *et al.* **Germ-free C57BL/6J mice are resistant to high-fat-diet-induced insulin resistance and have altered cholesterol metabolism.** *FASEB J* 24, 4948-4959 (2010).
- 26 Larsen, N. *et al.* **Gut microbiota in human adults with type 2 diabetes differs from non-diabetic adults.** *PLoS One* 5, e9085 (2010).
- 27 Qin, J. *et al.* **A metagenome-wide association study of gut microbiota in type 2 diabetes.** *Nature* 490, 55-60 (2012).
- 28 Karlsson, F. H. *et al.* **Gut metagenome in European women with normal, impaired and diabetic glucose control.** *Nature* 498, 99-103 (2013).
- 29 Vrieze, A. *et al.* **Impact of oral vancomycin on gut microbiota, bile acid metabolism, and insulin sensitivity.** *J Hepatol* 60, 824-831 (2014).
- 30 Vrieze, A. *et al.* **Transfer of intestinal microbiota from lean donors increases insulin sensitivity in individuals with metabolic syndrome.** *Gastroenterology* 143, 913-916 e917 (2012).
- 31 Dao, M. C. *et al.* ***Akkermansia muciniphila* and improved metabolic health during a dietary intervention in obesity: relationship with**

- gut microbiome richness and ecology.** *Gut* 65, 426-436 (2016).
- 32 Everard, A. *et al.* **Cross-talk between *Akkermansia muciniphila* and intestinal epithelium controls diet-induced obesity.** *Proc Natl Acad Sci U S A* 110, 9066-9071 (2013).
- 33 Shin, N. R. *et al.* **An increase in the *Akkermansia* spp. population induced by metformin treatment improves glucose homeostasis in diet-induced obese mice.** *Gut* 63, 727-735 (2014).
- 34 Nielsen, F. H. **Evolutionary events culminating in specific minerals becoming essential for life.** *Eur J Nutr* 39, 62-66 (2000).
- 35 Chen, C. J. *et al.* **Arsenic and diabetes and hypertension in human populations: a review.** *Toxicol Appl Pharmacol* 222, 298-304 (2007).
- 36 Navas-Acien, A. *et al.* **Urine arsenic concentrations and species excretion patterns in American Indian communities over a 10-year period: the Strong Heart Study.** *Environ Health Perspect* 117, 1428-1433 (2009).
- 37 Rahman, M. M., Ng, J. C. & Naidu, R. **Chronic exposure of arsenic via drinking water and its adverse health impacts on humans.** *Environ Geochem Health* 31 Suppl 1, 189-200 (2009).
- 38 Diaz-Villasenor, A. *et al.* **Arsenic-induced alteration in the expression of genes related to type 2 diabetes mellitus.** *Toxicol Appl Pharmacol* 225, 123-133 (2007).
- 39 Merali, Z. & Singhal, R. L. **Diabetogenic effects of chronic oral cadmium administration to neonatal rats.** *Brit J Pharmacol* 69, 151-157 (1980).
- 40 Schwartz, G. G., Il'yasova, D. & Ivanova, A. **Urinary cadmium,**

- impaired fasting glucose, and diabetes in the NHANES III.** *Diabetes Care* 26, 468-470 (2003).
- 41 Kelishadi, R. *et al.* **Effect of zinc supplementation on markers of insulin resistance, oxidative stress, and inflammation among prepubescent children with metabolic syndrome.** *Metab Syndr Relat Disord* 8, 505-510 (2010).
- 42 Larsen, S. C. *et al.* **Interaction between genetic predisposition to obesity and dietary calcium in relation to subsequent change in body weight and waist circumference.** *Am J Clin Nutr* 99, 957-965 (2014).
- 43 Li, P. *et al.* **Effects of calcium supplementation on body weight: a meta-analysis.** *Am J Clin Nutr* 104, 1263-1273 (2016).
- 44 Miao, X. *et al.* **Zinc homeostasis in the metabolic syndrome and diabetes.** *Front Med* 7, 31-52 (2013).
- 45 Fazeli, M., Hassanzadeh, P. & Alaei, S. **Cadmium chloride exhibits a profound toxic effect on bacterial microflora of the mice gastrointestinal tract.** *Hum Exp Toxicol* 30, 152-159 (2011).
- 46 Breton, J. *et al.* **Ecotoxicology inside the gut: impact of heavy metals on the mouse microbiome.** *BMC Pharmacol Toxicol* 14, 62 (2013).
- 47 Lepage, P. *et al.* **Twin study indicates loss of interaction between microbiota and mucosa of patients with ulcerative colitis.** *Gastroenterology* 141, 227-236 (2011).
- 48 Lu, K. *et al.* **Arsenic exposure perturbs the gut microbiome and its metabolic profile in mice: an integrated metagenomics and metabolomics analysis.** *Environ Health Perspect* 122, 284-291 (2014).

- 49 Carmody, R. N. *et al.* **Diet dominates host genotype in shaping the murine gut microbiota.** *Cell Host Microbe* 17, 72-84 (2015).
- 50 Griffin, N. W. *et al.* **Prior dietary practices and connections to a human gut microbial metacommunity alter responses to diet interventions.** *Cell Host Microbe* 21, 84-96 (2017).
- 51 Coronado-Gonzalez, J. A. *et al.* **Inorganic arsenic exposure and type 2 diabetes mellitus in Mexico.** *Environ Res* 104, 383-389 (2007).
- 52 Brauner, E. V. *et al.* **Long-term exposure to low-level arsenic in drinking water and diabetes incidence: a prospective study of the diet, cancer and health cohort.** *Environ Health Perspect* 122, 1059-1065 (2014).
- 53 Dheer, R. *et al.* **Arsenic induces structural and compositional colonic microbiome change and promotes host nitrogen and amino acid metabolism.** *Toxicol Appl Pharmacol* 289, 397-408 (2015).
- 54 Zhang, L. *et al.* **Persistent organic pollutants modify gut microbiota-host metabolic homeostasis in mice through aryl hydrocarbon receptor activation.** *Environ Health Perspect* 123, 679-688 (2015).
- 55 Wilck, N. *et al.* **Salt-responsive gut commensal modulates TH17 axis and disease.** *Nature* 551, 585-589 (2017).
- 56 Robberecht, H., Bruyne, T. & Hermans, N. **Biomarkers of the metabolic syndrome: Influence of minerals, oligo- and trace elements.** *J Trace Elem Med Biol* 43, 23-28 (2017).
- 57 Lim, M. Y. *et al.* **The effect of heritability and host genetics on the gut microbiota and metabolic syndrome.** *Gut* 66, 1031-1038 (2017).
- 58 Sung, J. *et al.* **Healthy Twin: a twin-family study of Korea--protocols**

- and current status.** *Twin Res Hum Genet* 9, 844-848 (2006).
- 59 Grundy, S. M. *et al.* **Diagnosis and management of the metabolic syndrome.** *Circulation* 112, E285-E290 (2005).
- 60 Lee, H. L. *et al.* **Abdominal obesity, insulin resistance, and the risk of colonic adenoma.** *Korean J Gastroenterol* 49, 147-151 (2007).
- 61 Caporaso, J. G. *et al.* **QIIME allows analysis of high-throughput community sequencing data.** *Nat Methods* 7, 335-336 (2010).
- 62 Lamichhane, S. *et al.* **Strategy for Nuclear-Magnetic-Resonance-based metabolomics of human feces.** *Anal Chem* 87, 5930-5937 (2015).
- 63 Le Gall, G. *et al.* **Metabolomics of fecal extracts detects altered metabolic activity of gut microbiota in ulcerative colitis and irritable bowel syndrome.** *J Proteome Res* 10, 4208-4218 (2011).
- 64 Hao, J. *et al.* **Bayesian deconvolution and quantification of metabolites in complex 1D NMR spectra using BATMAN.** *Nat Protoc* 9, 1416-1427 (2014).
- 65 Xia, J. & Wishart, D. S. **Web-based inference of biological patterns, functions and pathways from metabolomic data using MetaboAnalyst.** *Nat Protoc* 6, 743-760 (2011).
- 66 Chong, J. *et al.* **MetaboAnalyst 4.0: towards more transparent and integrative metabolomics analysis.** *Nucleic Acids Res* 46, W486-W494 (2018).
- 67 Langille, M. G. *et al.* **Predictive functional profiling of microbial communities using 16S rRNA marker gene sequences.** *Nat Biotechnol* 31, 814-821 (2013).
- 68 Segata, N. *et al.* **Metagenomic biomarker discovery and explanation.**

- Genome Biol* 12, R60 (2011).
- 69 Morgan, X. C. *et al.* **Dysfunction of the intestinal microbiome in inflammatory bowel disease and treatment.** *Genome Biol* 13, R79 (2012).
- 70 Arumugam, M. *et al.* **Enterotypes of the human gut microbiome.** *Nature* 473, 174-180 (2011).
- 71 J Emsley. **Nature's building blocks: An A-Z guide to the elements.** (*OUP Oxford*, 2011).
- 72 Fordtran, J. S., Rector, F. C., Jr. & Carter, N. W. **The mechanisms of sodium absorption in the human small intestine.** *J Clin Invest* 47, 884-900 (1968).
- 73 Visscher, M. B. **The absorption and excretion of potassium in the intestine.** *J Lancet* 73, 173-174 (1953).
- 74 Heaney, R. P. & Nordin, B. E. **Calcium effects on phosphorus absorption: implications for the prevention and co-therapy of osteoporosis.** *J Am Coll Nutr* 21, 239-244 (2002).
- 75 Messa, P. **The ups and downs of dialysate calcium concentration in haemodialysis patients.** *Nephrol Dial Transplant* 28, 3-7 (2013).
- 76 Conceicao, E. P. S. *et al.* **Dietary calcium supplementation in adult rats reverts brown adipose tissue dysfunction programmed by postnatal early overfeeding.** *J Nutr Biochem* 39, 117-125 (2017).
- 77 Laraichi, S. *et al.* **Dietary supplementation of calcium may counteract obesity in mice mediated by changes in plasma fatty acids.** *Lipids* 48, 817-826 (2013).
- 78 Martinez de Victoria, E. **Calcium, essential for health.** *Nutr Hosp* 33, 341 (2016).

- 79 Pilvi, T. K. *et al.* **Effects of high-calcium diets with different whey proteins on weight loss and weight regain in high-fat-fed C57BL/6J mice.** *Br J Nutr* 102, 337-341 (2009).
- 80 Hansen, C. L., Woodhouse, S. & Kramer, M. **Effect of patient obesity on the accuracy of thallium-201 myocardial perfusion imaging.** *Am J Cardiol* 85, 749-752 (2000).
- 81 Eshak, E. S. *et al.* **Associations between dietary intakes of iron, copper and zinc with risk of type 2 diabetes mellitus: A large population-based prospective cohort study.** *Clin Nutr* 37, 667-674 (2018).
- 82 Payahoo, L. *et al.* **Effects of zinc supplementation on the anthropometric measurements, lipid profiles and fasting blood glucose in the healthy obese adults.** *Adv Pharm Bull* 3, 161-165 (2013).
- 83 Sun, Q. *et al.* **Prospective study of zinc intake and risk of type 2 diabetes in women.** *Diabetes Care* 32, 629-634 (2009).
- 84 Kreznar, J. H. *et al.* **Host genotype and gut microbiome modulate insulin secretion and diet-induced metabolic phenotypes.** *Cell Rep* 18, 1739-1750 (2017).
- 85 Aoki, R. *et al.* **A proliferative probiotic *Bifidobacterium* strain in the gut ameliorates progression of metabolic disorders via microbiota modulation and acetate elevation.** *Sci Rep* 7, 43522 (2017).
- 86 Chen, J. *et al.* ***Bifidobacterium adolescentis* supplementation ameliorates visceral fat accumulation and insulin sensitivity in an experimental model of the metabolic syndrome.** *Br J Nutr* 107,

- 1429-1434 (2012).
- 87 Plovier, H. *et al.* **A purified membrane protein from *Akkermansia muciniphila* or the pasteurized bacterium improves metabolism in obese and diabetic mice.** *Nat Med* 23, 107-113 (2017).
- 88 Woting, A. *et al.* **Alleviation of high fat diet-induced obesity by oligofructose in gnotobiotic mice is independent of presence of *Bifidobacterium longum*.** *Mol Nutr Food Res* 59, 2267-2278 (2015).
- 89 Chaplin, A. *et al.* **Calcium supplementation modulates gut microbiota in a prebiotic manner in dietary obese mice.** *Mol Nutr Food Res* 60, 468-480 (2016).
- 90 Nadeem Aslam, M. *et al.* **Calcium reduces liver injury in mice on a high-fat diet: alterations in microbial and bile acid profiles.** *PLoS One* 11, e0166178 (2016).
- 91 Zhang, S. *et al.* **Subchronic exposure of mice to cadmium perturbs their hepatic energy metabolism and gut microbiome.** *Chem Res Toxicol* 28, 2000-2009 (2015).
- 92 Huang, L. *et al.* **Study on high permeabilized opening of lung mitochondrial permeability transition pore and apoptosis induced by beryllium sulfate in mice.** *J Toxicol* (2015).
- 93 Genova, M. W. *et al.* **Mitochondrial production of oxygen radical species and the role of coenzyme Q as an antioxidant.** *Exp Biol Med* 228, 506-513 (2003).
- 94 Reichardt, N. *et al.* **Phylogenetic distribution of three pathways for propionate production within the human gut microbiota.** *ISME J* 8, 1323-1335 (2014).
- 95 Human Microbiome Project, C. **Structure, function and diversity of**

- the healthy human microbiome.** *Nature* 486, 207-214 (2012).
- 96 Lloyd-Price, J. *et al.* **Strains, functions and dynamics in the expanded Human Microbiome Project.** *Nature* 550, 61-66 (2017).
- 97 Xie, H. *et al.* **Shotgun metagenomics of 250 adult twins reveals genetic and environmental impacts on the gut microbiome.** *Cell Syst* 3, 572-584 e573 (2016).
- 98 Ni, Y., Li, J. & Panagiotou, G. **A molecular-level landscape of diet-gut microbiome interactions: toward dietary interventions targeting bacterial genes.** *MBio* 6, e01263-01215 (2015).
- 99 Reck, M. *et al.* **Stool metatranscriptomics: A technical guideline for mRNA stabilisation and isolation.** *BMC Genomics* 16, 494 (2015).
- 100 Franzosa, E. A. *et al.* **Relating the metatranscriptome and metagenome of the human gut.** *Proc Natl Acad Sci U S A* 111, E2329-2338 (2014).
- 101 Chia, L. W. *et al.* **Deciphering the trophic interaction between *Akkermansia muciniphila* and the butyrogenic gut commensal *Anaerostipes caccae* using a metatranscriptomic approach.** *Antonie Van Leeuwenhoek* 111, 859-873 (2018).
- 102 Petriz, B. A. & Franco, O. L. **Metaproteomics as a complementary approach to gut microbiota in health and disease.** *Front Chem* 5, 4 (2017).
- 103 Jacobs, D. M. *et al.* **<sup>1</sup>H NMR metabolite profiling of feces as a tool to assess the impact of nutrition on the human microbiome.** *NMR Biomed* 21, 615-626 (2008).
- 104 Yen, S. *et al.* **Metabolomic analysis of human fecal microbiota: a comparison of feces-derived communities and defined mixed**

- communities.** *J Proteome Res* 14, 1472-1482 (2015).
- 105 Cha, K. H. *et al.* **Effects of fermented milk treatment on microbial population and metabolomic outcomes in a three-stage semi-continuous culture system.** *Food Chem* 263, 216-224 (2018).
- 106 Bhurosy, T. & Jeewon, R. **Overweight and obesity epidemic in developing countries: a problem with diet, physical activity, or socioeconomic status?** *ScientificWorldJournal* 2014, 964236 (2014).
- 107 Grun, F. & Blumberg, B. **Endocrine disruptors as obesogens.** *Mol Cell Endocrinol* 304, 19-29 (2009).
- 108 Holtcamp, W. **Obesogens: an environmental link to obesity.** *Environ Health Perspect* 120, a62-68 (2012).
- 109 Neel, B. A. & Sargis, R. M. **The paradox of progress: environmental disruption of metabolism and the diabetes epidemic.** *Diabetes* 60, 1838-1848 (2011).
- 110 K. A. Walsh. **Beryllium chemistry and processing.** (*ASM International*, 2009).
- 111 Newman, L. S. **To Be<sup>2+</sup> or not to Be<sup>2+</sup>: immunogenetics and occupational exposure.** *Science* 262, 197-198 (1993).
- 112 Iarc Working Group on The Evaluation of The Carcinogenic Risk of Chemicals. **IARC monographs on the evaluation of the carcinogenic risk of chemicals to humans.** Vol. 35 (*IARC*, 1993).
- 113 Administration, O. S. a. H. **Occupational exposure to beryllium. Final rule.** *Fed Regist* 82, 2470-2757 (2017).
- 114 Vaessen, H. A. & Szteke, B. **Beryllium in food and drinking water-a summary of available knowledge.** *Food Addit Contam* 17, 149-159 (2000).

- 115 Organization, W. H. in *Beryllium in drinking-water: background document for development of WHO guidelines for drinking-water quality* (2009).
- 116 Long, W. *et al.* **Differential responses of gut microbiota to the same prebiotic formula in oligotrophic and eutrophic batch fermentation systems.** *Sci Rep* 5, 13469 (2015).
- 117 Fadrosh, D. W. *et al.* **An improved dual-indexing approach for multiplexed 16S rRNA gene sequencing on the Illumina MiSeq platform.** *Microbiome* 2, 6 (2014).
- 118 Kuczynski, J. *et al.* **Using QIIME to analyze 16S rRNA gene sequences from microbial communities.** *Curr Protoc Bioinformatics* Chapter 10, Unit 10 17 (2011).
- 119 Callahan, B. J. *et al.* **DADA2: High-resolution sample inference from Illumina amplicon data.** *Nat Methods* 13, 581-583 (2016).
- 120 DeSantis, T. Z. *et al.* **Greengenes, a chimera-checked 16S rRNA gene database and workbench compatible with ARB.** *Appl Environ Microbiol* 72, 5069-5072 (2006).
- 121 McDonald, D. *et al.* **An improved Greengenes taxonomy with explicit ranks for ecological and evolutionary analyses of bacteria and archaea.** *ISME J* 6, 610-618 (2012).
- 122 Werner, J. J. *et al.* **Impact of training sets on classification of high-throughput bacterial 16s rRNA gene surveys.** *ISME J* 6, 94-103 (2012).
- 123 Dhariwal, A. *et al.* **MicrobiomeAnalyst: a web-based tool for comprehensive statistical, visual and meta-analysis of microbiome data.** *Nucleic Acids Res* 45, W180-W188 (2017).

- 124 Knights, D., Costello, E. K. & Knight, R. **Supervised classification of human microbiota.** *FEMS Microbiol Rev* 35, 343-359 (2011).
- 125 David, L. A. *et al.* **Diet rapidly and reproducibly alters the human gut microbiome.** *Nature* 505, 559-563 (2014).
- 126 Morgareidge, K., Cox, G. E. & Gallo, M. A. **Chronic feeding studies with beryllium in dogs.** *Food and Drug Research Laboratories, Inc. Submitted to the Aluminum Company of America, Alcan Research and Development, Ltd. , Kaweck-Berylco Industries, Inc. , and Brush-Wellman, Inc* (1976).
- 127 World Health Organization. **Guidelines for drinking-water quality: Fourth edition incorporating the first addendum.** (*World Health Organization*, 2017).
- 128 Thomas, K. J., 3rd & Rice, C. V. **Revised model of calcium and magnesium binding to the bacterial cell wall.** *Biometals* 27, 1361-1370 (2014).
- 129 Brahe, L. K., Astrup, A. & Larsen, L. H. **Is butyrate the link between diet, intestinal microbiota and obesity-related metabolic diseases?** *Obes Rev* 14, 950-959 (2013).
- 130 Hartstra, A. V. *et al.* **Insights into the role of the microbiome in obesity and type 2 diabetes.** *Diabetes Care* 38, 159-165 (2015).
- 131 Shoaie, S. *et al.* **Understanding the interactions between bacteria in the human gut through metabolic modeling.** *Sci Rep* 3, 2532 (2013).
- 132 Hijova, E. & Chmelarova, A. **Short chain fatty acids and colonic health.** *Bratisl Lek Listy* 108, 354-358 (2007).
- 133 Lin, H. V. *et al.* **Butyrate and propionate protect against diet-**

- induced obesity and regulate gut hormones via free fatty acid receptor 3-independent mechanisms.** *PLoS One* 7, e35240 (2012).
- 134 Sanz, Y., Santacruz, A. & Gauffin, P. **Gut microbiota in obesity and metabolic disorders.** *Proc Nutr Soc* 69, 434-441 (2010).
- 135 Perry, R. J. *et al.* **Acetate mediates a microbiome-brain-beta-cell axis to promote metabolic syndrome.** *Nature* 534, 213-217 (2016).
- 136 Ruiz-Nunez, B. *et al.* **Lifestyle and nutritional imbalances associated with Western diseases: causes and consequences of chronic systemic low-grade inflammation in an evolutionary context.** *J Nutr Biochem* 24, 1183-1201 (2013).
- 137 Hotamisligil, G. S. **Inflammation and metabolic disorders.** *Nature* 444, 860-867 (2006).
- 138 Caesar, R. *et al.* **Crosstalk between gut microbiota and dietary lipids aggravates WAT Inflammation through TLR signaling.** *Cell Metab* 22, 658-668 (2015).
- 139 Cani, P. D. *et al.* **Changes in gut microbiota control metabolic endotoxemia-induced inflammation in high-fat diet-induced obesity and diabetes in mice.** *Diabetes* 57, 1470-1481 (2008).
- 140 Silva, S. *et al.* **Beryllium alters lipopolysaccharide-mediated intracellular phosphorylation and cytokine release in human peripheral blood mononuclear cells.** *J Occup Environ Hyg* 6, 775-782 (2009).
- 141 Mack, D. G. *et al.* **Regulatory T cells modulate granulomatous inflammation in an HLA-DP2 transgenic murine model of beryllium-induced disease.** *Proc Natl Acad Sci U S A* 111, 8553-8558 (2014).

- 142 Kufe, D. W. **Mucins in cancer: function, prognosis and therapy.** *Nat Rev Cancer* 9, 874-885 (2009).
- 143 Schroeder, B. O. *et al.* **Bifidobacteria or fiber protects against diet-induced microbiota-mediated colonic mucus deterioration.** *Cell Host Microbe* 23, 27-40 e27 (2018).
- 144 Matsumoto, A., Hisada, Y. & Yoshimura, Y. **Calcium and phosphate concentrations, and alkaline and acid phosphatase activities in serum of the rat fed with low calcium and beryllium diets.** *J Oral Ther Pharmacol* 10, 253-259 (1991).
- 145 Guyatt, B. L., Kay, H. D. & Branion, H. D. **Beryllium “Rickets”.** *The Journal of Nutrition* 6, 313-324 (1933).
- 146 Kay, H. D. & Skill, D. I. **Beryllium rickets: The prevention and cure of beryllium rickets.** *Biochem J* 28, 1222-1227 (1934).
- 147 Schroeder, H. A. & Mitchener, M. **Life-term studies in rats: effects of aluminum, barium, beryllium, and tungsten.** *J Nutr* 105, 421-427 (1975).
- 148 Freundt, K. J. & Ibrahim, H. A. **Growth of rats during a subchronic intake of the heavy metals Pb, Cd, Zn, Mn, Cu, Hg, and Be.** *Pol J Occup Med* 3, 227-232 (1990).
- 149 Cani, P. D. *et al.* **Changes in gut microbiota control inflammation in obese mice through a mechanism involving GLP-2-driven improvement of gut permeability.** *Gut* 58, 1091-1103 (2009).
- 150 Chambers, E. S., Morrison, D. J. & Frost, G. **Control of appetite and energy intake by SCFA: what are the potential underlying mechanisms?** *Proc Nutr Soc* 74, 328-336 (2015).
- 151 Tolhurst, G. *et al.* **Short-chain fatty acids stimulate glucagon-like**

- peptide-1 secretion via the G-protein-coupled receptor FFAR2.** *Diabetes* 61, 364-371 (2012).
- 152 Jones, K. W. *et al.* **Effect of a dairy- and calcium-rich diet on weight loss and appetite during energy restriction in overweight and obese adults: a randomized trial.** *Eur J Clin Nutr* 67, 371-376 (2013).
- 153 Shin, S. K. *et al.* **The cross-sectional relationship between dietary calcium intake and metabolic syndrome among men and women aged 40 or older in rural areas of Korea.** *Nutr Res Pract* 9, 328-335 (2015).
- 154 Gomes, J. M. G., Costa, J. D. A. & Alfenas, R. C. G. **Effect of increased calcium consumption from fat-free milk in an energy-restricted diet on the metabolic syndrome and cardiometabolic outcomes in adults with type 2 diabetes mellitus: a randomised cross-over clinical trial.** *Br J Nutr* 119, 422-430 (2018).
- 155 Liu, S. *et al.* **Dietary calcium, vitamin D, and the prevalence of metabolic syndrome in middle-aged and older U.S. women.** *Diabetes Care* 28, 2926-2932 (2005).
- 156 Zemel, M. B. **Calcium modulation of hypertension and obesity: mechanisms and implications.** *J Am Coll Nutr* 20, 428S-435S; discussion 440S-442S (2001).
- 157 National Institutes of Health. **NIH consensus development panel on optimal calcium Intake. Optimal calcium intake.** Vol. 272 (*JAMA*, 1994).
- 158 Zemel, M. B. *et al.* **Calcium and dairy acceleration of weight and fat loss during energy restriction in obese adults.** *Obes Res* 12,

- 582-590 (2004).
- 159 Denke, M. A., Fox, M. M. & Schulte, M. C. **Short-term dietary calcium fortification increases fecal saturated fat content and reduces serum lipids in men.** *J Nutr* 123, 1047-1053 (1993).
- 160 Beydoun, M. A. *et al.* **Ethnic differences in dairy and related nutrient consumption among US adults and their association with obesity, central obesity, and the metabolic syndrome.** *Am J Clin Nutr* 87, 1914-1925 (2008).
- 161 Soares, M. J., Pathak, K. & Calton, E. K. **Calcium and vitamin D in the regulation of energy balance: where do we stand?** *Int J Mol Sci* 15, 4938-4945 (2014).
- 162 Nicar, M. J. & Pak, C. Y. **Calcium bioavailability from calcium carbonate and calcium citrate.** *J Clin Endocrinol Metab* 61, 391-393 (1985).
- 163 Hanzlik, R. P., Fowler, S. C. & Fisher, D. H. **Relative bioavailability of calcium from calcium formate, calcium citrate, and calcium carbonate.** *J Pharmacol Exp Ther* 313, 1217-1222 (2005).
- 164 van der Velde, R. Y. *et al.* **Calcium and vitamin D supplementation: state of the art for daily practice.** *Food Nutr Res* 58 (2014).
- 165 Li, K. *et al.* **Associations of dietary calcium intake and calcium supplementation with myocardial infarction and stroke risk and overall cardiovascular mortality in the Heidelberg cohort of the European Prospective Investigation into Cancer and Nutrition study (EPIC-Heidelberg).** *Heart* 98, 920-925 (2012).
- 166 Ermak, G. & Davies, K. J. **Calcium and oxidative stress: from cell**

- signaling to cell death.** *Mol Immunol* 38, 713-721 (2002).
- 167 Camello-Almaraz, M. C. *et al.* **Mitochondrial production of oxidants is necessary for physiological calcium oscillations.** *J Cell Physiol* 206, 487-494 (2006).
- 168 Foroozanfard, F. *et al.* **Calcium plus vitamin D supplementation influences biomarkers of inflammation and oxidative stress in overweight and vitamin D-deficient women with polycystic ovary syndrome: a randomized double-blind placebo-controlled clinical trial.** *Clin Endocrinol (Oxf)* 83, 888-894 (2015).
- 169 Sakhaee, K. *et al.* **Meta-analysis of calcium bioavailability: a comparison of calcium citrate with calcium carbonate.** *Am J Ther* 6, 313-321 (1999).
- 170 Bristow, S. M. *et al.* **Acute and 3-month effects of microcrystalline hydroxyapatite, calcium citrate and calcium carbonate on serum calcium and markers of bone turnover: a randomised controlled trial in postmenopausal women.** *Br J Nutr* 112, 1611-1620 (2014).
- 171 Lehmann, A. & Hornby, P. J. **Intestinal SGLT1 in metabolic health and disease.** *Am J Physiol Gastrointest Liver Physiol* 310, G887-898 (2016).
- 172 Larraufie, P. *et al.* **SCFAs strongly stimulate PYY production in human enteroendocrine cells.** *Sci Rep* 8, 74 (2018).
- 173 Tordoff, M. G. **Calcium: taste, intake, and appetite.** *Physiol Rev* 81, 1567-1597 (2001).
- 174 McCaughey, S. A., Fitts, D. A. & Tordoff, M. G. **Lesions of the subfornical organ decrease the calcium appetite of calcium-deprived rats.** *Physiol Behav* 79, 605-612 (2003).

- 175 Tremblay, A., Doyon, C. & Sanchez, M. **Impact of yogurt on appetite control, energy balance, and body composition.** *Nutr Rev* 73 Suppl 1, 23-27 (2015).
- 176 Stuart, R. O. *et al.* **Critical role for intracellular calcium in tight junction biogenesis.** *J Cell Physiol* 159, 423-433 (1994).
- 177 Datta, P. & Weis, M. T. **Calcium glycerophosphate preserves transepithelial integrity in the Caco-2 model of intestinal transport.** *World J Gastroenterol* 21, 9055-9066 (2015).

## APPENDICES

### Appendix A. Odds ratios of 29 fecal elements for the association between elements and risk of MetS.

Fecal elements (tertile status)	Healthy (N=240)	MetS (N=64)	OR [95% CI]	p-value
<b>Al:</b>				
low	81 (33.8%)	20 (31.2%)	Ref.	Ref.
middle	81 (33.8%)	20 (31.2%)	1.00 [0.50;2.01]	1
high	78 (32.5%)	24 (37.5%)	1.24 [0.63;2.46]	0.526
<b>As:</b>				
low	82 (34.2%)	19 (29.7%)	Ref.	Ref.
middle	82 (34.2%)	19 (29.7%)	1.00 [0.49;2.04]	1
high	76 (31.7%)	26 (40.6%)	1.47 [0.75;2.91]	0.259
<b>Ba:</b>				
low	76 (31.7%)	25 (39.1%)	Ref.	Ref.
middle	79 (32.9%)	22 (34.4%)	0.85 [0.44;1.64]	0.622
high	85 (35.4%)	17 (26.6%)	0.61 [0.30;1.21]	0.161
<b>Be:</b>				
low	87 (36.2%)	14 (21.9%)	Ref.	Ref.
middle	81 (33.8%)	20 (31.2%)	1.53 [0.72;3.30]	0.267
high	72 (30.0%)	30 (46.9%)	2.56 [1.28;5.36]	0.008*
<b>Bi:</b>				
middle	155 (64.6%)	47 (73.4%)	Ref.	Ref.
high	85 (35.4%)	17 (26.6%)	0.66 [0.35;1.21]	0.185

Fecal elements (tertile status)	Healthy (N=240)	MetS (N=64)	OR [95% CI]	p-value
Ca:				
low	74 (30.8%)	27 (42.2%)	Ref.	Ref.
middle	79 (32.9%)	22 (34.4%)	0.77 [0.40;1.46]	0.418
high	87 (36.2%)	15 (23.4%)	0.48 [0.23;0.95]	0.036*
Cd:				
low	85 (35.4%)	16 (25.0%)	Ref.	Ref.
middle	76 (31.7%)	25 (39.1%)	1.74 [0.87;3.57]	0.12
high	79 (32.9%)	23 (35.9%)	1.54 [0.76;3.19]	0.232
Co:				
low	84 (35.0%)	17 (26.6%)	Ref.	Ref.
middle	82 (34.2%)	19 (29.7%)	1.14 [0.55;2.38]	0.718
high	74 (30.8%)	28 (43.8%)	1.86 [0.95;3.74]	0.072
Cr:				
low	80 (33.3%)	21 (32.8%)	Ref.	Ref.
middle	83 (34.6%)	18 (28.1%)	0.83 [0.41;1.67]	0.599
high	77 (32.1%)	25 (39.1%)	1.23 [0.64;2.41]	0.533
Cs:				
low	83 (34.6%)	18 (28.1%)	Ref.	Ref.
middle	74 (30.8%)	27 (42.2%)	1.67 [0.86;3.34]	0.133
high	83 (34.6%)	19 (29.7%)	1.05 [0.51;2.18]	0.884
Cu:				
low	77 (32.1%)	24 (37.5%)	Ref.	Ref.

Fecal elements (tertile status)	Healthy (N=240)	MetS (N=64)	OR [95% CI]	p-value
middle	79 (32.9%)	22 (34.4%)	0.89 [0.46;1.74]	0.741
high	84 (35.0%)	18 (28.1%)	0.69 [0.34;1.37]	0.289
Fe:				
low	78 (32.5%)	23 (35.9%)	Ref.	Ref.
middle	80 (33.3%)	21 (32.8%)	0.89 [0.45;1.75]	0.737
high	82 (34.2%)	20 (31.2%)	0.83 [0.42;1.63]	0.587
Ga:				
low	78 (32.5%)	23 (35.9%)	Ref.	Ref.
middle	79 (32.9%)	22 (34.4%)	0.94 [0.48;1.84]	0.868
high	83 (34.6%)	19 (29.7%)	0.78 [0.39;1.54]	0.473
K:				
low	85 (35.4%)	16 (25.0%)	Ref.	Ref.
middle	78 (32.5%)	23 (35.9%)	1.56 [0.77;3.23]	0.219
high	77 (32.1%)	25 (39.1%)	1.72 [0.86;3.52]	0.129
Li:				
low	84 (35.0%)	17 (26.6%)	Ref.	Ref.
middle	81 (33.8%)	20 (31.2%)	1.22 [0.59;2.52]	0.592
high	75 (31.2%)	27 (42.2%)	1.77 [0.90;3.57]	0.1
Mg:				
low	85 (35.4%)	16 (25.0%)	Ref.	Ref.
middle	80 (33.3%)	21 (32.8%)	1.39 [0.68;2.90]	0.371
high	75 (31.2%)	27 (42.2%)	1.90 [0.96;3.88]	0.067

Fecal elements (tertile status)	Healthy (N=240)	MetS (N=64)	OR [95% CI]	p-value
Mn:				
low	77 (32.1%)	24 (37.5%)	Ref.	Ref.
middle	79 (32.9%)	22 (34.4%)	0.89 [0.46;1.74]	0.741
high	84 (35.0%)	18 (28.1%)	0.69 [0.34;1.37]	0.289
Na:				
low	81 (33.8%)	20 (31.2%)	Ref.	Ref.
middle	81 (33.8%)	20 (31.2%)	1.00 [0.50;2.01]	1
high	78 (32.5%)	24 (37.5%)	1.24 [0.63;2.46]	0.526
P:				
low	75 (31.2%)	26 (40.6%)	Ref.	Ref.
middle	80 (33.3%)	21 (32.8%)	0.76 [0.39;1.46]	0.412
high	85 (35.4%)	17 (26.6%)	0.58 [0.29;1.15]	0.118
Pb:				
low	85 (35.0%)	16 (26.2%)	Ref.	Ref.
middle	73 (30.0%)	28 (45.9%)	2.03 (1.02, 4.13)	0.009*
high	84 (35.0%)	18 (27.9%)	1.06 (0.50, 2.27)	0.075
Rb:				
low	83 (34.6%)	18 (28.1%)	Ref.	Ref.
middle	79 (32.9%)	22 (34.4%)	1.28 [0.64;2.60]	0.487
high	78 (32.5%)	24 (37.5%)	1.41 [0.71;2.85]	0.323
S:				
low	82 (34.2%)	19 (29.7%)	Ref.	Ref.

Fecal elements (tertile status)	Healthy (N=240)	MetS (N=64)	OR [95% CI]	p-value
middle	81 (33.8%)	20 (31.2%)	1.06 [0.53;2.16]	0.861
high	77 (32.1%)	25 (39.1%)	1.40 [0.71;2.78]	0.332
Se:				
low	82 (34.2%)	19 (29.7%)	Ref.	Ref.
middle	81 (33.8%)	20 (31.2%)	1.06 [0.53;2.16]	0.861
high	77 (32.1%)	25 (39.1%)	1.40 [0.71;2.78]	0.332
Sr:				
low	77 (32.1%)	24 (37.5%)	Ref.	Ref.
middle	81 (33.8%)	20 (31.2%)	0.79 [0.40;1.56]	0.502
high	82 (34.2%)	20 (31.2%)	0.78 [0.40;1.54]	0.479
Ti:				
low	77 (32.1%)	24 (37.5%)	Ref.	Ref.
middle	83 (34.6%)	18 (28.1%)	0.70 [0.35;1.39]	0.305
high	80 (33.3%)	22 (34.4%)	0.88 [0.45;1.71]	0.713
Tl:				
low	84 (35.0%)	17 (26.6%)	Ref.	Ref.
middle	86 (35.8%)	15 (23.4%)	0.86 [0.40;1.85]	0.706
high	70 (29.2%)	32 (50.0%)	2.24 [1.16;4.47]	0.016*
U:				
low	84 (35.0%)	17 (26.6%)	Ref.	Ref.
middle	78 (32.5%)	23 (35.9%)	1.45 [0.72;2.97]	0.297
high	78 (32.5%)	24 (37.5%)	1.51 [0.76;3.08]	0.242

Fecal elements (tertile status)	Healthy (N=240)	MetS (N=64)	OR [95% CI]	<i>p</i> -value
V:				
low	82 (34.2%)	19 (29.7%)	Ref.	Ref.
middle	77 (32.1%)	24 (37.5%)	1.34 [0.68;2.68]	0.397
high	81 (33.8%)	21 (32.8%)	1.12 [0.56;2.26]	0.754
Zn:				
low	77 (32.1%)	24 (37.5%)	Ref.	Ref.
middle	79 (32.9%)	22 (34.4%)	0.89 [0.46;1.74]	0.741
high	84 (35.0%)	18 (28.1%)	0.69 [0.34;1.37]	0.289

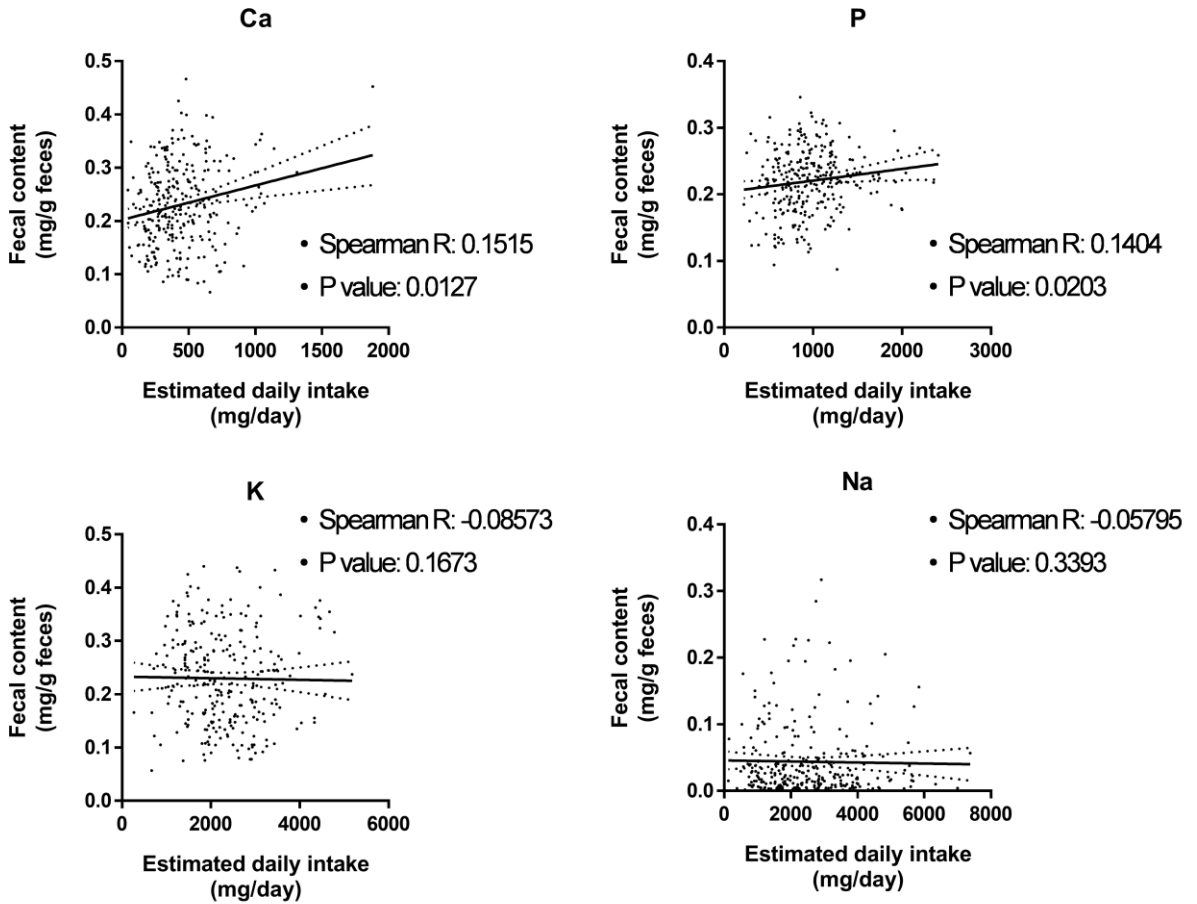
The low, middle, and high level groups of each element were determined using the tertile values. The low level group (tertile1) of each element was utilized as a reference. The significant values ( $P < 0.05$ ) were marked with an asterisk (\*)

**Appendix B. Significant associations between specific fecal elements (Be, Ca, and Tl) and microbial taxa by multivariate analysis using MaAsLin.**

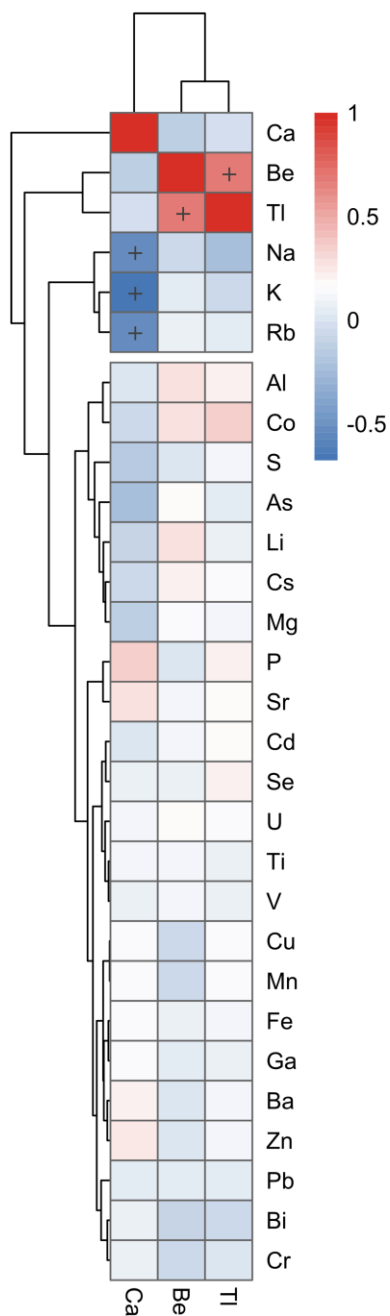
Elements	Feature	Coefficient	P value	Adjusted P value
Be	<i>Sutterella</i>	318.4856	0.00000	0.00053
	<i>Subdoligranulum</i>	-770.7603	0.00001	0.00053
	<i>Rothia</i>	-48.3169	0.00286	0.04284
	<i>Bifidobacterium</i>	-377.0052	0.00383	0.04353
Ca	<i>Bacteroides</i>	0.0083	0.00000	0.00000
	<i>Roseburia</i>	-0.0028	0.00000	0.00000
	<i>Haemophilus</i>	-0.0009	0.00000	0.00010
	<i>Parabacteroides</i>	0.0023	0.00000	0.00010
	<i>Prevotella</i>	-0.0092	0.00001	0.00033
	<i>Bifidobacterium</i>	0.0018	0.00007	0.00147
	<i>Faecalibacterium</i>	-0.0026	0.00028	0.00409
	<i>Alistipes</i>	0.0021	0.00032	0.00409
	<i>Lachnospira</i>	-0.0014	0.00099	0.00914
	<i>Veillonella</i>	-0.0007	0.00405	0.02862
	<i>Akkermansia</i>	0.0001	0.00775	0.04892
Tl	<i>Subdoligranulum</i>	-590.2033	0.00000	0.00004
	<i>Streptococcus</i>	-139.7455	0.00030	0.00731
	<i>Rothia</i>	-37.5445	0.00038	0.00757
	<i>Blautia</i>	-122.6066	0.00228	0.02279
	<i>Alistipes</i>	329.5262	0.00257	0.02371
	<i>Lactobacillus</i>	-122.9489	0.00391	0.03351
	<i>Bacteroides</i>	797.1077	0.00435	0.03390
	<i>Parabacteroides</i>	259.1554	0.00480	0.03390
	<i>Clostridium</i>	-205.0104	0.00669	0.04225

Associations were considered to be significant with a Benjamini and Hochberg false discovery rate (FDR)-corrected *P* value of < 0.05.

Appendix C. Scatter plots showing the relationship between food intake information and human fecal measurement data of four elements including Ca, P, K, and Na (N=275).



**Appendix D. Spearman’s rank correlation between three elements with the significant association in Table 2.4 and each element. Asterisks represent significant associations at FDR adjusted  $P$  values of  $< 0.05$  (N=304).**



**Appendix E. Primer information**

<b>Genes</b>	<b>Functions</b>	<b>Primer sequences</b>
GLP-1	gastrointestinal hormone	F: CAAACCAAGATCACTGACAAGAAAT R: GGGTTACACAATGCTAGAGGGA
IL-10	inflammation	F: ATAACTGCACCCACTTCCCA R: GGGCATCACTTCTACCAGGT
IL-17	inflammation	F: TCTCCACCGCAATGAAGACC R: CACACCCACCAGCATCTTCT
IL-1 $\beta$	inflammation	F: TCGCTCAGGGTCACAAGAAA R: CATCAGAGGCAAGGAGGAAAAC
MUC2	mucin production	F: AAACTCAGCTGGGAAGAACTG R: TTGGGAGTGGAAGTCTCAATGAT
MUC3	mucin production	F: CACCCCAGCACCTACCACTACT R: ATAGAAGAGGCTGGTGCCTGAC
Nos2	inflammation	F: CCAGCCTTGCATCCTCATTGG R: CCAAACACCAAGCTCATGCGG
Occl	tight junction	F: ATGTCCGGCCGATGCTCTC R: TTTGGCTGCTCTTGGGTCTGTAT
PYY	gastrointestinal hormone	F: CTTACAGACGACAGCGACA R: GGGAAATGAACACACACAGCC
RPL19	housekeeping gene	F: GAAGGTCAAAGGGAATGTGTTCA R: CCTTGTCTGCCTTCAGCTTGT
TNF $\alpha$	inflammation	F: AAATGGGCTCCCTCTCATCAGTTC R: TCTGCTTGGTGGTTTGCTACGAC
ZO1	tight junction	F: TTTTGGACAGGGGGAGTGG R: TGCTGCAGAGGTCAAAGTTCAAG

# 국문초록

## 장내 원소가 대사성 질환과

## 장내 마이크로비옴에 미치는 영향

보건학과 환경보건학 전공 차광현

비만과 당뇨 등을 포함한 대사증후군은 전세계적으로 주요 공중 보건 이슈 중 하나이다. 최근 보고되고 있는 연구들은 장내 미생물이 에너지 섭취, 대사 내독성증 등에 영향을 주어 대사증후군을 유발할 수 있음을 보여준다. 한편, 환경 속 화학물질에 대한 노출이 대사증후군과 연관될 수 있다는 다양한 증거들이 함께 보고되고 있다. 특히, 무기질, 금속을 포함하는 장내 원소들은 생물체의 대사 과정에서 중요한 역할을 한다. 지금까지 대사증후군에 각 원소들이 미치는 영향에 대한 연구는 대부분 장내 미생물의 역할을 고려하지 않고 주로 호스트 관점에서 수행되었으며, 비소, 카드뮴과 같은 소수의 원소들에 연구가 집중되어왔다. 따라서, 본 연구에서는 다양한 장내 원소에 대하여 장내 미생물, 대사증후군과의 연관성을 규명하고 이들 사이의 인과관계를 밝히고자 하였다.

먼저, 우리는 장내 원소가 장내 미생물 군집 그리고 대사증후군과 연관성을 나타내는지 확인하였다. 인체 대변 시료로부터 29개의 장내 원소 함량을 측정하였고, 대사증후군, 장내 미생물과의 상관관계 분석을 수행하였다. 베릴륨(Be), 칼슘(Ca), 탈륨(Tl)은 유의적인 대사증후군 odds ratio를 나타냈고, 대사증후군과 관련된 각각의 세부 바이오마커와도 유의적인 상관관계를 보였다. 또한 Be, Tl은 미생물 다양성 감소와 높은

연관성을 가지고 있었다. 특히, Be와 Ca는 대사증후군 억제 효과가 있는 것으로 보고되고 있는 *Akkermansia*, *Bifidobacterium* 등의 장내 미생물 분포에서 서로 음과 양의 상반된 연관성을 보여주었다. 또한 두 장내 원소는 장내 환경에서 미생물 대사 기능에도 서로 다르게 영향을 주었다.

둘째, 저농도 Be 노출이 장내 미생물 변화를 유도하고 대사증후군을 악화시킬 수 있는지를 평가했다. 고지방 식이 생쥐의 경우, 30 ppb의 Be 노출이 유의적인 체중 및 지방 증가로 이어졌지만, 일반 식이 그룹은 분명한 변화를 나타내지 않았다. 고지방 식이와 함께 3 ppb와 30 ppb의 Be에 노출시켰을 때 미생물 다양성 감소, *Akkermansia*의 현저한 감소와 같은 장내 미생물 변화가 나타났다. 인체 대변 시료 배양 실험에서도 저농도 Be 처리 시 미생물 다양성 감소와 *Bifidobacterium*의 감소가 야기되었다. 이밖에도 고지방 식이 그룹에서 베릴륨 노출에 의해 야기된 유의적인 단쇄 지방산 변화는 거식성 감소 및 식욕 증가와 관련이 있었고, 염증 관련 유전자의 유의적인 발현 증가와 혈중 LPS의 상승은 대사 내독소증과 만성 염증이 대사증후군을 더욱 악화시켰을 가능성을 보여주었다.

셋째, Ca-carbonate와 Ca-citrate가 고지방 식이 생쥐의 대사 항상성 개선에 미치는 영향을 평가하고 비교하였다. 높은 농도의 Ca-citrate 보충제는 Ca-carbonate에 비해 현저한 체중 감소와 함께 대사증후군 관련 혈장 바이오마커의 유의적인 변화를 나타냈다. Ca-carbonate와 Ca-citrate 보충제는 장내 미생물 구성에는 서로 유사한 변화를 가져왔지만, Ca-citrate 그룹이 단쇄 지방산 중 특히 식욕억제 호르몬인 GLP-1 분비와 관련이 있는 propionate를 더 현저하게 증가시켰다. 또한 Ca-citrate 그룹은 점막 기능 관련 유전자 발현 증가와 함께 염증성 사이토카인 유전자의 발현과 혈중 LPS 농도를 유의적으로 감소시켰다.

결론적으로, 본 연구는 장내 원소가 대사증후군과 높은 관련성을 가지며, Be, Ca와 같은 일부 원소는 장내 미생물의 군집 형성 및 기능성에 강한 상관관계를 가지고 있음을 보여주었다. 실제로 Be에 대한 노출은 고지방 식이 생쥐에서 장내 미생물 구성 및 대사에 영향을 줌과 동시에 매우 낮은 농도에서도 대사증후군을 악화시킬 수 있었다. Ca 보충제는 대사증후군 억제 효능이 알려진 장내 미생물의 증가와 함께 대사증후군 지연에 도움을 주었고 Ca-citrate가 Ca-carbonate에 비해 더 좋은 효과를 나타내었다. 이러한 연구결과는 장내 미생물과 질병 사이의 관계를 이해하는데 장내 원소 분석이 중요한 정보를 제공해줄 수 있음을 보여준다. 향후 이와 관련된 더욱 다양한 후속 연구가 필요할 것이다.

**표제어:** 대사증후군, 장내 미생물, 장내 원소, 베릴륨, 칼슘

**학번:** 2014-30750